



**TECHNICAL REPORT 0-6925-1**  
TXDOT PROJECT NUMBER 0-6925

# Improving the Performance-Graded Asphalt Binder Specification: Final Report

Ramez Hajj  
Angelo Filonzi  
Amit Bhasin, Ph.D., P.E.

November 2018; Published May 2019

<http://library.ctr.utexas.edu/ctr-publications/0-6925-1.pdf>



Technical Report Documentation Page

1. Report No. FHWA/TX-18/0-6925-1		2. Government Accession No.		3. Recipient's Catalog No.	
4. Title and Subtitle Improving the Performance-Graded Asphalt Binder Specification: Final Report				5. Report Date November 2018; Published May 2019	
				6. Performing Organization Code	
7. Author(s) Ramez Hajj Angelo Filonzi Amit Bhasin, Ph.D., P.E.				8. Performing Organization Report No. 0-6925-1	
9. Performing Organization Name and Address Center for Transportation Research The University of Texas at Austin 3925 W. Braker Lane, 4 <sup>th</sup> Floor Austin, TX 78759				10. Work Unit No. (TRAIS)	
				11. Contract or Grant No. 0-6925	
12. Sponsoring Agency Name and Address Texas Department of Transportation Research and Technology Implementation Division P.O. Box 5080 Austin, TX 78763-5080				13. Type of Report and Period Covered Technical Report September 2016–November 2018	
				14. Sponsoring Agency Code	
15. Supplementary Notes Project performed in cooperation with the Texas Department of Transportation and the Federal Highway Administration.					
16. Abstract The Performance Grading (PG) specification is currently used as the primary purchase specification and binder classification system in the state of Texas and many other parts of the world. Since its inception, binder production has evolved to include new technologies and additives that can be used to improve binder performance. However, in some cases such binders may also prematurely fail in asphalt pavements while still meeting the existing specification requirements. In light of this shortcoming with the PG specification, this project reviewed various new methods that can be utilized as alternatives or in a complimentary manner to the current specification. A variety of field and laboratory modified binders were evaluated using a suite of tests along with mixtures that incorporated these binders in order to evaluate the most effective performance indicators for asphalt binder specification. Parameters from the Multiple Stress Creep and Recovery (MSCR) test showed a good correlation with rutting of asphalt mixtures and parameters from the poker chip test showed a good correlation with cracking of asphalt binders. A method to measure low-temperature properties of the binder using a 4-mm diameter geometry with the Dynamic Shear Rheometer (DSR) was evaluated and the analytical method used with the resulting data was further developed for use as a surrogate to traditional tests. Based on the results, this study recommends the implementation of the MSCR, the 4-mm plate geometry for low temperature DSR testing in certain scenarios, and the poker chip test as an indicator for cracking resistance.					
17. Key Words performance grading, performance-graded asphalt binder, multiple stress creep and recovery (MSCR) test, dynamic shear rheometer (DSR)			18. Distribution Statement No restrictions. This document is available to the public through the National Technical Information Service, Springfield, Virginia 22161; www.ntis.gov.		
19. Security Classif. (of report) Unclassified		20. Security Classif. (of this page) Unclassified		21. No. of pages	
				22. Price	



**THE UNIVERSITY OF TEXAS AT AUSTIN  
CENTER FOR TRANSPORTATION RESEARCH**

## **Improving the Performance-Graded Asphalt Binder Specification: Final Report**

Ramez Hajj  
Angelo Filonzi  
Amit Bhasin, Ph.D., P.E.

---

CTR Technical Report:	0-6925-1
Report Date:	November 2018; Published May 2019
Research Project:	0-6925
Research Project Title:	Improving the Performance-Graded Asphalt Binder Specification
Sponsoring Agency:	Texas Department of Transportation
Performing Agency:	Center for Transportation Research at The University of Texas at Austin

Project performed in cooperation with the Texas Department of Transportation and the Federal Highway Administration.



## **DISCLAIMER**

The contents of this report reflect the views of the authors, who are responsible for the facts and the accuracy of the information presented herein. Mention of trade names or commercial products does not constitute endorsement or recommendations for use.

## **ACKNOWLEDGMENTS**

The authors recognize that this project was supported by the Texas Department of Transportation. The authors acknowledge and thank Dr. Andre de Fortier Smit and Darren Hazlett for all of their help and contributions to this work. The authors would like to acknowledge Arash Motamed, Jerry Peterson, and Ryan Barborak for their help with sampling materials and round robin testing. The authors would also like to thank Gerry Reinke for his guidance in carrying out the test using the 4 mm plate DSR geometry and acknowledge Victoria Hang and Erica Lopez for their help with laboratory testing. Finally, the authors would also like to acknowledge Mr. Tyler Seay for his many contributions to this project.

## **ABSTRACT**

The Performance Grading (PG) specification is currently used as the primary purchase specification and binder classification system in the state of Texas and many other parts of the world. Since its inception, binder production has evolved to include new technologies and additives that can be used to improve binder performance. However, in some cases such binders may also prematurely fail in asphalt pavements while still meeting the existing specification requirements. In light of this shortcoming with the PG specification, this project reviewed various new methods that can be utilized as alternatives or in a complimentary manner to the current specification. A variety of field and laboratory modified binders were evaluated using a suite of tests along with mixtures that incorporated these binders in order to evaluate the most effective performance indicators for asphalt binder specification. Parameters from the Multiple Stress Creep and Recovery (MSCR) test showed a good correlation with rutting of asphalt mixtures and parameters from the poker chip test showed a good correlation with cracking of asphalt binders. A method to measure low-temperature properties of the binder using a 4-mm diameter geometry with the Dynamic Shear Rheometer (DSR) was evaluated and the analytical method used with the resulting data was further developed for use as a surrogate to traditional tests. Based on the results, this study recommends the implementation of the MSCR, the 4-mm plate geometry for low temperature DSR testing in certain scenarios, and the poker chip test as an indicator for cracking resistance.

## EXECUTIVE SUMMARY

Over the last two decades, the state of Texas, and many other parts of the world, have used the Performance Grading (PG) specification as a purchase specification and a metric to evaluate the expected performance of asphalt binders. However, in recent years, this system has proven to be ineffective for predicting some premature binder-related pavement failures due to an increase in the use of non-traditional methods and modifiers during binder production, for which the PG specification was not designed. Similarly, in some cases the current PG framework underestimates the expected performance of certain modified binders. This study provides a comprehensive review of the current methods used in binder testing, as well as methods that have been recently developed and shown to effectively measure performance related properties of asphalt binders.

A thorough literature review was done to identify the methods that exist outside of the PG framework that can more accurately reflect the performance of the asphalt binder. Focus was placed on methods that mostly utilize existing or other standard laboratory equipment and do not require long testing times. Material sampling focused on three categories of binders: a set of binders with similar PG developed in the laboratory by modifying a single base binder with several different modifiers, a set of binders recovered from field cores with known performance, and a set of binders from new construction projects. Testing was performed on binders in the project with a variety of tests, ranging from the traditional PG tests, to new tests developed in the last few years. Tests that used the existing equipment, the Dynamic Shear Rheometer (DSR) and Bending Beam Rheometer (BBR) were prioritized. In addition, tests that involved nonlinear performance and fracture of binder were more closely examined to determine whether these tests could be effective in predicting actual cracking performance. Finally, mixture testing was performed using the Hamburg Wheel Tracking Device (HWT) and the Texas Overlay test on mixes using these binders to determine which tests correlated well with mixture performance.

Details of the aforementioned work and final recommendations are presented in this report. These recommendations include the implementation of the Multiple Stress Creep and Recovery test (MSCR) for high temperature performance of asphalt binders. In addition, the implementation of the 4 mm DSR geometry is recommended. This report includes details relevant to the use of the 4 mm geometry to account for errors that may arise due to machine compliance as well as an improvised and validated analysis method that can be used to analyze the results from this test. This method can serve as a more efficient alternative to using the BBR to measure low-temperature performance of asphalt binders, particularly

in the case of recycled binders and emulsion residues. Finally, the poker chip test is recommended for further implementation as an indicator for the cracking resistance of asphalt binders due to its good relationship with results from mixture testing. A draft specification for this test is also provided in this report.



# TABLE OF CONTENTS

<b>List of Figures</b>	<b>xiii</b>
<b>List of Tables</b>	<b>xix</b>
<b>Chapter 1. Introduction</b>	<b>1</b>
1.1 Introduction . . . . .	1
1.2 Tests to evaluate binder rutting . . . . .	2
1.3 Tests to evaluate binder cracking resistance and durability . . . . .	4
1.3.1 Low temperature cracking . . . . .	4
1.3.2 Fatigue cracking . . . . .	7
<b>Chapter 2. Material Selection and Sampling</b>	<b>21</b>
2.1 Binders from cores of existing pavements with good and poor performance .	21
2.2 Binders from producers and artificial blends produced in the laboratory . . .	21
2.3 Binders from new construction sites . . . . .	23
2.4 Aggregates for Laboratory Mixes . . . . .	23
2.5 Recycled Materials and Rejuvenators . . . . .	23
<b>Chapter 3. Binder Testing Using Current and New Methods</b>	<b>25</b>
3.1 Overview of current methods . . . . .	25
3.1.1 Aging . . . . .	25
3.2 Overview of new methods . . . . .	29
3.2.1 New methods for high temperature testing . . . . .	31
3.2.1.1 Multiple Stress Creep and Recovery (MSCR) test . . . . .	31
3.2.2 New methods for intermediate temperature testing . . . . .	32
3.2.2.1 Rheological indices related to brittleness and durability . .	32
3.2.2.2 Linear Amplitude Sweep (LAS) . . . . .	33
3.2.2.3 Monotonic testing in a realistic state of stress . . . . .	34
3.2.3 New methods for low temperature testing . . . . .	35
3.2.3.1 Measures of binder cracking resistance using the BBR and other equipment . . . . .	35
3.3 Materials and laboratory binder modification . . . . .	36

3.3.1	Binder set 1 . . . . .	36
3.3.2	Binder set 2 . . . . .	46
3.4	High temperature properties . . . . .	46
3.5	Low temperature properties and Delta Tc . . . . .	50
3.6	Intermediate temperature cracking indicators . . . . .	52
3.6.1	Relationships between cracking indicators . . . . .	63
3.7	Recovered binders from field sections . . . . .	63
3.8	Improving testing efficiency . . . . .	70
3.8.1	Methods and Materials . . . . .	73
3.8.2	Analysis of Data . . . . .	74
3.8.3	Results using different approaches . . . . .	77
3.8.3.1	Use of sigmoidal function, interconversion to time do- main, and conversion for axial loading . . . . .	78
3.8.3.2	Use of CAM model, interconversion to time domain, and correlation with BBR S and m-value . . . . .	80
3.8.3.3	Use of CAM model and approximate correlation with BBR S and m-value . . . . .	83
3.8.4	Sensitivity to Poisson's Ratio . . . . .	84
3.8.5	Discussion of 4 mm plate . . . . .	86
<b>Chapter 4.</b>	<b>Mixture Testing and Comparison with Binder Testing</b>	<b>89</b>
4.1	Mixture test methods . . . . .	89
4.1.1	Hamburg Wheel Tracking Device Test . . . . .	89
4.1.2	Overlay Test . . . . .	89
4.2	Mix design and materials . . . . .	90
4.3	Mixture test results . . . . .	91
4.4	Comparison with binder testing . . . . .	91
<b>Chapter 5.</b>	<b>Evaluating Repeatability of Select Test Methods</b>	<b>103</b>
5.1	Overview and materials . . . . .	103
5.2	Results . . . . .	105
<b>Chapter 6.</b>	<b>Summary and Conclusions</b>	<b>107</b>
<b>References</b>		<b>109</b>

**Appendix A**

**115**

**Appendix B**

**123**



## LIST OF FIGURES

Figure 3.1.	High temperature continuous grades at different doses of additive A1 . . . . .	38
Figure 3.2.	High temperature continuous grades at different doses of additive A2 . . . . .	38
Figure 3.3.	High temperature continuous grades at different doses of additive A3 . . . . .	39
Figure 3.4.	High temperature continuous grades at different doses of additive A4 . . . . .	39
Figure 3.5.	High temperature continuous grades at different doses of additive A5 . . . . .	40
Figure 3.6.	High temperature continuous grades at different doses of additive A6 . . . . .	40
Figure 3.7.	High temperature continuous grades at different doses of blending with binder B2 . . . . .	41
Figure 3.8.	Summary of high grades of binders in Set 1 . . . . .	41
Figure 3.9.	Low temperature continuous grades at different doses of additive A1 . . . . .	42
Figure 3.10.	Low temperature continuous grades at different doses of additive A2 . . . . .	42
Figure 3.11.	Low temperature continuous grades at different doses of additive A3 . . . . .	43
Figure 3.12.	Low temperature continuous grades at different doses of additive A4 . . . . .	43
Figure 3.13.	Low temperature continuous grades at different doses of additive A5 . . . . .	44
Figure 3.14.	Low temperature continuous grades at different doses of additive A6 . . . . .	44
Figure 3.15.	Low temperature continuous grades at different doses of blending with binder B2 . . . . .	45
Figure 3.16.	High temperature continuous grades after PPA modification . . . .	47
Figure 3.17.	Continuous low grades of Set 2 binders with their Set 1 counterparts	47

Figure 3.18.	Example of analysis of MSCR results for two cycles . . . . .	48
Figure 3.19.	Elastic Recovery of Set 1 binders at 100 Pa loading . . . . .	48
Figure 3.20.	Elastic Recovery of Set 1 binders at 3200 Pa loading . . . . .	49
Figure 3.21.	Non-recoverable creep compliance of Set 1 binders at 100 Pa loading . . . . .	49
Figure 3.22.	Non-recoverable creep compliance of Set 1 binders at 3200 Pa loading . . . . .	50
Figure 3.23.	Effect of SBS modification with the use of low temperature additives, elastic recovery at the end of 10 cycles and 100 Pa loading amplitude is shown . . . . .	51
Figure 3.24.	$\Delta T_c$ for binders in Binder Set 1 . . . . .	51
Figure 3.25.	$\Delta T_c$ for binders in Set 2 and corresponding Set 1 binders . . . . .	52
Figure 3.26.	Example of frequency sweep data shifted to a master curve . . . . .	53
Figure 3.27.	PG intermediate temperature parameter for Set 1 binders . . . . .	54
Figure 3.28.	PG intermediate temperature parameter for Set 2 binders . . . . .	54
Figure 3.29.	Glover-Rowe parameter for Set 1 binders . . . . .	55
Figure 3.30.	Glover-Rowe parameter for Set 2 binders . . . . .	55
Figure 3.31.	Crossover frequency parameter for Set 1 binders . . . . .	56
Figure 3.32.	Crossover modulus parameter for Set 1 binders . . . . .	56
Figure 3.33.	Crossover frequency parameter for Set 2 binders . . . . .	57
Figure 3.34.	Crossover modulus parameter for Set 2 binders . . . . .	57
Figure 3.35.	Relationship between crossover frequency and crossover modulus . . . . .	58
Figure 3.36.	Linear Amplitude Sweep Results . . . . .	59
Figure 3.37.	Poker chip maximum stress for PAV aged binders . . . . .	59
Figure 3.38.	Poker chip fracture energy for PAV aged binders . . . . .	60
Figure 3.39.	Poker chip failure strain for PAV aged binders . . . . .	60
Figure 3.40.	Poker chip maximum stress for unaged binders . . . . .	61
Figure 3.41.	Poker chip fracture energy for unaged binders . . . . .	61
Figure 3.42.	Poker chip failure strain for unaged binders . . . . .	62
Figure 3.43.	Current intermediate temperature parameter vs. $\Delta T_c$ . . . . .	63
Figure 3.44.	Current intermediate temperature parameter vs. Glover-Rowe parameter . . . . .	64
Figure 3.45.	Current intermediate temperature parameter vs. crossover modulus . . . . .	64
Figure 3.46.	$\Delta T_c$ vs. Glover-Rowe parameter . . . . .	65

Figure 3.47.	$\Delta T_c$ vs. crossover modulus . . . . .	65
Figure 3.48.	Glover-Rowe parameter vs. crossover modulus . . . . .	66
Figure 3.49.	Current intermediate temperature parameter vs. poker chip test PAV strength . . . . .	66
Figure 3.50.	$\Delta T_c$ vs. poker chip test PAV strength . . . . .	67
Figure 3.51.	Glover-Rowe parameter vs. poker chip test PAV strength . . . . .	67
Figure 3.52.	Crossover Modulus vs. poker chip test PAV strength . . . . .	68
Figure 3.53.	Poker chip test fracture energy vs. poker chip test PAV strength . .	68
Figure 3.54.	Poker chip test strength for binders recovered from field mixes . .	69
Figure 3.55.	Low True Grade based on 4 mm plate DSR test for binders recov- ered from field mixes . . . . .	70
Figure 3.56.	Raw data from 4 mm plate test . . . . .	74
Figure 3.57.	Master curve generated from 4 mm plate test . . . . .	76
Figure 3.58.	Stiffness true grades of the binders in this study based on the mas- ter curve created using the sigmoidal function compared to BBR Stiffness true grades . . . . .	79
Figure 3.59.	m-value true grades of the binders in this study based on the mas- ter curve created using the sigmoidal function compared to BBR Stiffness true grades . . . . .	79
Figure 3.60.	m-value true grades of the binders in this study based on the raw data at BBR temperatures compared with BBR m-value true grades	80
Figure 3.61.	Correlation between Stiffness measured in the DSR and BBR us- ing the raw data at each temperature and Ninomiya-Ferry inter- conversion (each symbol represents one asphalt binder) . . . . .	81
Figure 3.62.	Correlation between m-value measured in the DSR and BBR us- ing the raw data at each temperature and Ninomiya-Ferry inter- conversion (each symbol represents one asphalt binder) . . . . .	82
Figure 3.63.	Stiffness true grades of the binders in this study based on the Far- rar et al. method compared with BBR Stiffness true grades . . . . .	82
Figure 3.64.	m-value true grades of the binders in this study based on the Farrar et al. method compared with BBR m-value true grades . . . . .	83
Figure 3.65.	Stiffness true grades of the binders in this study based on the method used by Lu et al. compared with BBR Stiffness true grades	84

Figure 3.66.	m-value true grades of the binders in this study based on the method used by Lu et al. compared with BBR m-value true grades	85
Figure 3.67.	Effect of assuming different Poisson ratios on the Stiffness true grade as computed in the present study . . . . .	86
Figure 4.1.	Results of Hamburg Wheel Tracking Device test for binders in this study . . . . .	92
Figure 4.2.	Critical Fracture Energy for mixes made with different binders from this study . . . . .	92
Figure 4.3.	Crack Resistance Index for mixes made with different binders from this study . . . . .	93
Figure 4.4.	PG High Temperature vs. Number of Cycles to Failure . . . . .	93
Figure 4.5.	Non-Recoverable Compliance at 100 Pa loading amplitude vs. Number of Cycles to Failure . . . . .	94
Figure 4.6.	Percent Elastic Recovery at 100 Pa loading amplitude vs. Number of Cycles to Failure . . . . .	94
Figure 4.7.	Non-Recoverable Compliance at 3200 Pa loading amplitude vs. Number of Cycles to Failure . . . . .	95
Figure 4.8.	Percent Elastic Recovery at 3200 Pa loading amplitude vs. Number of Cycles to Failure . . . . .	95
Figure 4.9.	PG Intermediate Temperature Parameter vs. Critical Fracture Energy . . . . .	96
Figure 4.10.	PG Intermediate Temperature Parameter vs. Crack Resistance Index	97
Figure 4.11.	$\Delta T_c$ vs. Critical Fracture Energy . . . . .	97
Figure 4.12.	$\Delta T_c$ vs. Crack Resistance Index . . . . .	98
Figure 4.13.	Glover-Rowe Parameter vs. Critical Fracture Energy . . . . .	98
Figure 4.14.	Glover-Rowe Parameter vs. Crack Resistance Index . . . . .	99
Figure 4.15.	PAV-aged Poker Chip Strength vs. Critical Fracture Energy . . . . .	99
Figure 4.16.	PAV-aged Poker Chip Strength vs. Crack Resistance Index . . . . .	100
Figure 4.17.	RTFO-aged Poker Chip Strength vs. Critical Fracture Energy . . . . .	100
Figure 4.18.	RTFO-aged Poker Chip Strength vs. Crack Resistance Index . . . . .	101
Figure 4.19.	Crossover Modulus vs. Critical Fracture Energy . . . . .	101
Figure 4.20.	Crossover Modulus vs. Crack Resistance Index . . . . .	102
Figure 5.1.	Delta Tc tested by different operators using the same instrument . . . . .	105
Figure 5.2.	Delta Tc tested by different operators in different laboratories . . . . .	106



Figure 5.3. Glover-Rowe Parameter tested by different operators using the  
same instrument . . . . . 106



## LIST OF TABLES

Table 1.1.	Summary of Binder Properties that Relate to Performance; tests marked with <sup>+</sup> are part of current PG specification and others are the subject of research as potential to be used as replacements in the near future. . . . .	15
Table 2.1.	Softening agents with starting points for modification . . . . .	23
Table 3.1.	Binder with additive concentrations used to produce modified binders for this study . . . . .	37
Table 3.2.	Asphalt Binders Evaluated in the Present Study . . . . .	73
Table 4.1.	Aggregate gradation . . . . .	91



# CHAPTER 1. INTRODUCTION

## 1.1 INTRODUCTION

The purchase specification for asphalt binder plays a critical role in selecting and screening asphalt binders for design of asphalt mixtures. Binder specifications in the United States have evolved considerably over the past several decades from consistency and solubility based systems, to viscosity specifications, and finally to the performance-based specifications developed during the Strategic Highway Research Program (SHRP) and formalized in AASHTO M320. This latter system was developed during the late 1980's and early 1990's and is based largely upon rheological measurements taken in the linear viscoelastic range of the asphalt binder (SHRP A-370). Correlations between these measures and pavement performance were used to establish limits for purchase specifications of asphalt binders. The binder specifications are necessary but not sufficient to prevent premature pavement failure, which could also occur due to issues with aggregates, mixture proportioning, structural design and construction. However, in the nearly 25 years since the completion of the SHRP project, the formulations of asphalt binders used in paving applications have changed considerably. Much of these changes can be attributed to increased global demand for fuels and other petroleum-based products, which has led to the development of refining techniques that allow the extraction of increased amounts of higher value light products with lower sulfur contents from crude oil.

Crude oil sources are now more varied than when the performance grading (PG) purchase specification was developed. Today, unlike the late 1980's and early 1990's, asphalt binder modifiers such as but not limited to polymers, polyphosphoric acid, re-refined engine oil bottoms (REOB), paraffinic base oils, rendered oils, bio binders, and ground tire rubber are being used to formulate and manufacture asphalt binders. In addition to these modifiers, there has also been an increase in the use of higher percentages of reclaimed asphalt pavement (RAP) and reclaimed asphalt shingles (RAS).

Today's asphalt binders continue to meet the requirements of the PG specification, but highway agencies in the United States and Canada are increasingly experiencing premature failures of newly constructed pavements that are attributed to the quality of the asphalt binder. These failures occur despite general compliance with existing pavement and mix design standards, construction methods, and materials specifications. Many of these failures are in the form of low- and intermediate-temperature cracking and raveling, aggregate

loss, and instances of premature total surface course loss. Keeping in sync with the binder production and additive technologies that have emerged since the post SHRP work, it is important to comprehensively review the current PG specification framework. In fact, several studies and efforts have been made in the recent decade to address the aforementioned gap between the PG framework and the binder production and additive technologies. Table 1.1 lists some of the existing and newer test methods for typical distresses related to asphalt mixtures attributed to asphalt binders.

The overall objective of this research is to propose changes to the current performance-graded asphalt binder specifications, tests, and practices to remedy its gaps and shortcomings. The final outcome of this project will be modifications to the existing PG framework to more accurately capture the performance of asphalt binders. The research will also deliver a plan to implement the findings from this study as well as initiate this process through workshops through the course of the project. This chapter presents findings from the Task 2 of this project, i.e. to conduct a thorough review of the literature. The review presented in this chapter is categorized into two parts: (i) review of methods related to the rutting performance of asphalt binders and (ii) review of methods related to the cracking (low and intermediate temperature) performance of asphalt binders. Relatively more emphasis is placed on the latter because several recent studies have introduced tests to improve the current PG specification for rutting.

## **1.2 TESTS TO EVALUATE BINDER RUTTING**

The multiple stress creep recovery (MSCR) was perhaps the first test method that was developed to improve the existing Superpave high temperature PG specification. Bahia et al. (2001a) demonstrated that the relation between and measured rutting in asphalt mixtures was weak. To overcome this shortcoming, the repeated creep and recovery test using the DSR was explored as an alternative (Bahia et al., 2001b; D'Angelo et al., 2007). The outcome of these investigations was the development of the MSCR test protocol (D'Angelo et al., 2007) to measure the non-recoverable compliance of the binder,  $J_{nr}$ . The non-recoverable compliance was defined as the ratio of the non-recoverable strain at the end of a 9-second recovery period that followed a 1-second loading period to the constant stress that was applied during the loading period. At a given temperature, a binder with a higher value of non-recoverable compliance indicates a higher propensity to accumulate permanent deformation and therefore is more susceptible to rutting. D'Angelo et al. (2007) also reported that the values so obtained correlated better with rutting compared to the pa-

parameter as prescribed by the original Superpave PG specification. This finding was later substantiated by other researchers (Anderson et al., 2011b; Dubois et al., 2014; Zhou et al., 2014). Several other researchers have used non-recoverable compliance as a measure of rutting performance to evaluate binder properties in the laboratory, influence of recycled materials on binder properties, and the influence of polymer modified additives on binder performance (Abbas et al. 2013, Bernier et al. 2012). As a result of these and other similar studies, a new standard, AASHTO MP19, was proposed to replace the current AASHTO M320. In summary, per AASHTO MP19, the high temperature grade is based on the lower of the two temperatures that meet a criterion ( $G^*/\sin \delta > 1.0$  kPa) in unaged condition and a criterion ( $J_{nr} < 4.0, 2.0, 1.0, \text{ or } 0.5$  kPa<sup>-1</sup> depending on a sub-grade of “S”, “H”, “V” or “E”) in RTFO aged condition. This is different from the AASHTO M320 wherein the high temperature grade is based on the lower of the two temperatures that meet a criterion ( $G^*/\sin \delta > 1.0$  kPa) at unaged condition and another criterion ( $G^*/\sin \delta > 2.2$  kPa) in the RTFO aged condition. More recently, MP19 has been superseded by M332; the latter uses a cut-off value of 4.5 kPa<sup>-1</sup> for the “S” sub-grade.

A notable feature of the AASHTO MP19 specification is that it does not allow the use of “grade bump” to specify asphalt binders for locations with higher traffic volume and/or slower traffic speeds. Instead, a sub-grade (“S”, “H”, “V” or “E”) at the specific pavement temperature is utilized to accommodate for these factors.

Also, the use of the MSCR test protocol also allows the user to determine stress sensitivity and elastic recovery of the asphalt binder. Stress sensitivity is defined as the difference in  $J_{nr}$  measured at 0.1 kPa and 3.2 kPa compared to the measured at 0.1 kPa. However, it has been argued that the use of stress sensitivity is fundamentally incorrect because materials below their plastic yield limit will show little to no permanent strain at low stress levels. When such materials do deform at high stress levels, the stress sensitivity would appear to be infinity, falsely disqualifying the material.

Elastic recovery, or more correctly time-dependent recovery, can be considered as a complimentary measure to the non-recoverable compliance. For any given cycle, it is defined as the percentage of total strain that is recovered at the end of the recovery period. The percentage of elastic recovery is also a surrogate indicator for binders modified using elastomers. One study shows that the elastic recovery measured using the ductilometer showed very similar trends compared to elastic recovery measured using the MSCR test (Arega 2016). This was despite the fact that the former test was conducted on the original binder at 10 °C whereas the latter test was conducted on the RTFO aged binder at 64 °C.

This suggests that the elastic recovery from the MSCR test has a strong potential to replace the current method and specifications used to measure elastic recovery of asphalt binders. This can potentially save testing time and expensive capital equipment and maintenance, as well as enable the use of smaller specimens of binder for testing.

### **1.3 TESTS TO EVALUATE BINDER CRACKING RESISTANCE AND DURABILITY**

Cracking in asphalt mixtures occurs due to tensile failure of the asphalt binder in the mixture. While rutting resistance of the mixture depends both on the plastic deformation resistance of the binder and more importantly on the aggregate structure and packing, cracking resistance is largely dependent on the properties of the binder. The tensile failure could be induced by low temperature shrinkage (low-temperature cracking) or repeated traffic loading (fatigue cracking).

#### **1.3.1 Low temperature cracking**

When selecting the best asphalt binder for a particular use with low temperature properties in mind, mitigation of low-temperature cracking is the biggest concern. Breaking down the mechanics of low-temperature cracking, the change in temperature induces thermal stresses in a pavement. As a pavement cools down and no provisions are made for expansion or shrinkage along the length of the road, it causes the roadway to develop thermal stresses. Once the stresses exceed the tensile strength of the binder, a crack is initiated (Anderson et al., 2011a). Thus, a desirable binder has superior relaxation and strength properties.

According to the current Superpave specifications, stiffness and m-value of asphalt binders are measured using the Bending Beam Rheometer (BBR) test to determine low-temperature stiffness properties (Kennedy et al., 1994). The BBR applies a point load to an asphalt binder beam and measures its deflection to calculate stiffness (S) and relaxation properties (m-value). A low stiffness represents lower induced stress and thus a favorable property since stress is essentially the product of the: change in temperature, coefficient of thermal expansion, and stiffness. A high m-value indicates a desirable property due to the elevated ability to relax, resisting the generation of stresses. Mathematically speaking, the m-value represents the slope of the stiffness versus loading time in the log-log plot, or the rate of relaxation (Kennedy et al., 1994). The PG specification limits the stiffness of an asphalt binder beam to a maximum of 300 MPa and the m-value to a minimum of



0.300 (AAS, 2017). The more conservative true grade produced from these two parameters determines the asphalt binder's PG low temperature grade. Then, the true grade is rounded up to an increment of 6°C (AST, 2016). Previous work conflicts as to the importance and field performance predictability of the stiffness and m-value for specification grading purposes. According to the Superpave system, the binder performance is dependent on the stiffness and m-value (Kennedy et al., 1994). Yet, the strength of asphalt pavement determines when low-temperature cracking occurs, not the stiffness. Strength of asphalt binders is rarely measured, resulting in inconsistencies between lab and field performance. The asphalt binder specifications need to factor in strength, not just the stiffness of asphalt binders.

Along with the BBR, the Direct Tensile Test (DTT) was proposed for binders that failed the stiffness criterion to determine low temperature properties of asphalt binder. The DTT is not necessary if the stiffness of the binder is less than 300 MPa at the minimum pavement design temperature (Kennedy et al., 1994). The resulting failure strain of the DTT test is used to determine binder properties with no consideration of strength. Strength is also an input in the AASHTOWare Pavment ME Design Software. However, in practice, the DTT is rarely used to define the low temperature grade of the binder. Generally, the fracture properties of binders are not considered since BBR based S and m-values (rheological properties within the linear viscoelastic range) are used to characterize the low-temperature performance.

Another issue with the aforementioned BBR based approach is that usually only one parameter ends up determining the asphalt binder's low temperature PG grade. Normally, the m-value determines the true grade (Marasteanu et al., 2004), although stiffness-controlled binders are also possible to find. Marasteanu (2004) claims that thermal stresses are controlled more by stiffness than m-value, since a lower stiffness showed a lower thermal stress. When comparing the binders with similar stiffness values, Marasteanu found that a lower m-value resulted in lower thermal stress due to a slower accumulation of stresses. Regardless, stiffness and m-value may not be the best predictors of low-temperature cracking since strength needs consideration and m-value alone proves to be inaccurate in predicting the low-temperature PG grade.

Other studies point to the use of  $\Delta T_c$  as a better indicator of field performance. In previous work by Anderson et al. (Anderson et al., 2011a),  $\Delta T_c$  is defined as the difference between the critical temperature based on the stiffness and the critical temperature based on the m-value. As mentioned earlier, the more conservative value (higher temperature)

determines the binder's low temperature true grade.  $\Delta T_c$  is a measure of how close the stiffness and m-value parameters are to each other with respect to their influence over the low temperature true grade. The latest version of ASTM D7643 (2016) describes the process for selecting the low temperature true grade and defines  $\Delta T_c$ .

Anderson (2011a) looked further into  $\Delta T_c$  when he studied airfield pavements with the objective of predicting when preventative maintenance was needed to minimize the effects of non-load related cracking. Both transverse and block cracking occur due to environmental conditions (non-load related) such as low temperature and aging, respectively. In other words, block cracking occurs on pavements that are older, while transverse cracking happens when the temperature first drops during winter. Thus, binder was aged 20, 40, and 80 hours in the PAV to investigate the aging effects at low temperatures, not necessarily correlated to any particular service life (Anderson et al., 2011a). This work on cracking was also based on concepts developed by Glover. Glover (2005) related cracking behavior to ductility at low temperatures. He used the Maxwell element to better understand rheological properties of binders, in turn characterizing their in ductility. Glover found that ductility testing has low repeatability, so he developed a new parameter. The parameter  $G' / (\eta' / G')$  is inversely related to ductility in a log-log plot, quantifying the loss of flexibility.  $G'$  represents the storage modulus and  $\eta'$  the dynamic viscosity. As  $G' / (\eta' / G')$  increases, ductility decreases. In order to calculate  $G' / (\eta' / G')$ , the Dynamic Shear Rheometer (DSR) was run at 10 rad/s and 44.7 °C to simulate ductility at 15 °C and 1 cm/min. Glover determined a cracking warning of 3 kPa/s (5 cm for ductility) and a cracking limit of 0.9 kPa/s (3 cm for ductility). This concept will be revisited in the discussion on fatigue cracking.

Anderson used Glover's findings to further relate ductility and  $\Delta T_c$ . He found that as the stiffness decreases on a m-controlled binder, the low temperature true grade also decreases because the m-value and stiffness both contribute to the binder gaining relaxation. Binder oxidation over time exhibits the same trend but in the opposite direction, showing an increase in the low temperature grade as the binder ages. However, there is a faster loss of relaxation properties (m-value) relative to stiffness because m-value and stiffness are not linearly related. Therefore, the difference between  $T_c$  based on m-value and stiffness widens as the binder ages, producing a larger  $\Delta T_c$ . Anderson defines a cracking warning of 2.5°C and a cracking limit of 5°C. Using this knowledge of  $\Delta T_c$  and ductility, as  $\Delta T_c$  increases, ductility decreases. He verified this correlation using field and lab data, producing a consistent trend, though not linear. Therefore, according to Anderson, either  $G' / (\eta' / G')$  or  $\Delta T_c$  can be used to predict asphalt pavement cracking behavior (Anderson et al., 2011a).

### 1.3.2 Fatigue cracking

As of this writing, the parameter that is used to quantify a binder's resistance to fatigue cracking within the PG system is  $|G^*| \sin \delta$  measured at a frequency of 10 radians per second in or close to the linear viscoelastic range. The aforementioned parameter is typically measured using a Dynamic Shear Rheometer (DSR). The test procedure to measure this parameter uses binder aged in the Pressure Aging Vessel (PAV), which simulates long-term aging. This is because it is also believed that the critical stage for the pavement to experience fatigue cracking is later in its life (McGennis et al., 1994). Note that fatigue damage nucleation and growth is a continuous process and does not occur after the binder reaches a specific aging condition; the choice of using a long-term aged binder for evaluation is simply for practical convenience because it is not trivial to grade a binder for a specific pavement structure, location and aging trajectory.

Several studies have demonstrated that the  $|G^*| \sin \delta$  parameter is not effective to evaluate fatigue cracking resistance of asphalt binders. These studies have argued that the stress state used to measure this parameter is unrealistic as well as the effectiveness of this parameter as a measure of fatigue cracking resistance (Bahia et al., 1999; Masad et al., 2001). Other studies have shown a lack of correlation between this parameter and controlled field performance studies (Stuart and Mogawer, 2002; Tsai and Monismith, 2005).

In an attempt to address these limitations, several studies have attempted to develop a more effective method to evaluate the fatigue cracking resistance of asphalt binders. These studies have used different approaches to arrive at a parameter(s) that can most accurately reflect the fatigue cracking resistance of the asphalt binder. An examination of these studies reveals that the approaches used and proposed by different researchers can be classified into four broad categories, as classified in a review paper by Hajj and Bhasin (2018).

1. Use of cyclic loading to induce fatigue typically at a constant frequency and amplitude, or time sweep tests (this is also the most traditional definition of a fatigue test).
2. Employing a series of progressively increasing stress or strain amplitudes until failure, also referred to as amplitude sweep tests.
3. Measuring the ductility of the binder or a surrogate of ductility as an indicator of its resistance to cracking.
4. Measuring the strength or fatigue cracking resistance of the binder in a realistic stress state (e.g. using thin films).

The following sections will review the rationale, effectiveness, and limitations for each of the above approaches. The typical test methods associated with each of the above approaches, test results, and parameters extracted from these results are also briefly discussed.

### **Time sweep using DSR**

In a traditional time sweep test, a specimen is loaded sinusoidally at the same amplitude, frequency, and temperature over a large number of cycles. The specimen is repeatedly loaded until the material fails as by some criterion. This criterion is usually observed by a reduction in the modulus of the material, or observable damage to the specimen.

At the beginning of the 21st century, researchers began to apply the time sweep test to evaluate the fatigue cracking resistance of asphalt binders (Bahia et al., 2001a; Bonnetti et al., 2002) with focus on the fatigue life of modified asphalt binders, which were not originally considered by the Superpave grading criteria. The DSR's parallel plate geometry was the mechanism of choice for performing the time sweep test. Like the original Superpave criteria, this test was based on the dissipated energy concept, this time as a ratio of the energy dissipated in a given cycle over the total dissipated energy in the specimen (Bonnetti et al., 2002). In contrast with the Superpave method which uses the same loading conditions regardless of the project specifics, Bonnetti et al. (2002) recommended using a frequency and loading mode representative of the real traffic conditions that the binder was being used for.

However, the time sweep test was subjected to criticism due to issues with the specimen geometry. In one such study, Anderson et al. (2001) examined the fatigue behavior of binders when subjected to a time sweep using the Dynamic Shear Rheometer (DSR). Qualitatively, the modulus versus number of cycles data was typical for a fatigue test. However this behavior determined to be mostly related to the initial modulus of the material rather than actual damage in the material. In their study, Anderson et al. (2001) determined that the expected failure mechanism of the fatigue test through microdamage was only occurring at low temperatures. However, the fatigue cracking properties of an asphalt binder are typically tested at intermediate temperatures, at which the researchers found the dominating mechanism of failure to be instability flow. Besides the fact that low temperatures do not best simulate the actual conditions at which fatigue cracks nucleate, they are also difficult to use for testing in the DSR, due to machine compliance issues for very stiff specimens.

Anderson et al. (2001) also showed the inherent dependence of time sweep behavior on the specimen geometry. Specimen thickness has considerable effect on the failure mecha-

nism (fatigue damage vs. flow) and also showed an effect on the fatigue life of the binder. The issues of flow versus damage phenomenon and the influence of specimen thickness are very important with regard to characterizing binder fatigue and will be revisited later in this study.

Johnson et al. (2007) proposed using the failure criterion established by Tsai and Monismith (2005), 50% of reduction in binder complex modulus, to better understand the results of the time sweep test. While they continued to suggest that it was possible to determine the fatigue properties of a binder using DSR and the time sweep test, they also demonstrated possible issues with correlating binder fatigue to asphalt mixture fatigue. They also reported that the stress history of the binder had an effect on its fatigue life, and that healing should be taken into consideration when developing an effective test method.

The final criticism that has been proposed regarding the time sweep test is the length of time that it takes to perform the test. Agencies are often looking for a simple, robust method that can be performed quickly to determine binder properties. However, with regard to the time sweep, at the outset it is unknown how long it will take to actually cause the appropriate amount of damage to the specimen.

### **Amplitude sweep using DSR**

In order to overcome the limitations and shortcomings of the time sweep test, researchers went on to develop a modified test called the Linear Amplitude Sweep (LAS) (Johnson, 2010). Like the time sweep test, this method involved cyclic loading of the asphalt binder using a DSR with binder in the parallel plate geometry. However, this test was performed using an increasing amplitude after a predetermined number of load cycles. By consistently increasing the stress amplitude at predetermined intervals, this test theoretically creates the same type of damage as the time sweep test, but with less testing time required due to the accelerated damage of the high amplitude loading.

To interpret the results of this test, Wen and Bahia (2009) used Viscoelastic Continuum Damage (VECD) theory to analyze the fatigue behavior of binders in this geometry. A similar type of analysis had previously been used to evaluate fatigue damage in asphalt mixtures. The authors hypothesized that VECD analysis could provide a framework to unify the analysis of mixtures and binders in the same way. In summary, this approach uses the VECD theory to interpret the results from the amplitude sweep test and to determine the fatigue characteristics of the binder at a particular strain amplitude, which is determined by the type of strains that the binder would undergo in a pavement structure.

Further studies regarding this test revealed good correlation between fatigue performance of binders with fatigue performance of pavement sections from the Long Term Pavement Preservation (LTPP) database (Hintz et al., 2011). However, the researchers still had concerns about the effectiveness of this test for polymer-modified binders and discussed the importance of capturing the difference between material nonlinearity and fatigue damage (Hintz et al., 2011).

In summary, one can think of the amplitude sweep test as a series of short time sweeps at various increasing strain amplitudes. Therefore, it is very possible that the LAS test conducted using a parallel plate geometry with the DSR may also produce some of the concerns related to non uniform stress distribution and edge instability discussed earlier with regard to the time sweep test (Anderson et al., 2001). In other words, the question then is whether the failure in the DSR specimen is due to dispersed microcrack (damage) nucleation and growth of these microcracks or some other form of instability that begins at the edge of the specimen and grows inwards toward the center (Hajj and Bhasin, 2018).

### **Ductility and Works of Fracture**

The time and amplitude sweep tests used the same device (DSR) and test specimen (parallel plate geometry) as the standard Superpave test, but with an intent to improve upon the  $G^* \sin \delta$  parameter. This was achieved by both increasing the number of cycles that the test was performed on, and increasing strain amplitudes to determine the behavior of the binder beyond its linear viscoelastic range. In this sense, these tests can be considered as an evolution or improvement over the PG approach. The following section discusses other methods, some of which also utilize the same equipment and some that do not.

Previous field studies from the last 60 years (Doyle, 1958; Clark, 1958) have reported a correlation between asphalt binder ductility at low to intermediate temperatures and cracking observed in asphalt pavements. A detailed summary of these studies can be found in other literature (Ruan et al., 2003). In addition, recent studies have also shown a correlation between ductility of an asphalt binder and laboratory cracking resistance of asphalt mixtures using the binder (Elseifi et al., 2010). Several research studies have used the importance of ductility as the basis to develop methods to evaluate the fatigue cracking resistance of asphalt binders.

Andriescu et al. (2004) performed a double-edge-notched tensile (DENT) test to measure the works of fracture for asphalt binders. This test involves monotonic loading of a molded specimen until fracture, in a manner similar to the direct tension test (DTT). In

this test, however, small notches are created at different points on different specimens to consider the effect of ligament length. This test is also more commonly performed at intermediate temperature, instead of low temperature as the DTT test is performed. With this test, they saw little correlation with the Superpave  $G^* \sin \delta$  parameter, and suggested that their test, which measured nonlinear properties of the binder, was better capturing actual material failure.

Elseifi et al. (2010) also looked into studying the effects of ductility by applying a ductility test to dog bone specimens as specified in AASHTO T 51-06 (2007), which involves molding binder into a dog bone shape and applying tension to it at a constant deformation rate of 5 cm/min, in this case at 25°C. Dog bone shapes are used to avoid high stress concentrations at the boundary of the specimen. This test measures the ability of a binder to deform before fracturing. They also used the same specimen geometry to perform a Direct Tension Test (DTT) on asphalt binder specimens. Unexpectedly, they found an inverse relationship between the ductility of the binder at intermediate temperatures with its ductility at low temperatures. They were also able to correlate their ductility measurements with mixtures' stress and strain at failure in the Indirect Tensile Test, which is commonly used to evaluate a mixture's cracking resistance.

These ductility-related tests are desirable because ductility has been shown empirically to relate directly to premature cracking in the field. However, this approach faces the limitation of requiring a large volume of binder, which is not always feasible, such as in cases where recycled materials are used, or when PAV aging must be done which requires more time in the lab.

The above ductility studies all focused on actual ductility tests, but in the case of lacking the material to perform such tests, parameters which correlate empirically with binder ductility, as well as use the current equipment, are desirable. For example, Glover et al. (2005) suggested a new DSR parameter,  $G' / (\eta' / G')$ , which correlated strongly with dog bone ductility tests. This parameter can be calculated by conducting a traditional frequency sweep using the DSR, and then using the time-temperature superposition principle to formulate the material's master curve. They suggested that this parameter and a modified PAV aging procedure could be a good indicator of resistance to oxidation (and therefore a retained ductility with aging) for unmodified binders.

Rowe et al. (2014) later examined this parameter and rearranged the terms to form what is known as the Glover-Rowe parameter (equation 1.1).

$$D = \frac{G^*(\cos\delta)^2}{\sin\delta}\omega \quad (1.1)$$

Note that the dynamic viscosity,  $\eta'$ , is in fact defined as  $G''/\omega$ . Also, because  $G' = G^* \cos \delta$  and  $G'' = G^* \sin \delta$ , the parameter  $G''/(\eta'/G')$  can be reduced to the parameter shown in equation 1.1.

In Rowe's study, after constructing the master curve, the parameter at 15°C and a frequency of .005 rad/sec was calculated and used as the surrogate for binder ductility (Rowe et al., 2014). A higher value of this parameter indicates a more brittle (less ductile) binder. One study which looked at the ductility parameter versus field performance (Anderson et al., 2011a) proposed that damage begins at a parameter value of 180 kPa, and that when the parameter goes above 450 kPa, it corresponds to significant pavement cracking, which was also used by Rowe et al. (Rowe et al., 2014).

While ductility-based surrogates have shown to be effective for unmodified binders, they have also been subject to skepticism about their ability to predict ductility in polymer-modified binders. Glover et al. (2005) observed potential issues between their surrogate and ductility of polymer-modified asphalt. Tabatabaee et al. (2013) later suggested that there may in fact be issues regarding the correlation between the dog bone ductility test and actual fatigue cracking of polymer-modified binders.

It must be recognized that this parameter is a surrogate, and therefore is only related empirically, but not fundamentally, to binder ductility, and by proxy, fatigue cracking. The studies discussed above have shown a strong correlation between binder ductility and the rheological parameter for unmodified asphalt, but this has not been substantiated for modified asphalt.

### **Strength tests in a confined state**

The above methods have focused on measuring the properties of asphalt binders, both non-linear and linear, in a bulk state (for example, the 2 mm thick specimen in the DSR parallel plate geometry). However, those type of conditions present a binder stress state and response are significantly different compared to the actual stress state and material response of asphalt when it is confined in thin films between rigid aggregate particles in an asphalt mixture. Several studies have focused on the material behavior of thin films of binder in a confined state of stress. These studies are significant not only because they allow an insight into the material behavior in a confined state of stress, but also because they directly pro-



vide a measure of asphalt binder strength, which is key to understanding the load at which it will form an actual crack.

Marek and Herrin (1968) were possibly among the first to perform tensile tests on thin films of asphalt binder. They examined the effects of film thickness, loading rate, and binder source. Their work indicated cohesive failure at intermediate temperatures, as opposed to debonding of asphalt from aggregate. They also quantified the importance of film thickness on binder behavior.

Thin film testing was later used by Harvey and Cebon (2003), who used two realistic methods to perform tensile test on asphalt binders: a butt joint test and a double cantilever beam (DCB) test. Their results showed binders exhibiting either brittle or ductile failure depending on testing conditions and binder type. For thicker films of binder, they observed flow instabilities, while for the thinner films, the primary instability observed as voiding of the material.

Poulikakos and Partl (2011) later performed tensile tests on very thin films (less than  $20\mu m$ ) and measured the strength of the binder. At higher temperatures, they concluded that binders had lower strengths but exhibited more ductile behavior. They also used water conditioning to observe the effect of moisture, and found that moisture had more effect when mineral aggregates bonded the binder rather than steel plates.

Other researchers also looked at different aspect ratios (diameter to thickness ratio) to determine the effect of film thickness. Motamed et al. (2014) performed poker chip tests on asphalt binders using multiple specimen diameters and film thicknesses. The poker chip geometry consists of a thin film of asphalt binder with a very high aspect ratio confined between rigid plates and subjected to uniaxial tensile stress. This high aspect ratio helps to reduce edge effects and creates a similar stress state to the real one that asphalt binder experiences in a mix.

Sultana et al. (2014) also used the poker chip test to determine the behaviors of thin films of asphalt binder. Their findings indicated that most binders were within their linear viscoelastic range at low strains (less than 1%). They also observed cavitation based failure of specimens which hints at the failure mechanism of asphalt binder in its true stress state in a mix.

In another study, Sultana and Bhasin (2014) also related the tensile strength of asphalt binder to its chemical properties. Their findings included that a higher amount of the most polar fractions corresponded with a higher tensile strength. These fractions also correlated with smaller and more frequent cavitation instabilities. These findings demonstrate some

insight into the actual fundamental failure properties of asphalt materials.

The poker chip test is similar to the test performed using the Pneumatic Adhesion Tensile Testing Instrument (PATTI). A clear difference is that the PATTI test is normally used to study the adhesive properties of a binder in tension, while poker chip testing is a test of the actual material and its cohesive properties. However, it is theorized that a PATTI machine could be adopted to use for cohesive testing of asphalt binders at a single loading rate.

**Table 1.1. Summary of Binder Properties that Relate to Performance; tests marked with <sup>+</sup> are part of current PG specification and others are the subject of research as potential to be used as replacements in the near future.**

Performance	Property	Reference(s)
Construction	Viscosity <sup>+</sup>	AASHTO T316
Permanent Deformation	$G^*/\sin \delta$ <sup>+</sup>	AASHTO T315 and M320
	$J_{nr}$ and Elastic Recovery	AASHTO T350 and M332
Fatigue Cracking	$G^* \sin \delta$ <sup>+</sup>	AASHTO T315 and M320
	$ G^* (\omega \cos^2 \delta)/\sin \delta$	AASHTO T315, Rowe et al. 2014
	$G' / (\eta' / G')$	AASHTO T315, Glover et al. 2005
	LAS	AASHTO TP101
	BYET	Johnson et al. (2010)
	DENT at intermediate temperature	AASHTO TP113
Thermal and Fatigue Cracking	$\Delta T_c$	Rowe (2014)
Thermal Cracking	S & m <sup>+</sup>	AASHTO T313 and M320
	EBBR (Extended BBR)	Marks (2015)
	DT	AASHTO T314 and M320
	ABCD	AASHTO TP92
	SENB	Lee and Hesp (1994), Anderson et al. (2001), Tabatabaee et al. (2012)
	DENT (Low Temp.)	Andriescu and Hesp (2004), Zofka and Marasteanu (2007)

## REFERENCES for Chapter 1

- (2007). ASTM D113: Standard Test Method for Ductility of Bituminous Materials. In *ASTM D113-07*.
- (2016). ASTM D6373-16, Standard Specification for Performance Graded Asphalt Binder. Technical report, ASTM International, West Conshohocken, PA.
- (2017). AASHTO M320: Standard Specification for Performance Graded Asphalt Binder.
- Anderson, D. A., Hir, Y. M. L., Marasteanu, M. O., Planche, J.-p., Martin, D., and Gauthier, G. (2001). Evaluation of Fatigue Criteria for Asphalt Binders. *Transportation Research Record: Journal of the Transportation Research Board*, 1766:48–56.
- Anderson, M., Kriz, P., King, G., and Planche, J.-P. (2011a). Evaluation of the Relationship Between Asphalt Binder Properties and Non-load Related Cracking. *Journal of the Association of Asphalt Paving Technologists*, 80:615–664.
- Anderson, R., D’Angelo, J. A., and Bukowski, J. (2011b). Evaluation of the MSCR Test for Canadian Asphalt Binders. In *Proceedings of the Fifty-Sixth Annual Conference of the Canadian Technical Asphalt Association*.
- Andriescu, A., Hesp, S. A. M., and Youtcheff, J. S. (2004). Essential and Plastic Works of Ductile Fracture in Asphalt Binders. *Transportation Research Record: Journal of the Transportation Research Board*, 1875:1–8.
- Bahia, H., Hanson, D., Zeng, M., Zhai, H., Khatfi, M., and Anderson, R. (2001a). NCHRP 459: Characterization of Modified Asphalt Binders in Superpave Mix Design. Technical report.
- Bahia, H. U., Hanson, D. I., Zeng, M., Zhai, H., Khatri, M. A., and Anderson, R. M. (2001b). Characterization of modified asphalt binders in superpave mix design. Technical report, NCHRP Project 9-10.
- Bahia, H. U., Zhai, H., Bonnetti, K., and Kose, S. (1999). Non-Linear Viscoelastic and Fatigue Properties of Asphalt Binders. In *Association of Asphalt Paving Technologists*.

- Bonnetti, K. S., Nam, K., and Bahia, H. U. (2002). Measuring and Defining Fatigue Behavior of Asphalt Binders. *Transportation Research Record: Journal of the Transportation Research Board*, 1810:33–43.
- Clark, R. (1958). Practical results of asphalt hardening on pavement life. *Journal of the Association of Asphalt Paving Technologists*, 27:196–208.
- D'Angelo, J., Kluttz, R., Dongre, R. N., Stephens, K., and Zanzotto, L. (2007). Revision of the Superpave High Temperature Binder Specification: The Multiple Stress Creep Recovery Test. *Journal of the Association of Asphalt Paving Technologists*, 76:123–162.
- Doyle, P. (1958). Cracking characteristics of asphalt cement. *Proc of Assoc of Asphalt Paving Technologists*, 27:581–597.
- Dubois, E., Mehta, Y., and Nolan, A. (2014). Correlation between multiple stress creep recovery (MSCR) results and polymer modification of binder. *Construction and Building Materials*, 65:184–190.
- Elseifi, M. A., Asce, A. M., Mohammad, L. N., Glover, I., Negulescu, I., Daly, W. H., and Abadie, C. (2010). Relationship between Molecular Compositions and Rheological Properties of Neat Asphalt Binder at Low and Intermediate Temperatures. *Journal of Materials in Civil Engineering*, 22(December):1288–1294.
- Farrar, M. J., Sui, C., Salmans, S., and Qin, Q. (2015). Determining the Low-Temperature Rheological Properties of Asphalt Binder Using a Dynamic Shear Rheometer (DSR). Technical report, Western Research Institute, Laramie, WY.
- Glover, C. J., Davison, R. R., Domke, C. H., Ruan, Y., Juristyarini, P., Knorr, D. B., and Jung, S. H. (2005). Development of a New Method for Assessing Asphalt Binder Durability with Field Validation. Technical report, Texas Department of Transportation.
- Hajj, R. and Bhasin, A. (2018). The search for a measure of fatigue cracking in asphalt binders - A review of different approaches. *International Journal of Pavement Engineering*, 19(3):205–219.
- Hajj, R., Filonzi, A., Rahman, S., and Bhasin, A. (2019). Considerations for Using the 4 mm Plate Geometry in the Dynamic Shear Rheometer for Low Temperature Evaluation of Asphalt Binders. *Transportation Research Record: Journal of the Transportation Research Board*.

- Harvey, J. A. F. and Cebon, D. (2003). Failure mechanisms in viscoelastic films. *Journal of Materials Science*, 38(5):1021–1032.
- Hintz, C., Velasquez, R., Johnson, C., and Bahia, H. (2011). Modification and Validation of the Linear Amplitude Sweep Test for Binder Fatigue Specification. *Transportation Research Record: Journal of the Transportation Research Board*, 2207.
- Johnson, C. (2010). *Estimating Asphalt Binder Fatigue Resistance Using an Accelerated Test Method*. PhD thesis, University of Wisconsin- Madison.
- Johnson, C. M., Bahia, H., and Wen, H. (2007). Evaluation of Strain-Controlled Asphalt Binder Fatigue Testing in the Dynamic Shear Rheometer. In *4th International SIIV Congress*.
- Kennedy, T. W., Huber, G., Cominsky, R., Hughes, C., Von Quintus, H., and Moulthrop, J. (1994). Superior performing asphalt pavements (Superpave): The product of the SHRP asphalt research program. Technical report.
- Lu, X., Uhlback, P., and Soenen, H. (2017). Investigation of bitumen low temperature properties using a dynamic shear rheometer with 4 mm parallel plates. *International Journal of Pavement Research and Technology*, 10:15–22.
- Marasteanu, M. O., Li, X., Clyne, T. R., Voller, V., Timm, D. H., and Newcomb, D. (2004). Low Temperature Cracking of Asphalt Concrete Pavement. Technical report, Retrieved from the University of Minnesota Digital Conservancy.
- Marek, C. and Herrin, M. (1968). Tensile Behavior and Failure Characteristics of Asphalt Cements in Thin Films. In *Association of Asphalt Paving Technologists Proceedings*, pages 1–54.
- Masad, E., Somadevan, N., Bahia, H., and Kose, S. (2001). Modeling and Experimental Measurements of Strain Distribution in Asphalt Mixes. *Journal of Transportation Engineering*, 127(December):477–485.
- McGennis, R. B., Shuler, S., and Bahia, H. U. (1994). Background of Superpave Asphalt Binder Test Methods. Technical Report July, Federal Highway Administration, Office of Technology Applications.

- Motamed, A., Bhasin, A., and Liechti, K. M. (2014). Using the poker-chip test for determining the bulk modulus of asphalt binders. *Mechanics of Time-Dependent Materials*, pages 197–215.
- Oshone, M. T. (2018). *Performance Based Evaluation of Cracking in Asphalt Concrete Using Viscoelastic and Fracture Properties*. PhD thesis, University of New Hampshire.
- Poulikakos, L. D. and Partl, M. N. (2011). Micro Scale Tensile Behaviour of thin bitumen films. *Proceedings of the Society for Experimental Mechanics, Inc.*, 51(7):1171–1183.
- Rowe, G. M., King, G., and Anderson, M. (2014). The Influence of Binder Rheology on the Cracking of Asphalt Mixes in Airport and Highway Projects. *Journal of Testing and Evaluation*, 42(5).
- Ruan, Y., Davison, R. R., and Glover, C. J. (2003). An investigation of asphalt durability: Relationships between ductility and rheological properties for unmodified asphalts. *Petroleum Science and Technology*, 21(1 & 2):231–254.
- Stuart, K. and Mogawer, D. (2002). Validation of the Superpave Asphalt Binder Fatigue Cracking Parameter Using the FHWA's Accelerated Loading Facility. In *Asphalt Paving Technology*.
- Sui, C., Farrar, M., Harnsberger, P., Tuminello, W., and Turner, T. (2011). New Low-Temperature Performance-Grading Method. *Transportation Research Record: Journal of the Transportation Research Board*, 2207:43–48.
- Sui, C., Farrar, M. J., Tuminello, W. H., and Turner, T. F. (2010). New Technique for Measuring Low-Temperature Properties of Asphalt Binders with Small Amounts of Material. *Transportation Research Record: Journal of the Transportation Research Board*, (2179):23–28.
- Sultana, S. and Bhasin, A. (2014). Effect of chemical composition on rheology and mechanical properties of asphalt binder. *Construction and Building Materials*, 72:293–300.
- Sultana, S., Bhasin, A., and Liechti, K. M. (2014). Rate and confinement effects on the tensile strength of asphalt binder. *Construction and Building Materials*, 53:604–611.
- Tabatabaee, H. A., Clopotel, C., Arshadi, A., and Bahia, H. (2013). Critical Problems with Using the Asphalt Ductility Test as a Performance Index for Modified Binders. *Transportation Research Record: Journal of the Transportation Research Board*, 2370:84–91.

- Tsai, B.-W. and Monismith, C. (2005). Influence of Asphalt Binder Properties on the Fatigue Performance of Asphalt Concrete Pavements. *Journal of the Association of Asphalt Paving Technologists*, 74(January).
- Wen, H. and Bahia, H. (2009). Characterizing Fatigue of Asphalt Binders with Viscoelastic Continuum Damage Mechanics. *Transportation Research Record: Journal of the Transportation Research Board*, 2126:55–62.
- Yusoff, N. I. M., Jakarni, F. M., Nguyen, V. H., Hainin, M. R., and Airey, G. D. (2013). Modelling the rheological properties of bituminous binders using mathematical equations. *Construction and Building Materials*, 40:174–188.
- Zhou, F., Li, H., Chen, P., and Scullion, T. (2014). Laboratory evaluation of asphalt binder rutting, fracture, and adhesion tests. Technical report, No. FHWA/TX-14/0-6674-1. Texas. Dept. of Transportation. Research and Technology Implementation Office.



## **CHAPTER 2. MATERIAL SELECTION AND SAMPLING**

The goal of this portion of the study was to obtain or synthesize a wide assortment of binders for use in subsequent tasks. In addition, other materials such as additives and aggregates were also identified for use. Three types of binders were selected for evaluation:

1. Binders from cores of existing pavements with good and poor performance.
2. Binders from producers and artificial blends produced in the laboratory.
3. Binders from new construction sites.

### **2.1 BINDERS FROM CORES OF EXISTING PAVEMENTS WITH GOOD AND POOR PERFORMANCE**

The main advantage of using binders from existing pavements with good and poor performance is that the measured properties can be directly related to known field performance. The limitation of these binders is that the aging condition relative to the fresh binder and laboratory procedures (RTFO and PAV) cannot be accurately established. However, these limitations will be overcome using binders described in the two subsequent sections.

Field sections were identified with the help of TxDOT engineers that included premature failures that were believed to be binder-related. As these field cores were selected, they were noted as either “good” or “bad” performers in the field. Note that poor performing sections have been carefully selected in this case to reflect sections where the potential cause for failure is very likely to be the asphalt binder. The binder was extracted from these cores using a standard binder extraction process, and it was tested using a suite of binder tests (both related to PG system as well as beyond) described later in this report. Due to the small amount of binder that is obtained from these cores, binder testing, but not mixture testing was performed. However, mixture testing is not necessary, since the mixture performance is already evident based on field performance of the mix.

### **2.2 BINDERS FROM PRODUCERS AND ARTIFICIAL BLENDS PRODUCED IN THE LABORATORY**

One straight run base asphalt binder was obtained from a producer who supplies asphalt binders to the state of Texas. The base binder had a Performance Grade of PG 64-22. This binder was used for modification with various softening and stiffening agents to artificially change the PG of the binder. In the case of softening, the goal was to create binders with

a true grade of PG 64-28, and for stiffening, the goal was to create a set of binders with a true grade of PG 70-22. Later in this report, these names are just reported as "Additive X" with X being a numeral, to protect the identity of the materials.

The softening agents selected were:

1. Aromatic Oil
2. Biobinder
3. Vacuum Gas Oil
4. Microcrystalline Wax
5. Rejuvenator 1
6. Rejuvenator 2
7. Softening Agent 1
8. Recycled Engine Oil Bottom (REOB)
9. PG 52-34 Binder

The binders developed using these agents were each to be used in the binder tests performed later on in this study, and in the mixture tests as well. However, before the step in which these tests are performed, it is critical to determine the “optimal” content at which each of these additives should dose the binder in order to reduce the true low grade to -28, within one degree, or as far as the grade could be reduced without adding too much of the product. In order to obtain an estimate of the amount of additive required to dose the asphalt binder, two approximate values were found from the literature or obtained from the producer. These two points were then used as the initial “guess” for the first dosing attempt. Binder properties using these two concentrations were then measured and used to develop a linear relationship along with a third control point. This relationship provided a clearer insight into the influence of the binder properties as a function of the concentration of the additive. Table 2.1 shows the softening agents used and the starting points for their additions.

On the stiffening side, two stiffeners were used:

1. Polyphosphoric Acid (PPA)
2. Elastomer (SBS)

For specific portions of this study, other binders used in the state of Texas were sourced from producers for further testing as well. These binders included a wide assortment of PG grades.

**Table 2.1. Softening agents with starting points for modification**

<b>Softening Agent</b>	<b>Lower Dose</b>	<b>Higher Dose</b>
Aromatic Oil	2%	4%
Biobinder	1.5%	5%
Vacuum Gas Oil	3%	6%
Microcrystalline Wax	3%	6%
Rejuvenator 1	2%	4%
Rejuvenator 2	2%	3%
Softening Agent 1	2%	3%
REOB	3%	10%
PG 52-34 Binder	50%	60%

### **2.3 BINDERS FROM NEW CONSTRUCTION SITES**

Asphalt binders that were used in construction sites around the state of Texas were selected for evaluation in this study. Four of the selected sites used PG 64-22 binder and two used binder with a performance grade of PG 76-22. While there will not be any long term performance data on these pavement sections, the advantages of obtaining binder from fresh construction sites are twofold. First, the binder will be available in larger amounts compared to binder extracted from field cores, meaning a larger suite of tests can be run on the binder. Second, after laboratory testing of the binder, it will be possible to track the performance of the pavement section over its life and determine how the binder is performing in the field with relation to the laboratory parameters. RAP or RAS, as used was also sampled from the sites as well as loose mix, for a total of six construction sites.

### **2.4 AGGREGATES FOR LABORATORY MIXES**

Siliceous aggregates were sampled from a source that provides aggregate for construction in Texas. These aggregates were used to develop mixes for testing in the Hamburg Wheel Tracking Device and Overlay Tester to correlate mixture performance with the binder test results observed in the lab.

### **2.5 RECYCLED MATERIALS AND REJUVINATORS**

Recycled asphalt pavements (RAP) are being used more frequently today in construction in the state of Texas. To consider this effect within the scope of the project, of the new

construction mixes discussed above, RAP was sampled from all projects that used it. In addition, the two rejuvenators used above for softening were also be applied to measure the effect of adding rejuvenating agents within the PG specification.

## **CHAPTER 3. BINDER TESTING USING CURRENT AND NEW METHODS**

### **3.1 OVERVIEW OF CURRENT METHODS**

The current form of the Performance Grading (PG) system used in Texas is defined by the Texas Department of Transportation (TxDOT) in Item 300 of their standard specifications. This system, very similar to the Superpave PG system, assigns any given binder a grade consisting of two numbers, the first referred to as the high PG, and the second referred to as the low PG. The high and low PG are indicative of the highest and lowest pavement temperature in which the binder can be used without being susceptible to rutting and thermal cracking, respectively. It is important to emphasize that the selection of an appropriate binder grade for a pavement application in any given geographic area is necessary but not sufficient to avoid the aforementioned distresses. Factors such as binder content, aggregate gradation, and construction quality also influence the ultimate performance of the pavement. The PG system evaluates binders at three levels of aging which are intended to reflect the three stages of aging in the binder related to mixture production, immediately after construction and towards the end of the service life of the pavement. These three conditions are referred to as the “unaged binder”, short-term aged binder simulated using the Rolling Thin Film Oven (RTFO), and long-term aged binder simulated using the Pressure Aging Vessel (PAV).

#### **3.1.1 Aging**

The RTFO procedure is described in detail in AASHTO T 240. This procedure involves subjecting the unaged asphalt binder to aging (due to loss of volatile organics and oxidation) by exposing it to high temperatures (163°C) and constant air flow (4 liters/minute). The binder is placed in glass bottles with an open mouth that allows air to be blown into the bottle. The bottles rotate horizontally to create a thin film of asphalt to facilitate aging, with 35 grams of binder in each bottle. This test is run for 85 minutes.

The PAV procedure is applied to binders that have already been aged using the RTFO procedure. The binders are aged in thin films in metal pans with standardized dimensions using 50 grams of RTFO aged binder in each pan. Aging occurs in a pressurized chamber that is subjected to heat of 100°C and 2070 kPa of pressure. It should be noted that the

PAV method has recently faced scrutiny in the literature in terms of its effectiveness in simulating field aging for various types of asphalt binder. However, since it is currently used in the PG specification, this approach for long term aging was used in this study.

Two pieces of equipment are primarily used to determine the PG of an asphalt binder: the Dynamic Shear Rheometer (DSR) and the Bending Beam Rheometer (BBR). The current specification uses the DSR to characterize the linear viscoelastic properties of the binder at high and intermediate temperatures. The DSR test involves using a disk shaped sample of the binder placed between two rigid circular plates. A sinusoidal load is applied to the binder at a predetermined frequency and amplitude that keeps the binder in its linear viscoelastic range.

In this test, two parameters are measured, the complex shear modulus  $G^*$  and the phase angle  $\delta$ . The complex shear modulus describes the material's resistance to deformation when subjected to a sinusoidal loading with constant stress amplitude or strain amplitude. A higher value corresponds with a stiffer material. The phase angle describes the lag between the applied shear stress and the resulting shear strain. This parameter reflects the extent to which the binder behaves as an elastic solid versus a viscous fluid. A phase angle of  $0^\circ$  corresponds to a linear elastic solid material and a value of  $90^\circ$  corresponds to a viscous fluid. In terms of rutting resistance, the critical condition for the pavement to experience this distress is when the pavement is relatively new (less oxidation has taken place in the binder) and when the temperatures are high. The parameter used from the DSR to describe this is  $G^*/\sin(\delta)$ . A higher value of this parameter is desirable because it indicates a higher stiffness of the material and lower phase angle which also corresponds to lower viscous fluid like behavior.

This test is performed on a RTFO aged sample of the binder as well as an unaged sample of the binder. Although rutting resistance is relevant only after the binder has experienced short term aging (or RTFO aged binder), the use of unaged binder sample was introduced in the SHRP specifications as a check on the consistency of the binder. For these materials, a DSR plate of 25 mm diameter is used, with a specimen thickness of 1 mm. For unaged material, a minimum value for  $G^*/\sin(\delta)$  of 1.00 kPa at the high PG temperature is required. For the RTFO aged material, a minimum of 2.20 kPa at the high PG temperature is required.

At intermediate temperature, a similar philosophy is applied. For intermediate temperatures, the primary pavement distress of concern is fatigue cracking. Fatigue cracking is thought to be more prevalent in stiffer materials due to studies showing a correlation be-

tween ductilometer measurements and fatigue cracking in the mid-20th century. Note that this is currently a subject of scrutiny in the community, and will be discussed further later in this chapter. Fatigue cracks are also thought to occur late in the life of the pavement; therefore, the fatigue cracking resistance of binder is measured on PAV aged material. However, due to the hardware and capacity limitations of the DSR, the stiff, PAV aged material cannot be tested using the 25 mm diameter plates as this would require a very high level of torque to measure reasonable deformation in the material sample. Therefore, a smaller plate of diameter 8 mm and a specimen thickness of 2 mm is used while evaluating PAV aged samples. This decreases the required torque to shear the specimen and obtain target deformations.

As mentioned above, a softer specimen is considered to be preferable for fatigue cracking (as discussed later this is not entirely accurate because stiffness, strength and ductility of the binder need to be considered). The parameter that is evaluated is  $G^* \sin(\delta)$ , and minimizing this parameter is desired. The aforementioned parameter is an indicator of the dissipated energy in any given load cycle, which for an elastic material corresponds to damage accumulated in that load cycle. The rationale for minimizing this parameter or specifying a maximum value for this parameter was to ensure that the energy dissipated per load cycle was minimized to ensure adequate fatigue cracking resistance. The current PG specification requires a maximum value of 5000 kPa for the PAV aged material at the intermediate temperature. The intermediate temperature is defined in many states by Equation 3.1.

$$T_i = \frac{\text{High PG} + \text{Low PG}}{2} + 4 \quad (3.1)$$

However, TxDOT uses a slightly different variation of the intermediate temperature definition. In Texas, PG 64 is typical for construction of asphalt pavements due to climatic conditions, but PG 70 or 76 is often used when “grade bumping” is necessary. Grade bumping refers to artificially requiring a higher high PG than what would be required based on temperature considerations alone in order to offset higher than typical traffic volume and/or slower than typical traffic speed. Therefore, 64°C is still used in place of the high grade in this calculation (Equation 3.2), regardless of the actual high grade of the binder, when the high grade is greater than 64.

$$T_i = \frac{64 + \text{Low PG}}{2} + 4 \quad (3.2)$$

Thermal cracking, or temperature-related cracking, is the third major pavement distress that is covered by the PG system. Similar to fatigue cracking, binders are most susceptible to thermal cracking toward the end of their life. Therefore, thermal cracking resistance of asphalt binders is also typically evaluated using long-term or PAV aged binders. The Bending Beam Rheometer (BBR) is the specified equipment for low temperature PG testing of asphalt binders. Recently, the DSR has been investigated as a tool for evaluating the performance of asphalt binders at low temperatures as well, which is further discussed in this report in a later section.

The purpose of the BBR is to perform a creep test to measure the stiffness and stress relaxation properties of asphalt binders. The test is a three point bending test performed on a beam made of asphalt binder. The beam is usually a rectangular prism with a width of 12.5 mm and a thickness of 6.25 mm. The beam is 127 mm long, but the supports are placed 102 mm apart for the purpose of the test. Beams are conditioned and tested in a fluid bath filled with fluid that has a low freezing point, since the test is performed at low temperatures. In the case of this study, methanol was used since it does not dissolve asphalt binder.

A 0.98 N (plus or minus 0.05 N) load is applied to the beam at its midpoint between the two supports, and is held for 240 seconds. During this period, the beam deflection is measured as a function of loading time, as a creep test. Creep Stiffness is calculated based on Equation 3.3. It should be noted that this definition of stiffness is not the true relaxation modulus of the material, but rather the inverse of creep compliance, since the test being performed is in fact a creep test and not a relaxation test. The second parameter that is measured is called the m-value, which denotes the absolute value of the slope of the Stiffness versus time curve at a given time. This parameter reflects the ability of the binder to relax. A higher m-value indicates that the binder is able to relax more quickly and relieve thermal stresses produced within it when the temperature changes.

$$S(t) = \frac{PL^3}{48I\delta(t)} \quad (3.3)$$

where:

P = applied load

L = distance between supports

I = cross-sectional moment of inertia

$\delta(t)$  = deflection



The current specification states that a binder should have a maximum Stiffness value of 300 MPa at a time of 60 seconds at the low PG temperature plus 10°C. Previously, the actual PG temperature was used for testing and a time of 7200 seconds was found to be the best time to use for PG grading, but in order to reduce testing time and the time for the bath to reach the test temperature, the current specification was adopted. As described earlier, a higher m-value is desirable to ensure that the binder relieves stresses and does not become susceptible to cracking. Therefore, a minimum m-value of 0.3 is required at a time of 60 seconds at the low PG temperature plus 10°C. Both of these requirements are required to be met in order to assign a binder a low temperature grade. In the end, it is either value of S or m that gives the grade assignment, which can term a binder as either S-controlled or m-controlled depending on which value is responsible for grade assignment.

### **3.2 OVERVIEW OF NEW METHODS**

The current binder specification has largely represented an improvement upon the previously utilized penetration and viscosity-based specifications. However, in the nearly 25 years since the completion of the SHRP project, the formulations of asphalt binders used in paving applications have changed considerably. Much of these changes can be attributed to increased global demand for fuels and other petroleum-based products, which has led to the development of refining techniques that allow the extraction of increased amounts of higher value light products with lower sulfur contents from crude oil.

Crude oil sources are now more varied than when the performance grading (PG) purchase specification was developed. Today, unlike the late 1980s and early 1990s, polymers, polyphosphoric acid, re-refined engine oil bottoms (REOB), paraffinic base oils, rendered oils, bio binders, and ground tire rubber are just some of the materials that are increasingly being used to formulate and manufacture asphalt binders. In addition to these modifiers, the asphalt paving industry is also interested in the increased use of higher percentages of reclaimed asphalt pavement (RAP) and reclaimed asphalt shingles (RAS). This desire to reduce the negative impact on environment and promote the use of sustainable paving materials has driven the use of softer asphalt binder grades, which are often produced by adding various products to stiff binders.

Today's asphalt binders continue to meet the requirements of the PG specification, but highway agencies in the United States and Canada are increasingly experiencing premature failures of newly constructed pavements. These failures occur despite general compliance with existing pavement and mix design standards, construction methods, and materials

specifications. Unlike in the pre-SHRP period, many of these failures are typified by low- and intermediate-temperature cracking and raveling, aggregate loss, and instances of total surface course loss within five years. Concern is often expressed over embrittlement and a lack of adhesion and tackiness of the asphalt binders.

Based upon changes in asphalt binder formulation and manufacture, current asphalt binder specifications, tests, and practices merit a comprehensive review to assure their effective contribution to satisfactory pavement performance. Modifications and enhancements to the AASHTO M320 specification have occurred over the years to address changes in formulation and performance, particularly with respect to the proliferation of polymer modified asphalt binders. Many of these efforts have been led by individual states or regions resulting in the existence of a number of surrogate test measures (elastic recovery, toughness and tenacity, etc.). National efforts to improve the grading system have largely focused on higher strain level, nonlinear behaviors of the binder. NCHRP 9-10 introduced the concept of the Multiple Stress Creep and Recovery test, which has since been refined through follow-up efforts by FHWA and others. With respect to fatigue the Asphalt Research Consortium developed the Linear Amplitude Sweep test and NCHRP 9-59 is evaluating the relationship between binder fatigue properties and asphalt mixture fatigue performance in order to propose a test that better relates to fatigue performance. NCHRP 9-23 proposed modifications to the long-term asphalt aging temperatures for asphalt binders and it may be likely that NCHRP 9-52 and 9-54 will lead to new insights and modifications to laboratory aging of asphalt mixtures, which may itself modify how asphalt binders should be aged. In short, the Superpave binder specification is continually evolving from a system based on the measurement of small strain rheological properties towards one that is based on large deformation and failure properties of the binder.

A performance specification for asphalt binders is a critical component of the material selection and mixture design process because (i) it serves as a screening tool to select a binder that is not inherently susceptible to distresses under a given environmental and loading condition, and (ii) it serves as a purchase specification and quality control tool for state agencies to ensure the quality of the binder and for binder producers to meet certain requirements. These two aspects of a binder specification must be borne in mind while evaluating existing or developing new specification type test methods and criteria for asphalt binders. The following are some of the tests and parameters evaluated in this study that can potentially be used to improve the current asphalt binder specification.

### 3.2.1 New methods for high temperature testing

#### 3.2.1.1 Multiple Stress Creep and Recovery (MSCR) test

The Multiple Stress Creep and Recovery (MSCR) test method is probably the first method that was developed to replace the existing Superpave high temperature PG specification. Chapter 1 of this report describes in detail the development of the MSCR test. A brief overview of the test in the context that it was used in this study is provided below.

Due to the new studies that have been done on MSCR, a new standard, AASHTO MP19 was proposed to replace the current AASHTO M320. In summary, per AASHTO MP19, the high temperature grade is based on the lower of the two temperatures that meet a  $G^*/\sin(\delta)$  criterion ( $> 1.0$  kPa) in unaged condition and a non-recoverable compliance,  $J_{nr}$ , criterion ( $< 4.0, 2.0, 1.0,$  or  $0.5$   $kPa^{-1}$  depending on a sub-grade of "S", "H", "V" or "E") in RTFO aged condition. This is different from the AASHTO M320 wherein the high temperature grade is based on the lower of the two temperatures that meet a  $G^*/\sin(\delta)$  criterion ( $> 1.0$  kPa) at unaged condition and another  $G^*/\sin(\delta)$  criterion ( $> 2.2$  kPa) in the RTFO aged condition. More recently, MP19 has been superseded by M332; the latter uses a cut-off value of  $4.5$   $kPa^{-1}$  for the "S" sub-grade.

A notable feature of the AASHTO MP19 specification is that it does not allow the use of grade bump to specify asphalt binders for locations with higher traffic volume and/or slower traffic speeds. Instead, a sub-grade (S, H, V, or E) at the specific pavement temperature is utilized to accommodate for these factors. Also, the use of the MSCR test protocol also allows the user to determine stress sensitivity and elastic recovery of the asphalt binder. Stress sensitivity is defined as the difference in  $J_{nr}$  measured at  $0.1$  kPa and  $3.2$  kPa compared to the  $J_{nr}$  measured at  $0.1$  kPa. Elastic recovery, or more correctly time-dependent recovery, can be considered as a complimentary measure to the non-recoverable compliance. For any given cycle, it is defined as the percentage of total strain that is recovered at the end of the recovery period. The percentage of elastic recovery is also a surrogate indicator for binders modified using elastomers. In the present study, both  $J_{nr}$  and the percent elastic recovery are evaluated as potential indicators of rutting resistance.

## 3.2.2 New methods for intermediate temperature testing

### 3.2.2.1 Rheological indices related to brittleness and durability

Researchers have demonstrated that several rheological indices can be derived to serve as surrogate indicators of brittleness that can also be measured using the DSR. These parameters have been primarily proposed for thermally induced cracking and surface raveling but have also shown promise for identifying asphalt binders susceptible to fatigue cracking as a result of oxidation induced embrittlement. Glover et al. (2005) proposed the rheological parameter,  $G' / (\eta' / G')$ , as an indicator of ductility based on a derivation of a mechanical analog to represent the ductility test consisting of springs and dashpots. They have also demonstrated that this parameter is directly correlated to measured ductility for unmodified binders. However, it is also important to emphasize that this correlation was not strong when including both modified and unmodified binders. The Glover parameter can be calculated based on DSR frequency sweep testing results, making it much more practical than directly measuring ductility using traditional methods. Rowe (2011) re-defined the Glover parameter in terms of  $|G^*|$  and  $\delta$  based on analysis of a black space diagram as shown in Equation 3.4 and suggested use of the new parameter on the right hand side, termed the Glover-Rowe (G-R) parameter, in place of the original Glover parameter.

$$\frac{G'}{\eta'/G'} = \frac{|G^*|(\cos(\delta))^2}{\sin(\delta)} \quad (3.4)$$

where:

$G'$  = storage modulus

$\eta'$  = viscosity

$|G^*|$  = complex shear modulus

$\delta$  = phase angle

Rowe proposed measuring the G-R parameter based on construction of a master curve from frequency sweep testing at 5°C, 15°C, and 25°C in the DSR and interpolating to find the value of G-R at 15°C and 0.005 rad/sec to assess binder brittleness (Rowe et al. 2013). A higher G-R value indicates increased brittleness. It has been proposed that a G-R parameter value of 180 kPa corresponds to damage onset whereas a G-R value exceeding 450 kPa corresponds to significant cracking based on a study relating binder ductility to field block cracking and surface raveling by Anderson et al. (2011).

Additional rheological indices have been proposed as indicators of aging susceptibil-

ity. The rheological index, R, has been proposed to assess oxidation sensitivity as related cracking resistance of binder based on the rheological model proposed for asphalt binders during the SHRP program (Christensen and Anderson 1992). The R value is the distance between the  $|G^*|$  master curve and glassy modulus ( $|G^*|_g$ ) at the frequency where  $\delta$  equals  $45^\circ$ , termed the cross-over frequency ( $\omega_c$ ). The cross over frequency corresponds to the frequency where loss and storage moduli are equal. The R value is related to the relaxation spectra and chemical composition of the binder. R values increase with oxidation and thus, high R values are anticipated to indicate increased cracking susceptibility. Harder, more brittle asphalts generally have lower cross over frequencies. In recent work, Farrar et al. (2012) proposed the  $|G^*|$  value at the cross over frequency, termed cross over modulus,  $|G^*|_c$ , as a rheological index to track oxidation. If the asphalt binder is thermorheologically simple, then the crossover modulus is independent of temperature. In addition, it has been demonstrated that the cross over modulus is correlated to oxygen uptake in binders and hence, can be used in place of FTIR or other chemical analyses to assess oxidation.

It is proposed that the aforementioned rheological indices be considered as simple indices related to cracking susceptibility. In addition, the relative change in rheological indices between the RTFO and PAV aging conditions can be assessed as a means to identify oxidation susceptible materials prone to cracking. Note that all parameters can be obtained through temperature-frequency sweep testing and generation of master curves.

### **3.2.2.2 Linear Amplitude Sweep (LAS)**

The time sweep test was developed in NCHRP 9-10 (Bahia et al. 2001) in an attempt to overcome the limitations of the current specification. The time sweep test consists of applying repeated cyclic loading at fixed amplitude to an 8 mm diameter asphalt binder specimen in the DSR. Changes in loading resistance with respect to number of loading cycles are used to evaluate damage resistance and determine fatigue failure. It has been demonstrated that results of binder time sweep testing are correlated with mixture beam fatigue results (Bahia et al. 2001) and direct tension testing (Hintz 2012). However, the time sweep has been deemed impractical for specification due to the need to select an appropriate loading amplitude for testing to produce failure in a reasonable amount of time, which requires knowledge of the material's damage resistance a priori.

The Linear Amplitude Sweep (LAS) test (AASHTO TP 101) has been proposed as a surrogate to the time sweep as a practical specification test (Johnson 2010, Hintz et al. 2011, Hintz and Bahia 2013b). The LAS test is similar to the time sweep in that it con-

sists of cyclic loading in the DSR and utilizes the same specimen geometry. However, in the LAS test loading amplitudes are systematically increased to accelerate damage. The LAS test also includes a frequency sweep to obtain a fingerprint of the material's undamaged material response, which can be run directly before the amplitude sweep, on the same specimen. Total testing time, including thermal equilibration, is approximately 30 minutes. Simplified Viscoelastic Continuum Damage (S-VECD) theory can be applied to LAS (or time sweep) results to allow for estimating fatigue life at any strain amplitude of interest. Recently, the analysis protocol has been enhanced to include a failure criterion to improve predictability (Wang et al. 2014). The new protocol includes an improved method for defining fatigue failure in the LAS test based on energy principles, which is material-dependent and is effective in capturing the benefits of asphalt modification for binder fatigue resistance. In addition, a failure criterion has been developed which can predict when the fatigue failure will occur under loading conditions other than those used in model characterization testing. Fatigue life predictions using this newly developed failure criterion coupled with the S-VECD model are able to predict measured time sweep fatigue lives reasonably well. In addition, fatigue life predictions generally related well with the field fatigue performance measured in the FHWA-ALF study (Wang et al. 2014), as well as LTPP field performance (Hintz et al. 2011). It has also been demonstrated that when a strain ratio from mix to binder of 80 is used, fatigue life predictions from LAS results are consistent with mixture fatigue life predictions (Safaei et al. 2014).

### **3.2.2.3 Monotonic testing in a realistic state of stress**

As previously discussed in Chapter 1, the poker chip test has been proposed as an indicator of the true strength and fracture properties of an asphalt binder in the state of stress similar to what it actually experiences in a mix. Previous work (Hajj et al. 2017) indicates that this test can identify large differences in binder strength for binders assigned similar PG grades. This method differs from the other methods evaluated in this study because it does not make use of the existing equipment used in the Superpave binder grading methods. However, this method was included for two primary reasons: first, to evaluate if binder tests in a confined stress state that actually test the material through nonlinear behavior and into fracture better predict mixture behavior in a similar stress state; second, because as mentioned before, there are equipment, such as the PATTI device, which could perform a similar test on asphalt binders, as well as a growing market of rheometers that can be used for Dynamic Mechanical Analysis (DMA) in tension-compression.

### **3.2.3 New methods for low temperature testing**

#### **3.2.3.1 Measures of binder cracking resistance using the BBR and other equipment**

The tests reviewed here are focused on low-temperature cracking resistance of the asphalt binder. However, recent studies have demonstrated that the  $\Delta T_c$ , which is the difference in the critical low temperature based on the stiffness (S) criterion and the critical low temperature based on the m-value criterion is also correlated with intermediate temperature fatigue cracking resistance (e.g. as measured using the overlay tester). Therefore, it is important to evaluate and consider the low-temperature properties of the asphalt binder.

The current AASHTO M320 asphalt specification is primarily based on the use of the Bending Beam Rheometer (BBR). The BBR is an excellent tool to measure the low temperature stiffness (S) and rate of relaxation (m-value) of the asphalt binder. In rare cases when the stiffness value fails to meet these requirements, the specification allows for a strength test (DT or direct tension test) (McGennis et al. 1994). Higher stiffness or lower m-value are indicators of higher thermal stresses. However, failure only occurs when the thermal stresses (in combination with external load related stresses), exceed the tensile strength of the material. The BBR does not provide a measure for the strength of the material and unfortunately despite substantial development work during SHRP, the DT test has not gained widespread usage due to difficulties in testing.

Other researchers have tried to overcome the limitations of the BBR and develop a simple and easy to use method for testing low temperature cracking resistance of asphalt binders. The common feature in these newer tests is that they involve testing the asphalt binder at its failure condition, e.g., measurement of binder fracture properties. Kim et al. (2014) developed the Asphalt Binder Cracking Device (ABCD) for low temperature characterization. The test method is described in AASHTO TP92 and involves casting a sample of asphalt inside an instrumented ring before cooling the sample induce thermal contraction. This contraction continues until the critical thermal strain at which point the sample fractures, and the critical temperature is recorded. While the test has shown good correlations to field performance, one noted drawback is the overall testing time.

Hesp and co-workers developed a double edged notch test (DENT) test to evaluate the low-temperature cracking resistance of asphalt binders (Kodrat et al. 2007). The DENT test can be conducted using simple fixtures on any device capable of applying displacement rates from 3 to 50 mm/minute and measuring displacement within an accuracy of plus or minus 0.05 mm and load up to 500 N. While results from the DENT test correlate well

with the field performance, it would still require specialized capital equipment. Behnia et al. have developed the use of an acoustic based method to evaluate the low-temperature cracking resistance of asphalt mixtures (Behnia and Dave 2011). However, they have also concluded that this method must be used in conjunction with mechanical tests to evaluate the low-temperature cracking resistance of asphalt mixtures. Tabatabaee et al. (2012) describe a single edge notched beam (SENB) test using the BBR equipment, but with asphalt binder samples cast to have a mid-span notch. The test results are shown to correlate better to LTPP data than other methods. More recently, Bhasin et al. (2015) have used a variation of the BBR device, the BBR-Pro, to obtain the rheological properties of the binder as well as its tensile strength. The test specimens and procedure for the BBR-Pro are very similar to the method used with the conventional BBR. The test is conducted by applying a constant or monotonically increasing rate of loading to the binder beam specimen at any given temperature until the beam specimen fails.

Due to the emphasis in this study placed on developing a specification that utilizes the current PG equipment (DSR and BBR) and does not involve long testing or aging times, the  $\Delta T_c$  parameter was investigated extensively in this study.

### **3.3 MATERIALS AND LABORATORY BINDER MODIFICATION**

The three types of binders that were used in this study were covered in a previous chapter. These binder types included new binders from new constructions as well as directly from producers, binders extracted from field cores, and finally, the binders described below in Set 1 and 2, which are laboratory-produced binders developed using commercial modifiers. The new binders from producers were largely used to evaluate low temperature properties of binders, which is described later in this chapter, due to their wide range of high and low temperature grades.

#### **3.3.1 Binder set 1**

The modification process has been discussed in a previous chapter of this report. For low temperature additives, a PG 64-22 base binder was selected. The additives described earlier in this report were each added to the neat asphalt binder in various concentrations, at least two of which were determined based on existing literature or producer recommendations. An “optimum” concentration for each additive was determined to achieve a low PG grade that was 6 degrees lower than the original grade of the control binder B1. Most laboratory



**Table 3.1. Binder with additive concentrations used to produce modified binders for this study**

<b>Binder</b>	<b>Concentration</b>
Control (B1)	N/A
B1+A1	4.5%
B1+A2	6.6%
B1+A3	6.3%
B1+A4	2.1%
B1+A5	2.0%
B1+A6	4.6%
B1+A7	10.0%
B1+B2	44.5%

binders were within 1 degree of this target after modification. Table 3.1 shows a list of the additives used and the concentration for each additive. In addition to the seven final additives selected to change the low temperature properties, one low grade (PG 52-34) binder (B2) was also selected to blend with B1. Finally, three of the binders that were selected from recent construction projects (B3, B4, B5) were evaluated in this part of the study in order to run a full suite of tests on them. It is therefore possible to track these construction projects in the future in order to compare binder performance measured in the lab with the proposed new test methods to the performance of these mixes in the field.

The procedure used for blending and estimating the optimum additive concentration is briefly summarized below. Each additive was mixed with the base binder for two hours in a high shear mixer. The unaged and RTFO aged DSR properties were then measured for binder at each concentration, so that the optimum concentration could be determined. Figures 3.1 - 3.7 show the high PG grades for all binders at many different concentrations based on unaged and RTFO DSR grading. It is notable that, in general, all low temperature additives caused a reduction in high temperature continuous grade as well. In most cases, the effect of aging based on unaged and RTFO aging was similar, with the exception of A1, which caused much more change in the RTFO aged binder. Figure 3.8 provides a summary of the high grades of the binders in this set.

The low temperature continuous grades of each modified binder were also evaluated using the conventional BBR method. All binders were graded based on Stiffness and m-value, and at at least three concentrations for each of the modified binders. Figures 3.9 - 3.15 show the low PG grades for all binders at many different concentrations based on

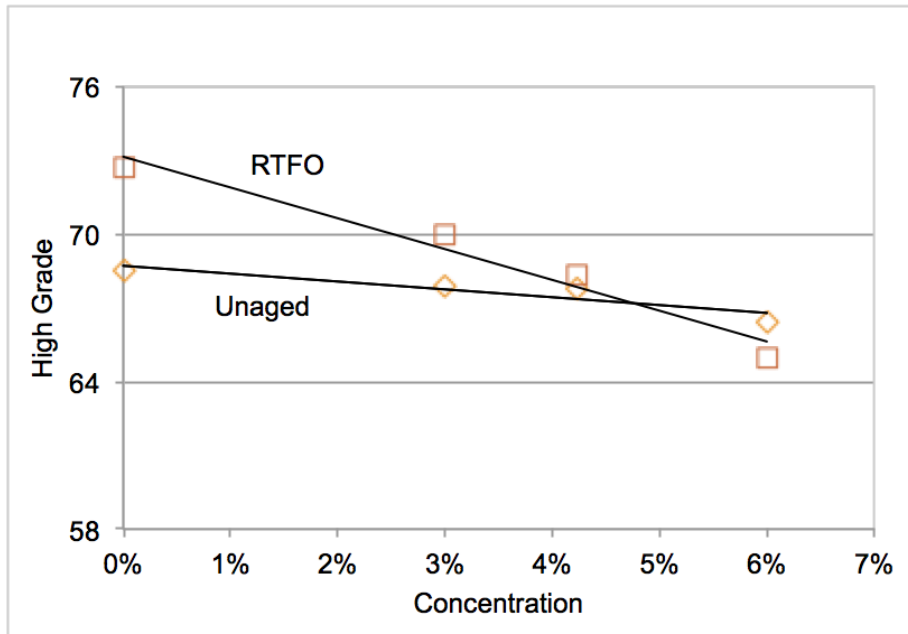


**Figure 3.1. High temperature continuous grades at different doses of additive A1**

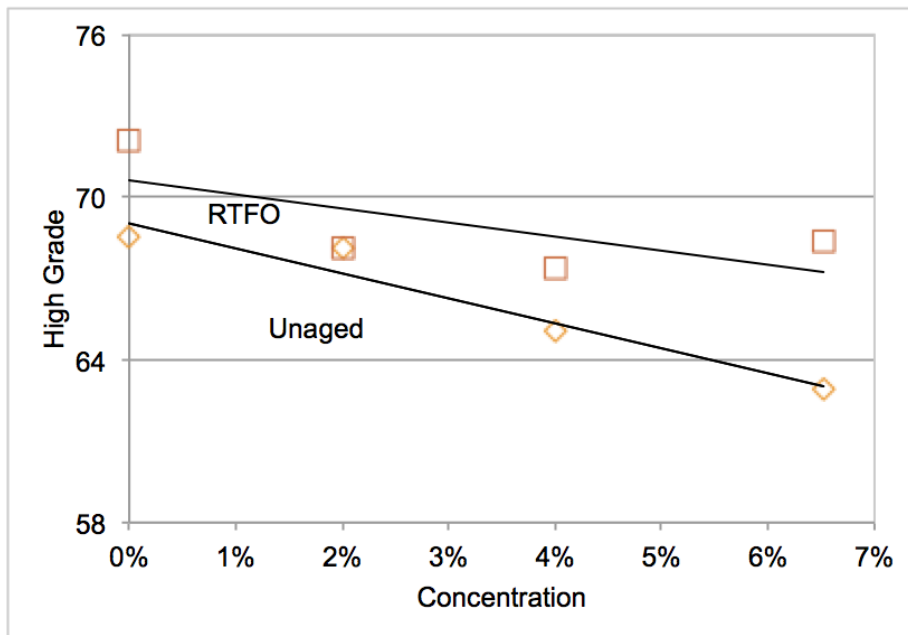


**Figure 3.2. High temperature continuous grades at different doses of additive A2**

Stiffness and m-value grading. Note that none of the modified binders were stiffness controlled (all were m-value controlled), so the higher line always represents the m-value true

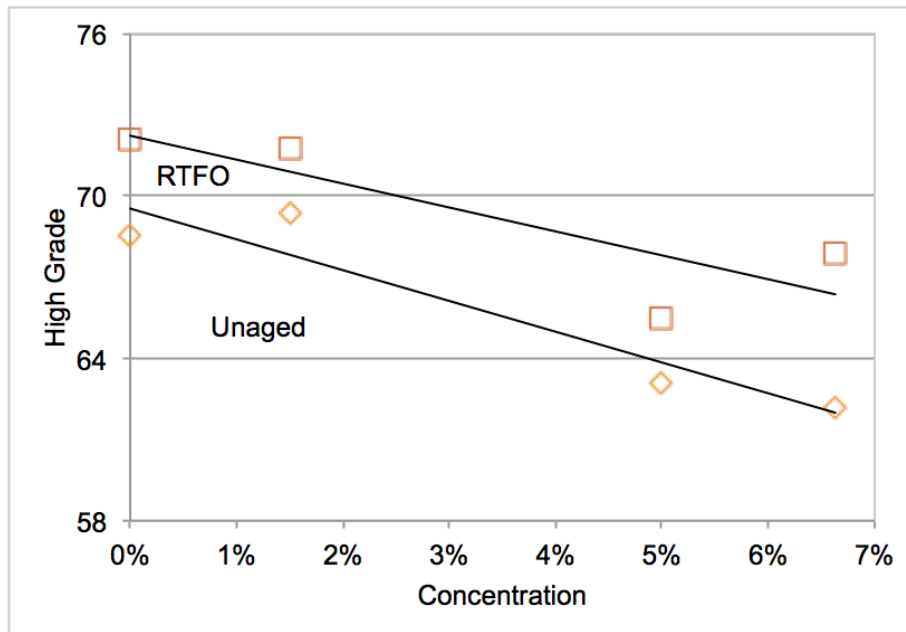


**Figure 3.3. High temperature continuous grades at different doses of additive A3**

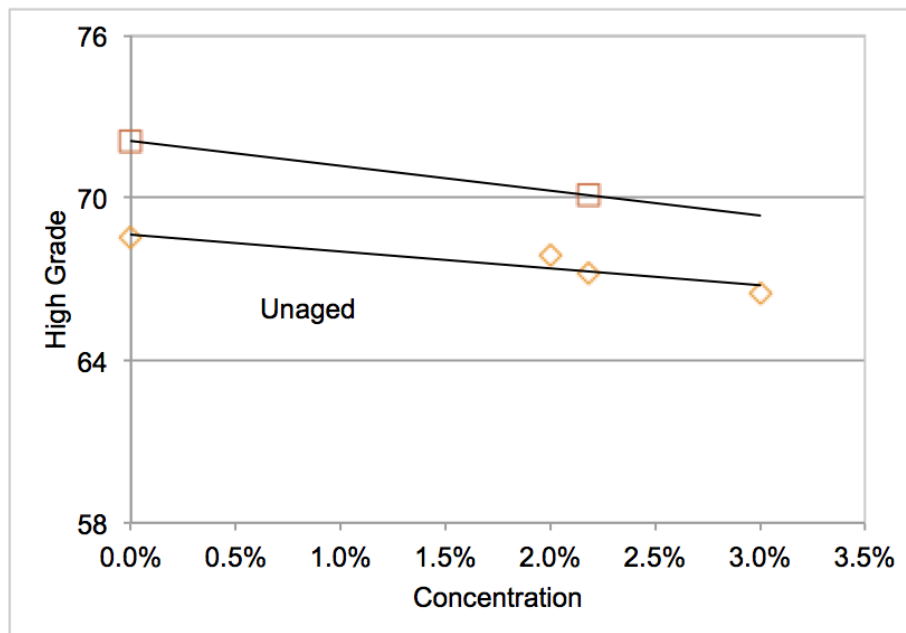


**Figure 3.4. High temperature continuous grades at different doses of additive A4**

grade. It is also notable that the vertical distance between the two lines represents the value of  $\Delta T_c$ , as it is the difference between the Stiffness and m-value true grades, so it is possible

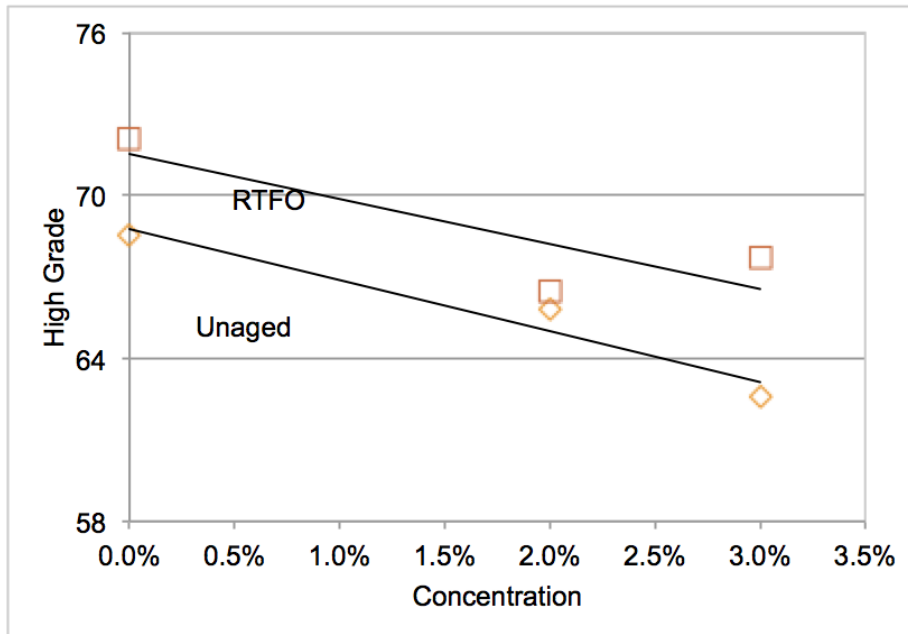


**Figure 3.5. High temperature continuous grades at different doses of additive A5**

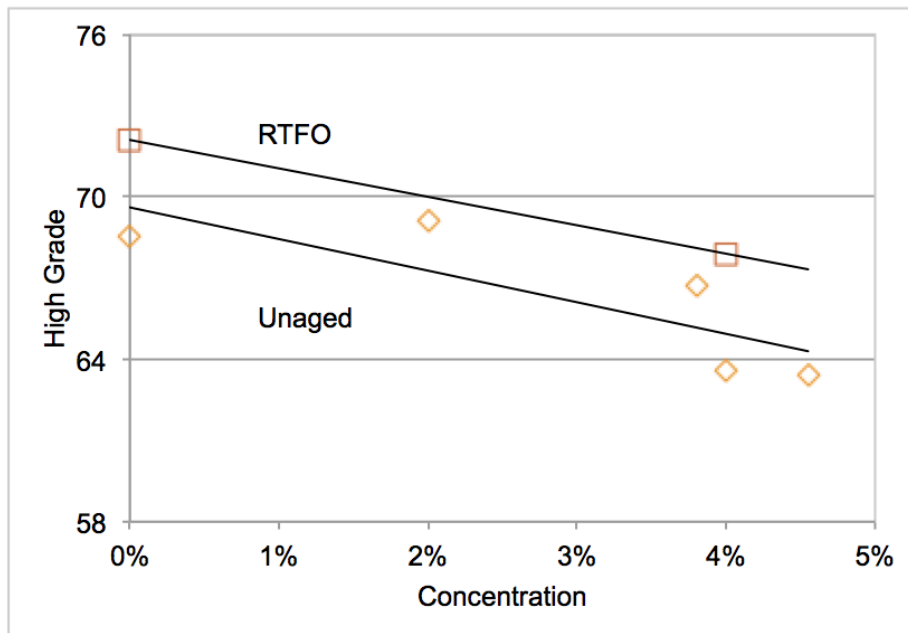


**Figure 3.6. High temperature continuous grades at different doses of additive A6**

from these plots to see the evolution of  $\Delta T_c$  with various modifications.

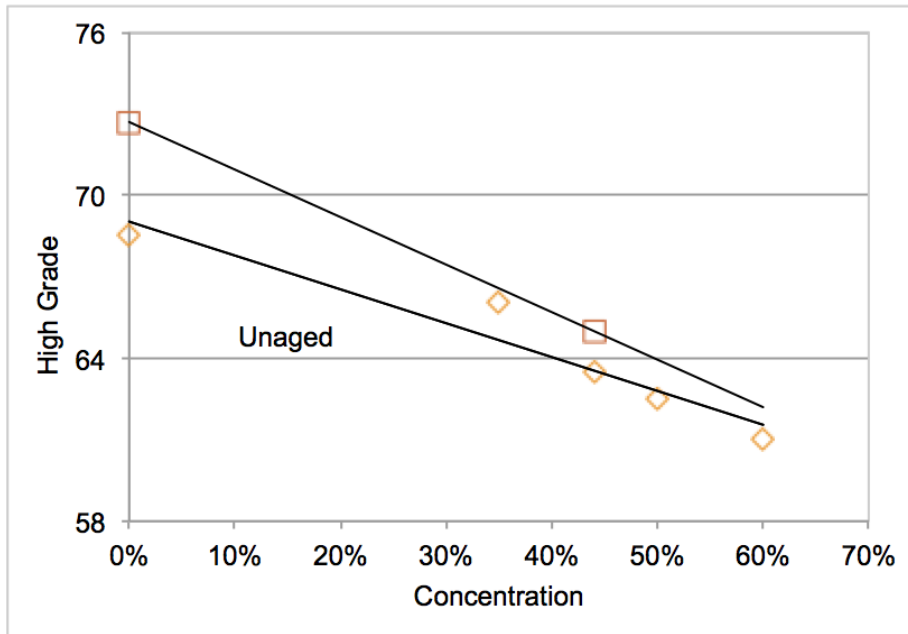


**Figure 3.7. High temperature continuous grades at different doses of blending with binder B2**

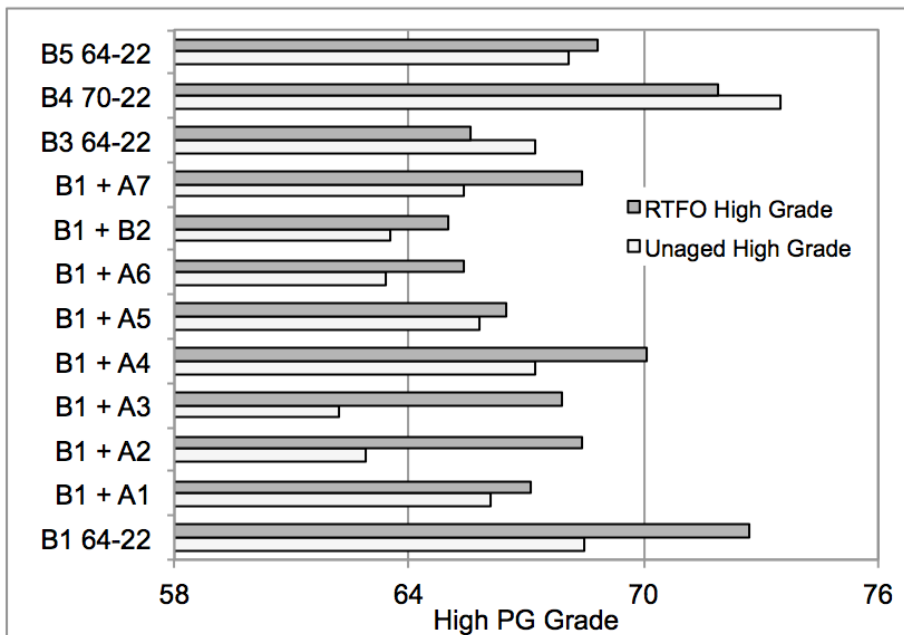


**Figure 3.8. Summary of high grades of binders in Set 1**

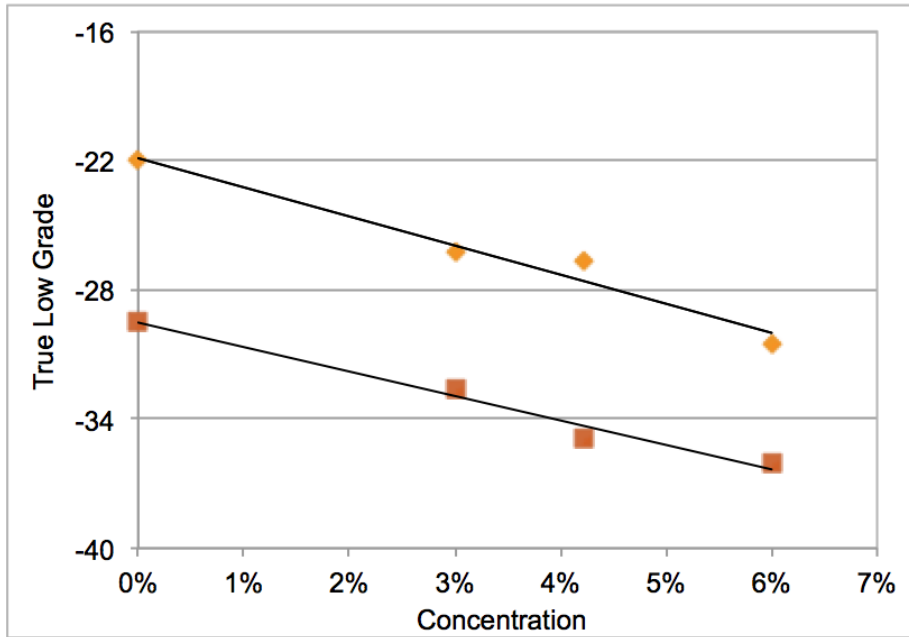


**Figure 3.9. Low temperature continuous grades at different doses of additive A1**

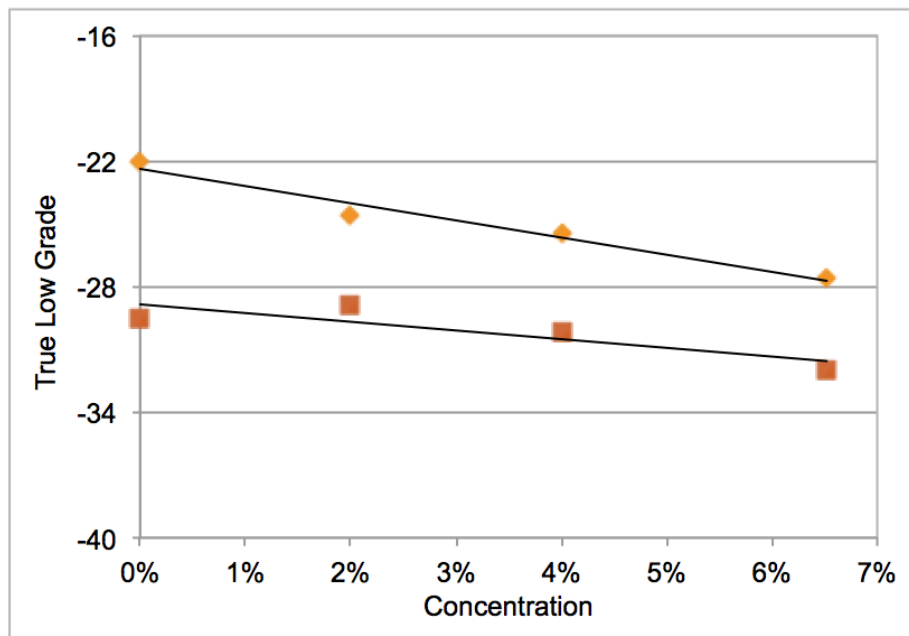


**Figure 3.10. Low temperature continuous grades at different doses of additive A2**

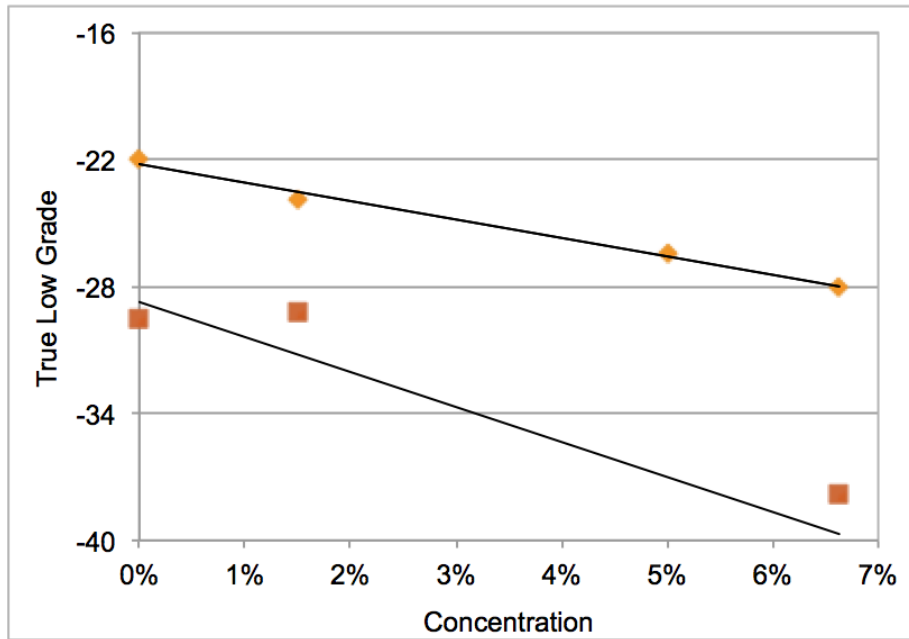


Figure 3.11. Low temperature continuous grades at different doses of additive A3

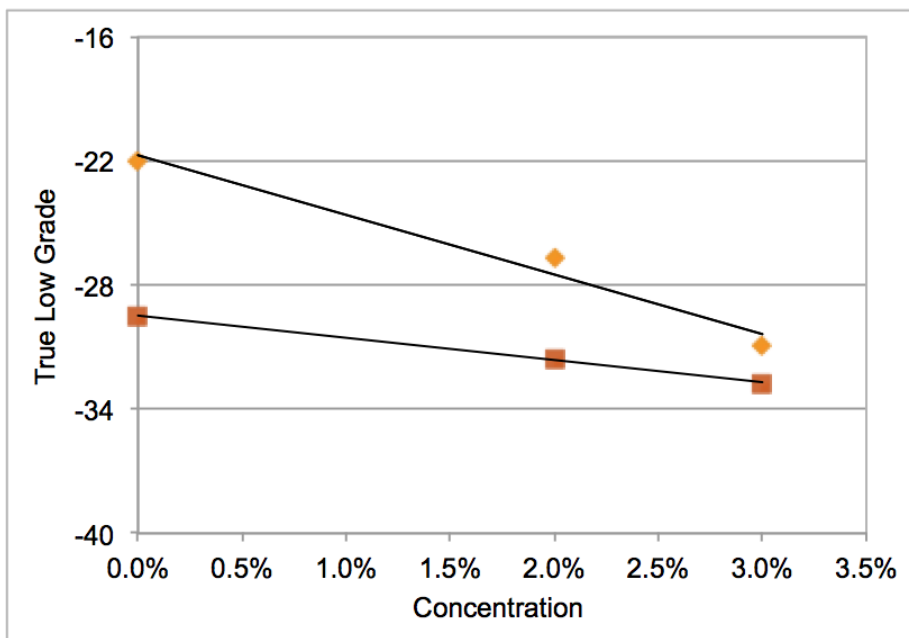
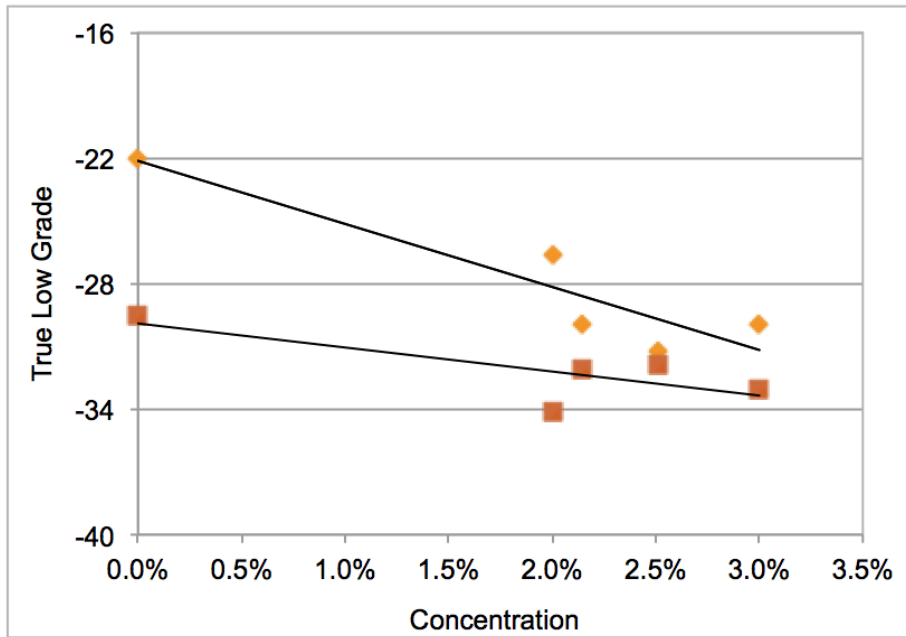
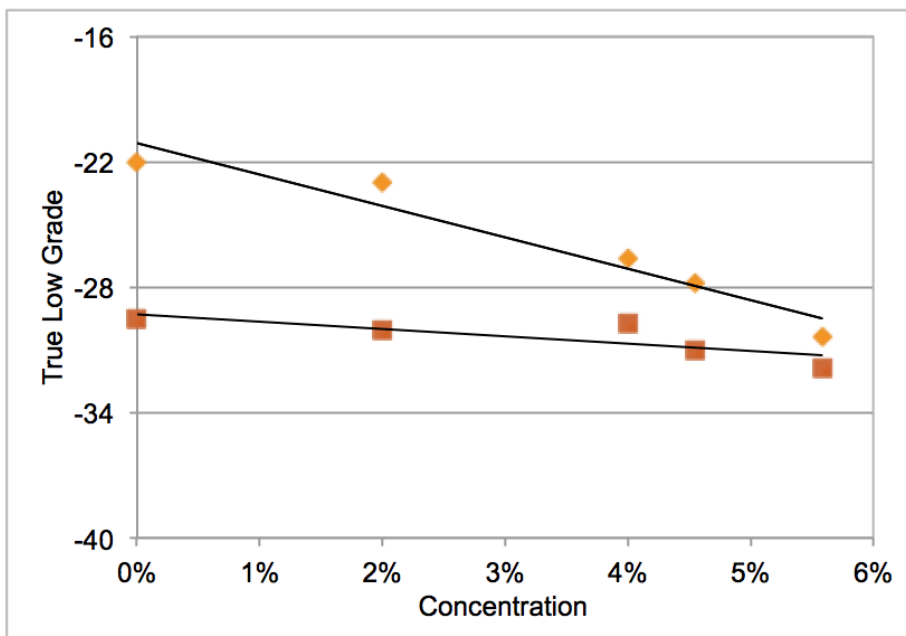


Figure 3.12. Low temperature continuous grades at different doses of additive A4



**Figure 3.13. Low temperature continuous grades at different doses of additive A5**



**Figure 3.14. Low temperature continuous grades at different doses of additive A6**



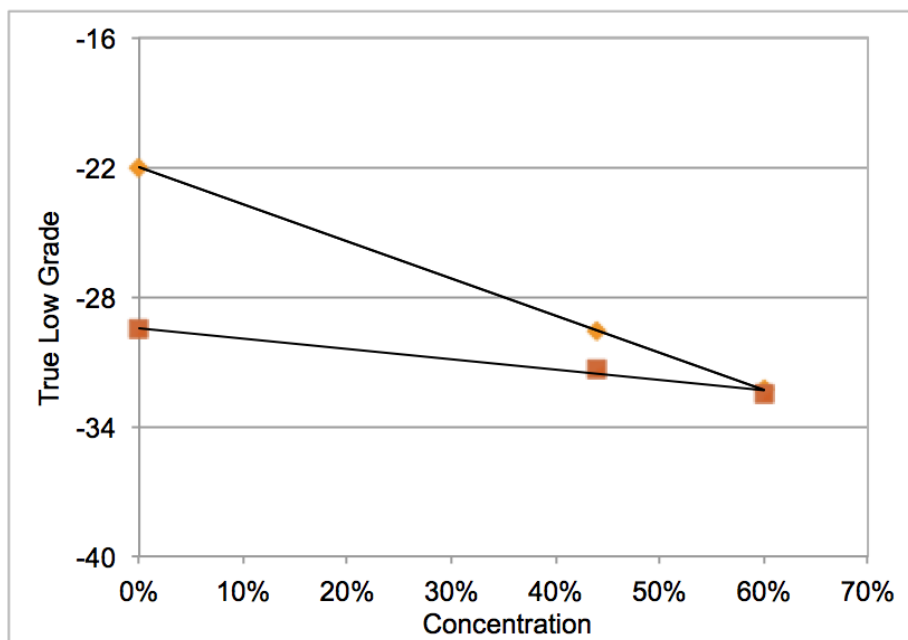


**Figure 3.15. Low temperature continuous grades at different doses of blending with binder B2**

### 3.3.2 Binder set 2

A second set of binders that included a modifier to improve the high temperature properties was also evaluated. Modification of binders with elastomers is a very common technique that is used not only to increase the high temperature grade of the binder, but also to provide the binder with additional elastic recovery. One of the most common polymers used is styrene-butadiene-styrene (SBS), which was evaluated in this study. In addition, many producers use polyphosphoric acid (PPA) to modify asphalt for high temperature performance. However, PPA is not allowed in some cases owing to performance related issues that have been observed in the field.

The neat asphalt binder was modified with both PPA and SBS, in addition to modifying some of the above blends of B1 + additive with each of these, as listed below:

- B1 + PPA
- B1 + A2 + PPA
- B1 + A3 + PPA
- B1 + A4 + PPA
- B1 + A2 + SBS
- B1 + A3 + SBS

In all cases, 0.6% PPA was used, and 1% SBS was used. Figure 3.16 shows the continuous high grades of the PPA modified binders, compared to the same binders without PPA modification. All of the binders modified with PPA were controlled by the unaged criterion. Figure 3.17 shows the continuous low grades of each binder in Set 2, compared with their Set 1 counterparts. It is notable that all low true grades were still assigned based on m-value. These results show little change due to SBS in low temperature properties, but a slightly larger change for some binders due to PPA modification.

## 3.4 HIGH TEMPERATURE PROPERTIES

As discussed in a previous section, the Multiple Stress Creep and Recovery (MSCR) test was performed on the binders involved in this study. The MSCR data was analyzed as shown in Figure 3.18 to determine the non-recoverable compliance and the elastic recovery at the end of 10 repeated loading and recovery cycles, at both 100 Pa and 3200 Pa of applied stress. Figures 3.19 - 3.22 show the MSCR results for all of the binders in Set 1. It is notable that most of the low temperature additives had a small effect on MSCR properties of the binder when compared with each other, although all of them made the performance slightly

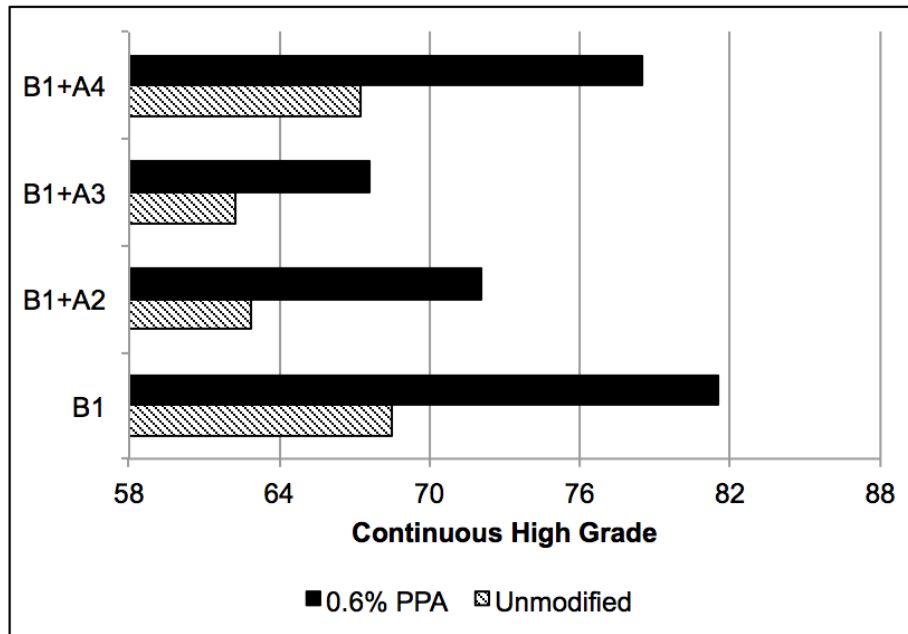


**Figure 3.16. High temperature continuous grades after PPA modification**

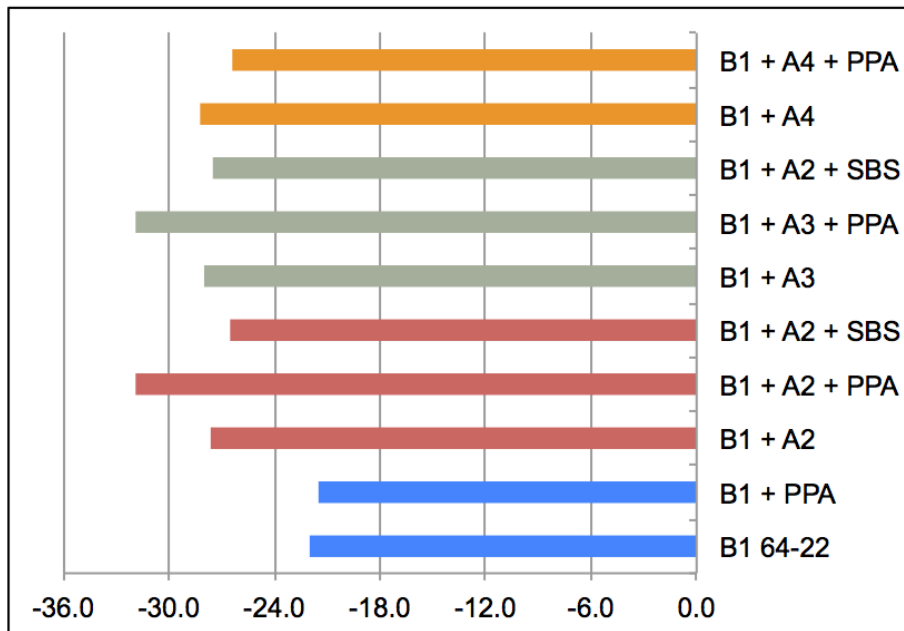


**Figure 3.17. Continuous low grades of Set 2 binders with their Set 1 counterparts**

worse than the original binder, most likely due to the reduction in high PG properties.

It is important to note the effect of SBS modification on the MSCR test. In most cases, it

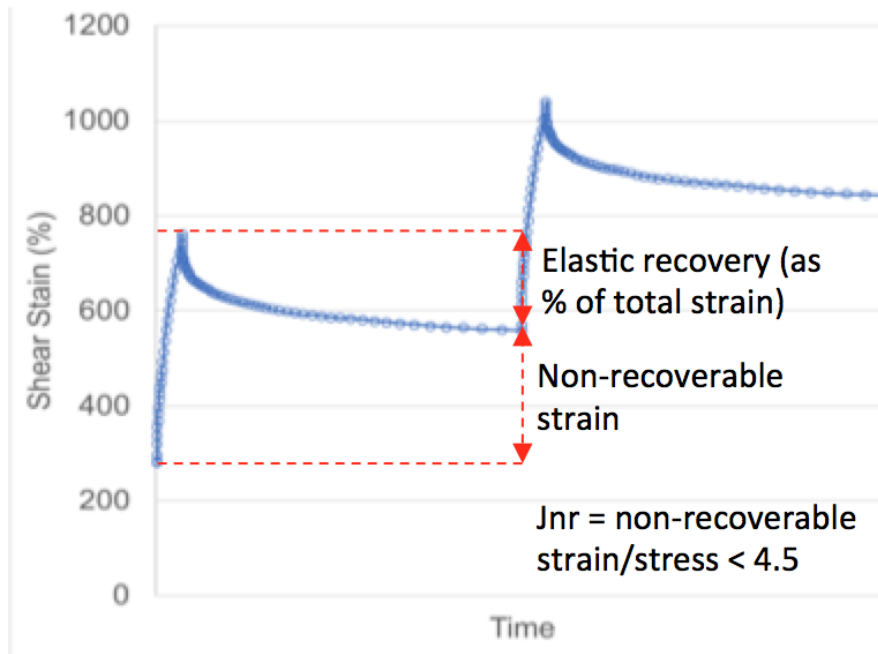


Figure 3.18. Example of analysis of MSCR results for two cycles

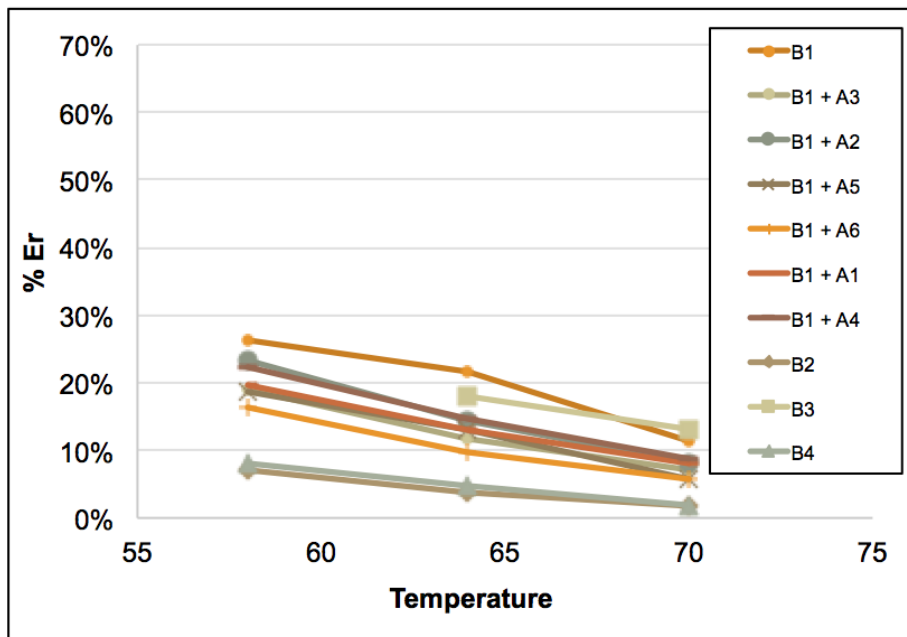


Figure 3.19. Elastic Recovery of Set 1 binders at 100 Pa loading

has been documented that SBS modification can significantly improve the elastic recovery

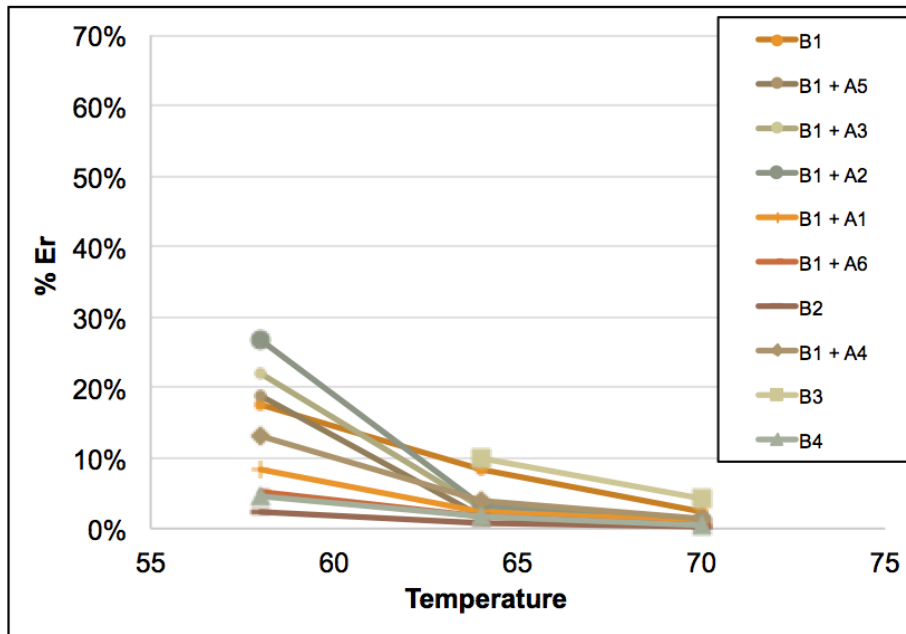


Figure 3.20. Elastic Recovery of Set 1 binders at 3200 Pa loading

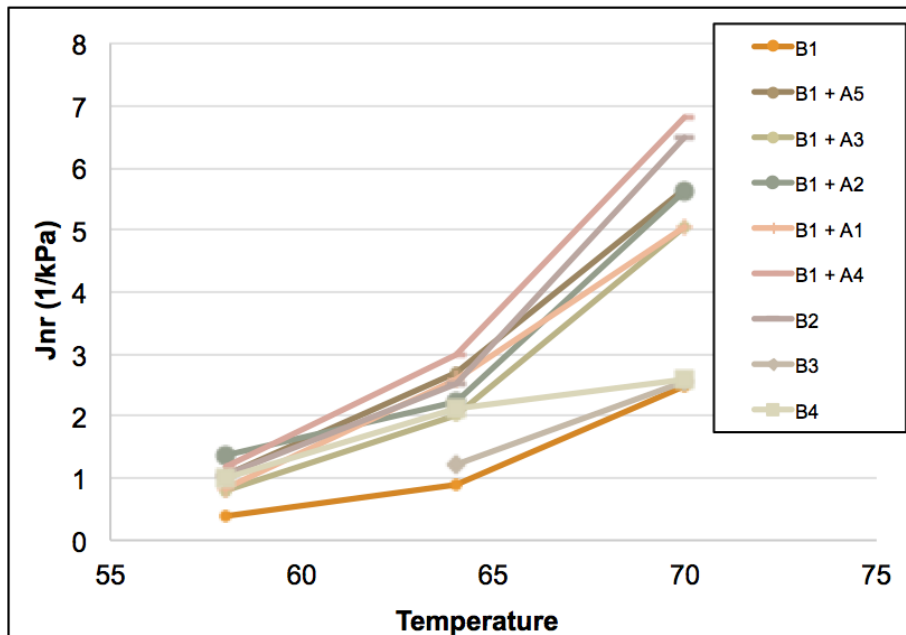
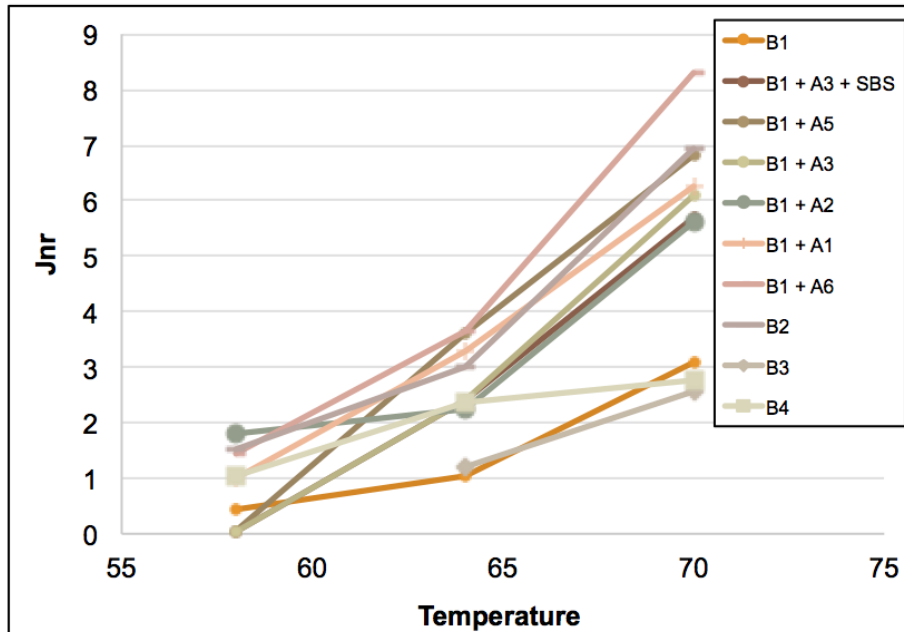


Figure 3.21. Non-recoverable creep compliance of Set 1 binders at 100 Pa loading

of asphalt binders. Figure 3.23 shows the percent elastic recovery (%ER) for two of the binders, both with and without SBS modification. Note that the same trend was observed



**Figure 3.22. Non-recoverable creep compliance of Set 1 binders at 3200 Pa loading**

for a stress level of 3200 Pa. This figure demonstrates that SBS modification will not affect all binders equally, especially modified asphalt, and therefore, it is preferable to specify an elastic recovery requirement, rather than specifying an amount of SBS requirement.

### 3.5 LOW TEMPERATURE PROPERTIES AND DELTA TC

As mentioned above, the primary low temperature property evaluated in this study was the  $\Delta T_c$  parameter, due in part to the ease of using it, and in part because it has been shown to relate to both thermal and fatigue cracking resistance. Figure 3.24 shows the  $\Delta T_c$  values for each of the binders in Binder Set 1. Note that in general, adding the low temperature additives improved the  $\Delta T_c$  of the binder, which is expected since these are proposed to be good additives for low temperature performance. However, two of them were clear exceptions and caused a substantial increase in  $\Delta T_c$ . Figure 3.25 shows  $\Delta T_c$  for the binders in Set 2, along with their Set 1 counterparts, to show the effect of PPA and SBS modification on this parameter. However, it is also important to note that this parameter has the potential to have large errors, due in part to the allowable error for measurements in the BBR accumulating for different temperatures.

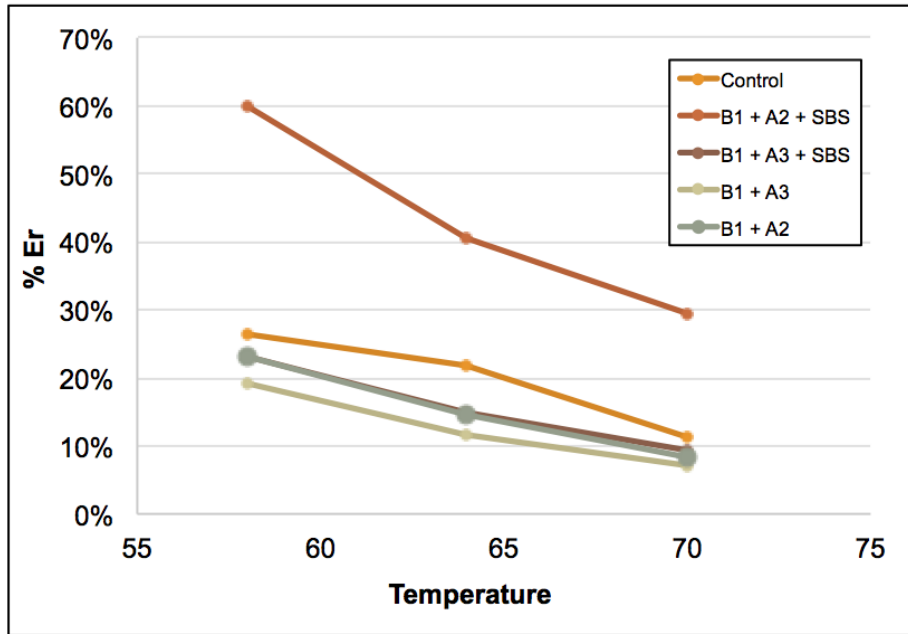


Figure 3.23. Effect of SBS modification with the use of low temperature additives, elastic recovery at the end of 10 cycles and 100 Pa loading amplitude is shown

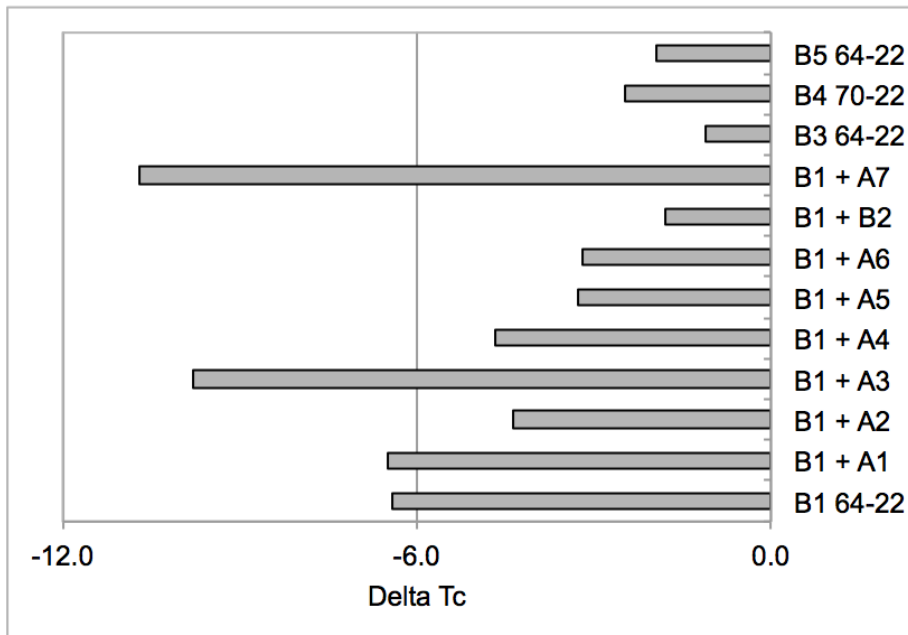


Figure 3.24.  $\Delta T_c$  for binders in Binder Set 1

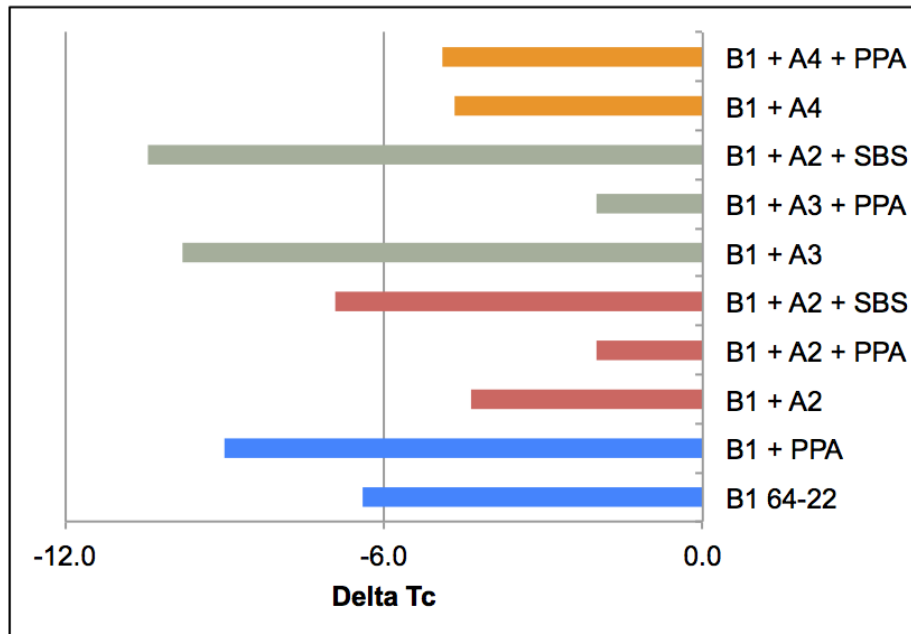


Figure 3.25.  $\Delta T_c$  for binders in Set 2 and corresponding Set 1 binders

### 3.6 INTERMEDIATE TEMPERATURE CRACKING INDICATORS

As mentioned above, the parameters that were evaluated for intermediate temperature cracking in this study were primarily those that can already be performed in the Dynamic Shear Rheometer, in order to facilitate the writing of a new specification without the need for new equipment. In addition to the tests that can be performed in shear with the parallel plate geometry, the poker chip test was also evaluated due to recent advances in rheometer technology which allow for the ability to conduct Dynamic Mechanical Analysis (DMA) testing using rheometers. Many of the tests that were evaluated require a frequency sweep test to be conducted at intermediate temperature, and then for the data to be shifted to a master curve using the Time Temperature Superposition Principle (TTSP). An example of a master curve developed using this method is shown in Figure 3.26. In this study, temperatures of 5°C, 15°C, and 25°C were used to develop a master curve at a reference temperature of 15°C.

Many parameters were extracted from this test, including the PG parameter  $G^* \sin(\delta)$  at the defined intermediate temperature for the base binder. This is shown in Figure 3.27 for the Set 1 binders and Figure 3.28 for the Set 2 binders at 25°C. In addition to that parameter, the Glover-Rowe parameter, crossover frequency, and crossover modulus were



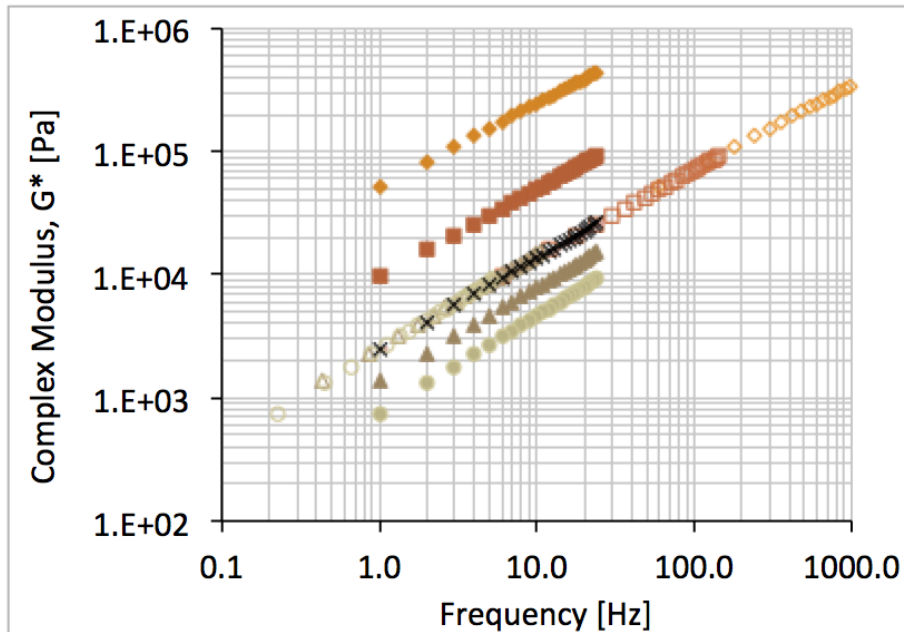


**Figure 3.26. Example of frequency sweep data shifted to a master curve**

obtained from the master curve. Beyond the master curve development, a Linear Amplitude Sweep test was run on all binders at their PG intermediate temperatures after the frequency sweep test was completed. All of these tests were performed on PAV aged material. In addition, a poker chip test was run on the binders at 18°C in all three aging conditions—unaged, RTFO aged, and PAV aged.

Figure 3.29 shows the Glover-Rowe parameter for each of the binders that was evaluated in Set 1 of this study. It is notable that all of the low temperature additives provided substantial improvement to the Glover-Rowe value of the original binder B1, as opposed to the  $\Delta T_c$  parameter, for which some of the additives caused a worse value than the original binder. In general, the modified binders and the field binders would all pass the specification limit of 450 kPa. Figure 3.30 shows the parameter for the Set 2 binders. Most binders remained within the specification limit when modified with PPA or SBS, although some change was observed due to SBS and PPA modification.

The crossover frequency was also determined for these binders, based on the point where the phase angle was equal to 45° on the master curve at a reference temperature of 15°C. From this computation, it was also possible to determine the crossover modulus, which was defined as  $G^*$  at the crossover frequency. Figure 3.31 shows the crossover frequency of each binder evaluated in Set 1, and Figure 3.32 shows the crossover modulus for each

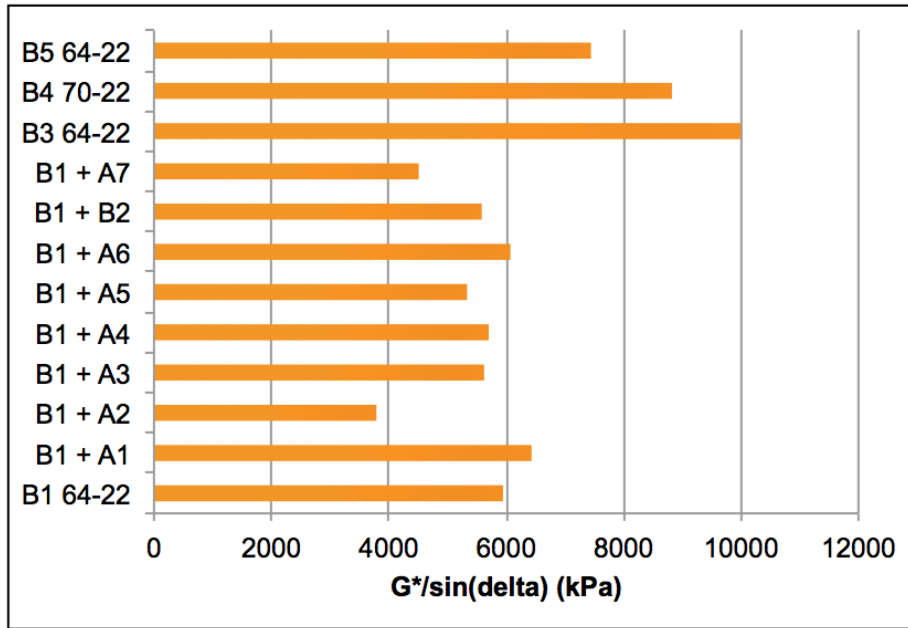


Figure 3.27. PG intermediate temperature parameter for Set 1 binders

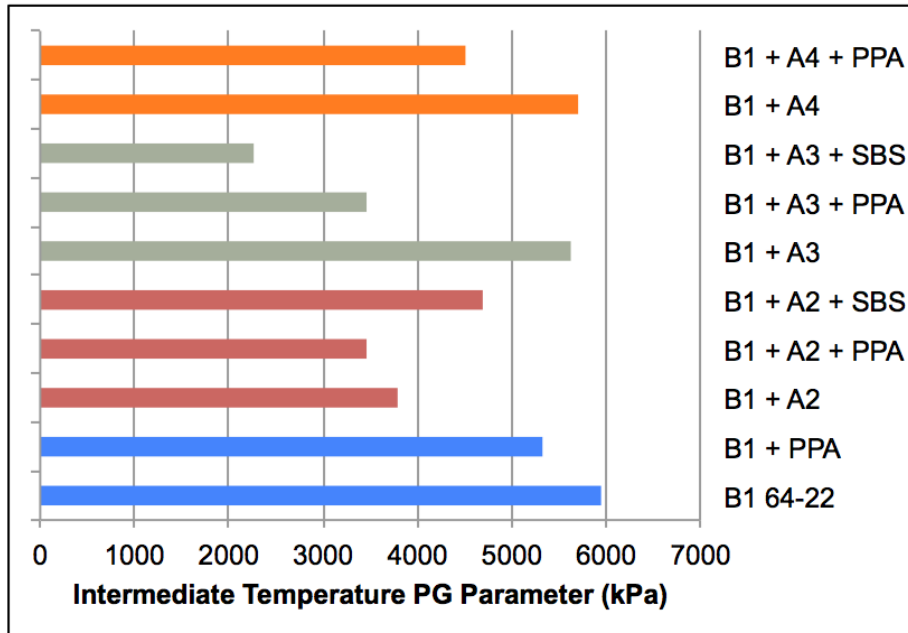


Figure 3.28. PG intermediate temperature parameter for Set 2 binders

binder evaluated in Set 1.

It is notable that for the binders here, it appears that the crossover frequency and

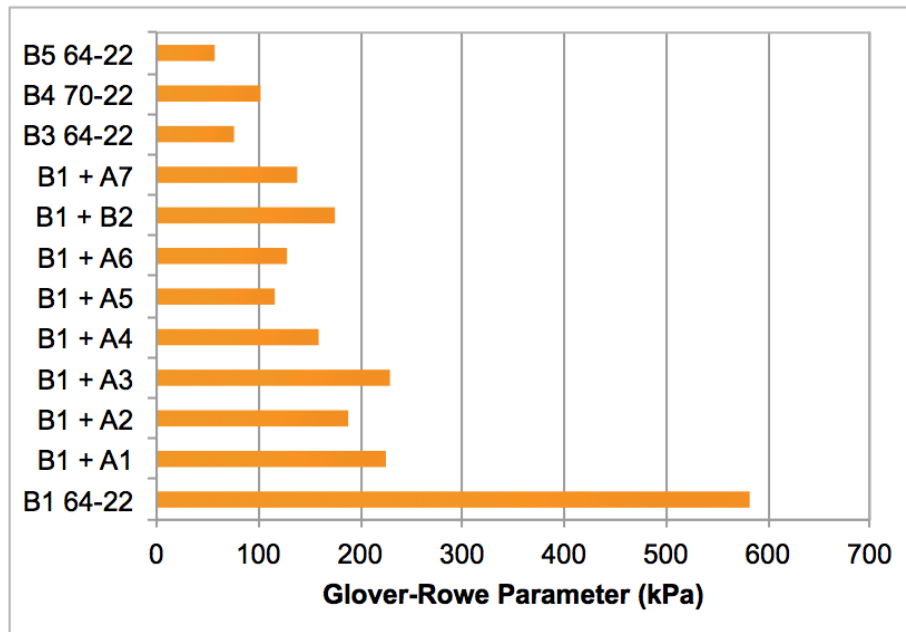


Figure 3.29. Glover-Rowe parameter for Set 1 binders

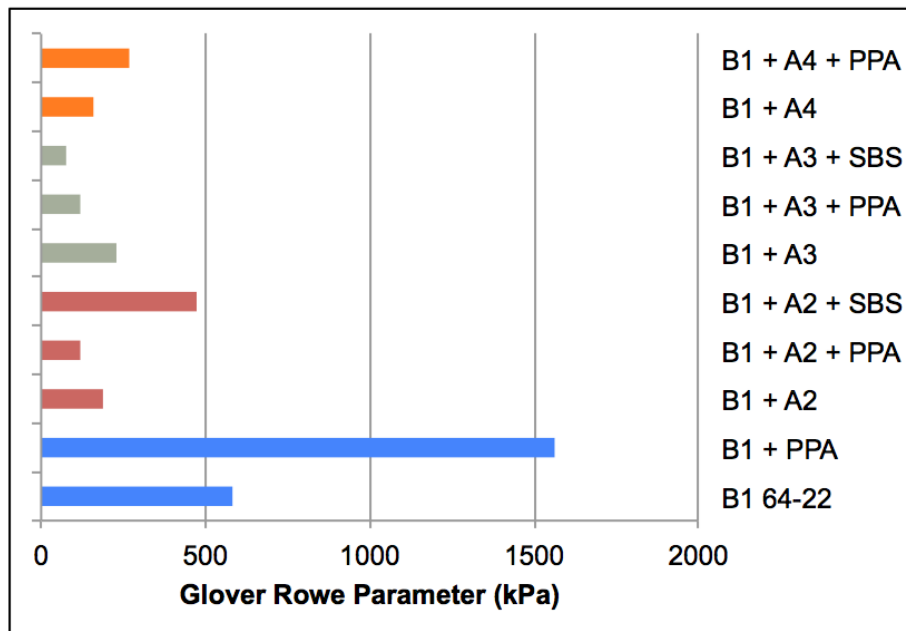
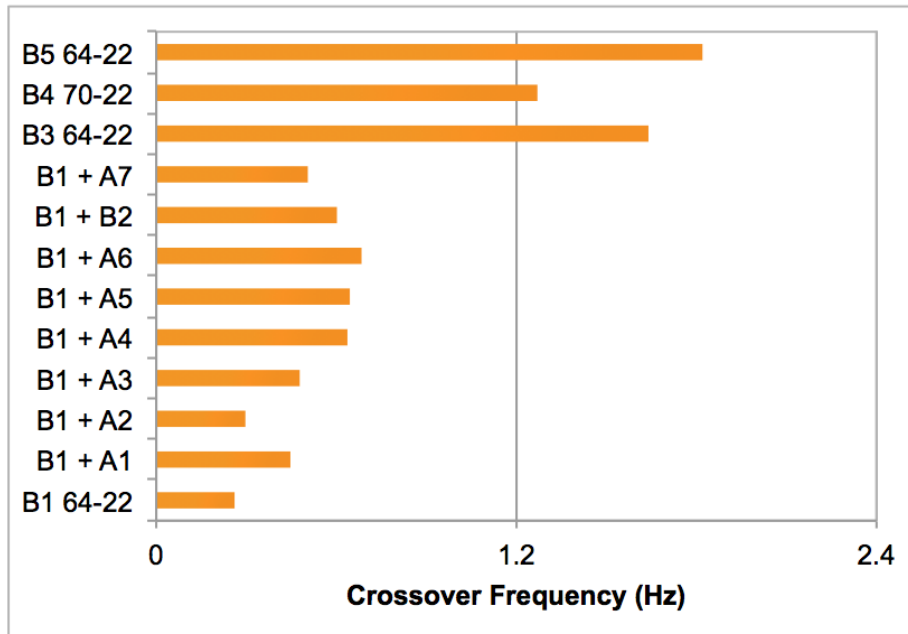


Figure 3.30. Glover-Rowe parameter for Set 2 binders

crossover modulus are very well correlated with each other (Figure 3.35).

It is generally observed that the modification of neat asphalt binder with SBS or PPA



**Figure 3.31. Crossover frequency parameter for Set 1 binders**

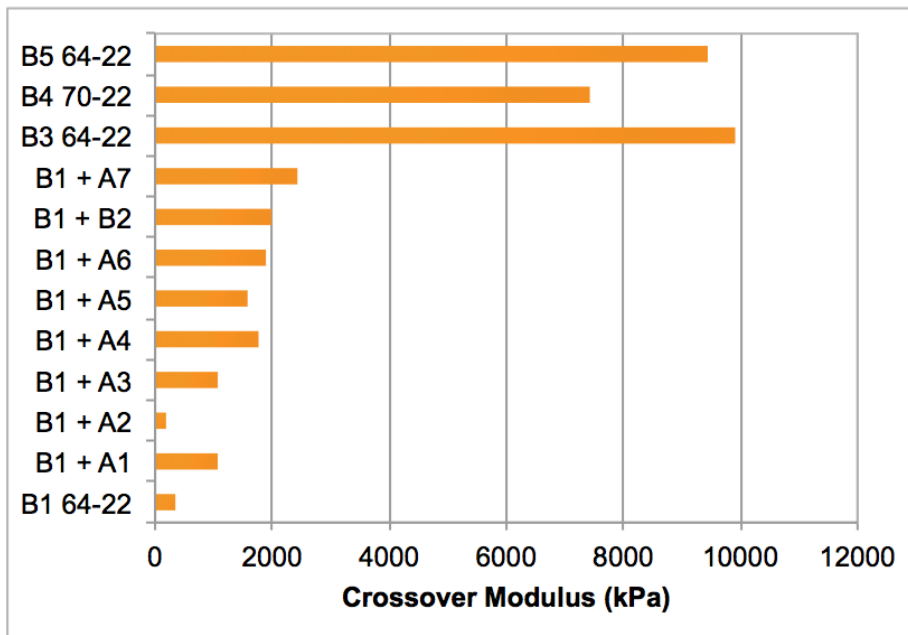


**Figure 3.32. Crossover modulus parameter for Set 1 binders**

has limited effect on the intermediate temperature properties of the binder. However, once modified with low temperature additives and then modified with SBS or PPA, substantial

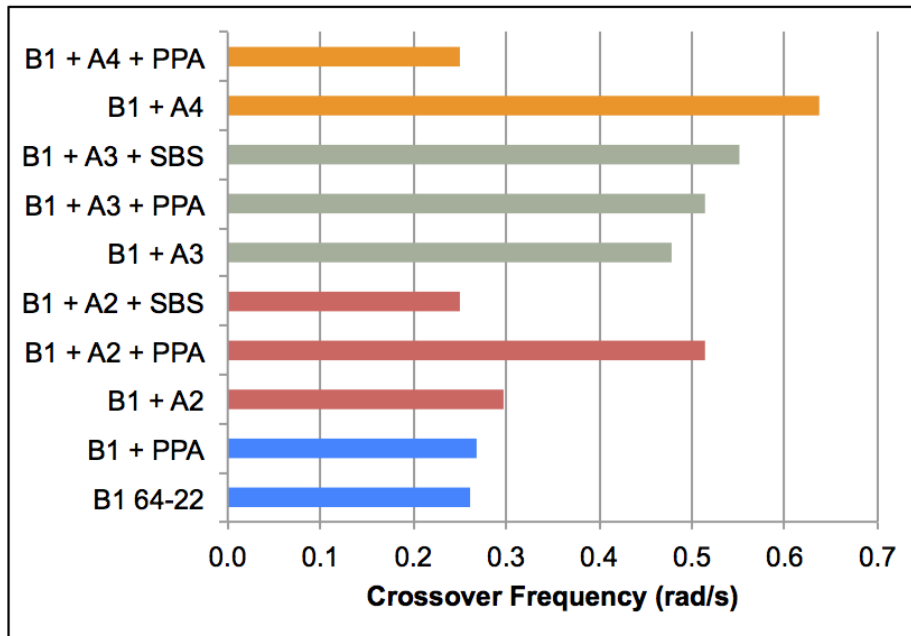


Figure 3.33. Crossover frequency parameter for Set 2 binders

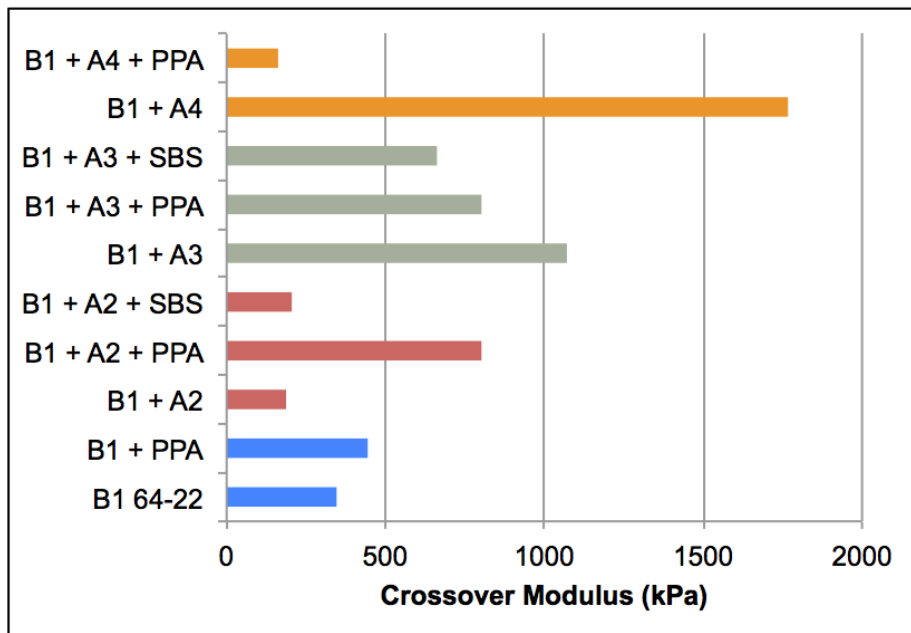
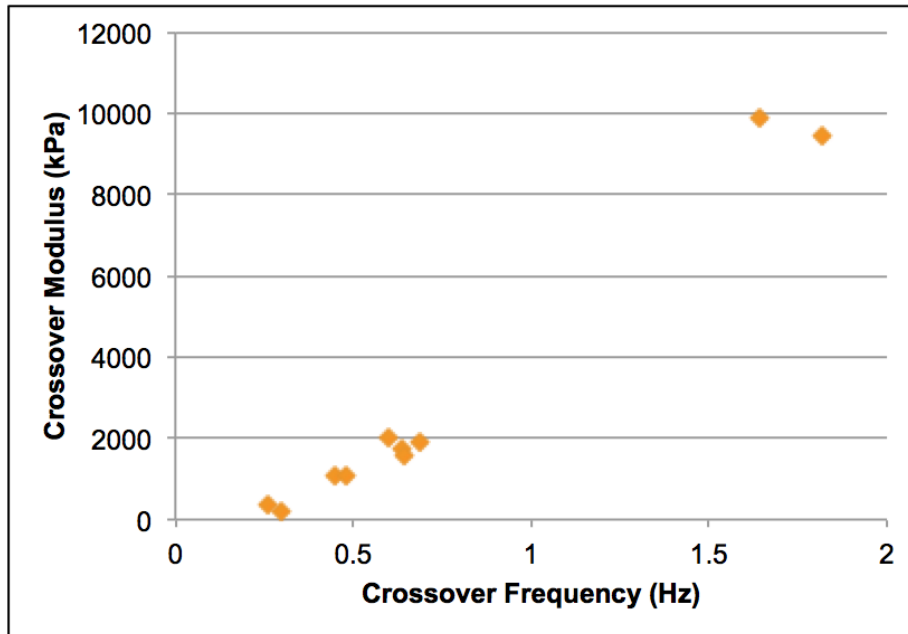


Figure 3.34. Crossover modulus parameter for Set 2 binders

effects were observed on these properties.

Two other tests were performed. First was the Linear Amplitude Sweep Test (LAST).



**Figure 3.35. Relationship between crossover frequency and crossover modulus**

The results for some of the binders tested are shown in Figure 3.36. Additionally, a strain controlled poker chip test was performed on the Set 1 binders in this study. This test was performed on binders in all three aging conditions- unaged, RTFO, and PAV aged. The engineering stress-strain curve was developed based on the load and displacement data recorded from the test. Then, three main parameters were measured- the peak stress, the fracture energy at the peak stress, and the failure strain at the peak stress. The results for the binders in all aging conditions are shown in Figures 3.37 - 3.42.

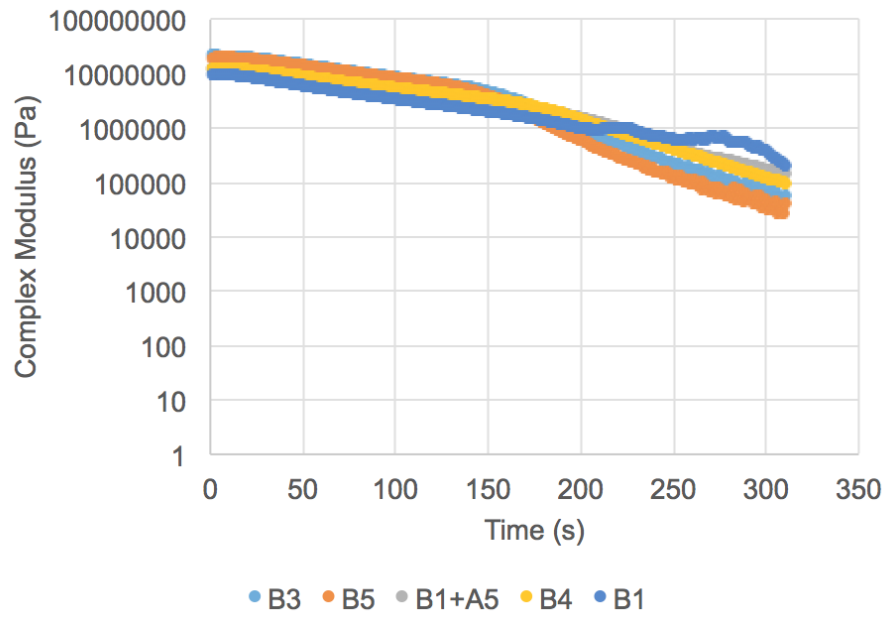


Figure 3.36. Linear Amplitude Sweep Results

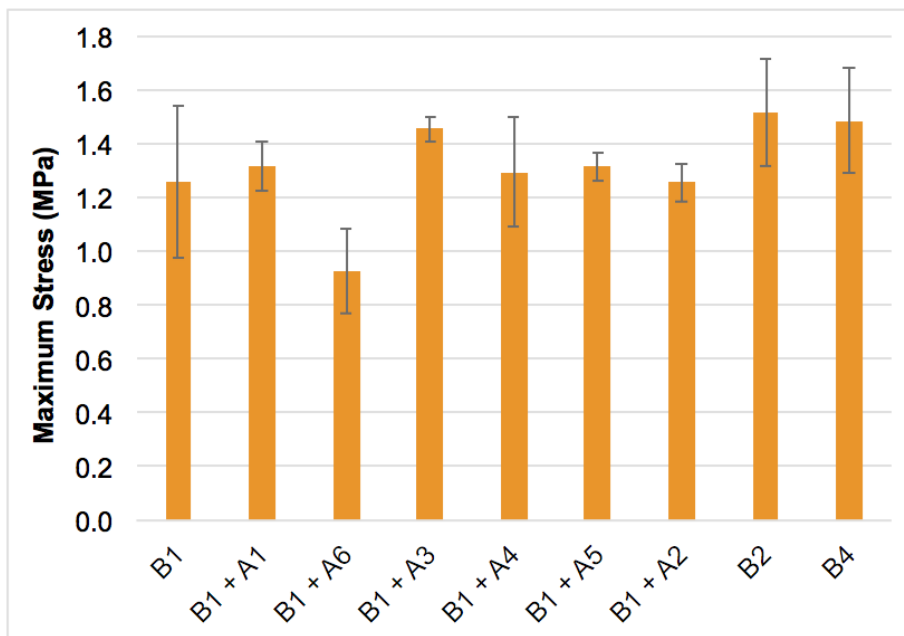


Figure 3.37. Poker chip maximum stress for PAV aged binders

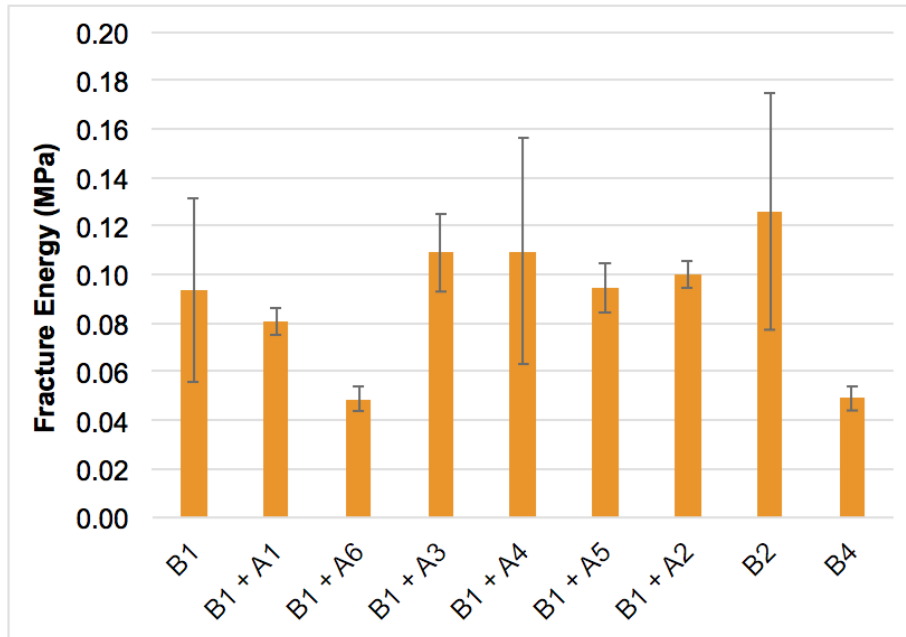


Figure 3.38. Poker chip fracture energy for PAV aged binders

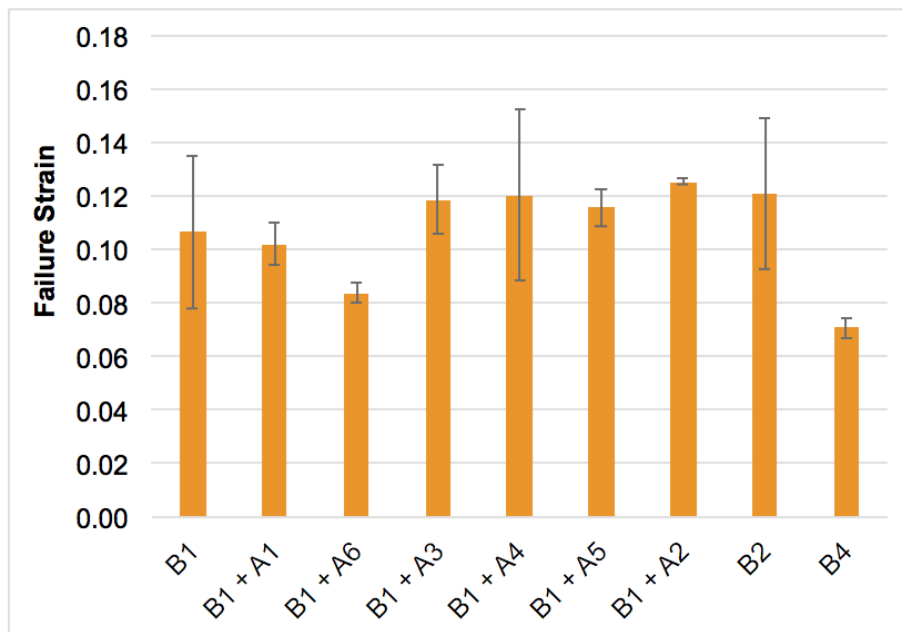


Figure 3.39. Poker chip failure strain for PAV aged binders



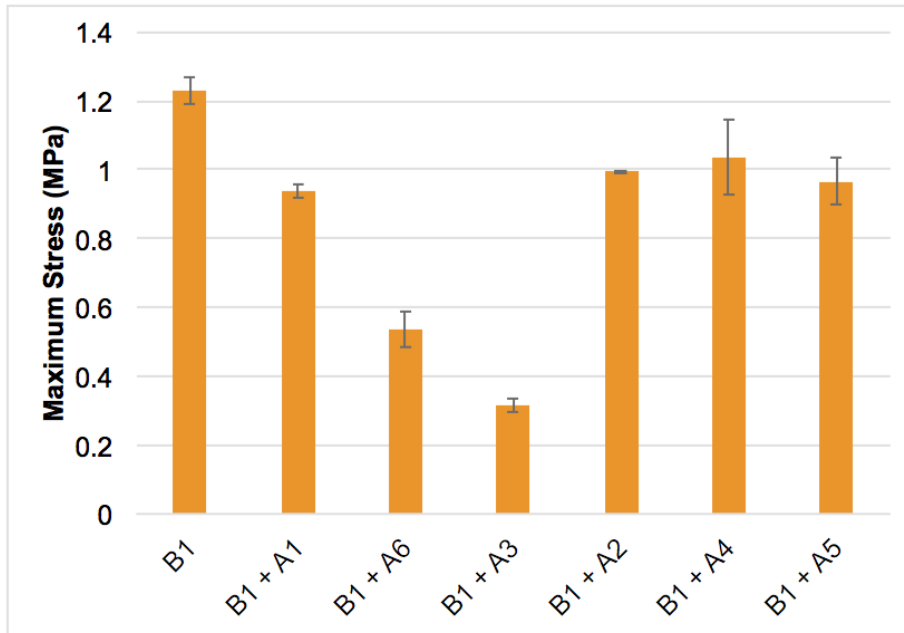


Figure 3.40. Poker chip maximum stress for unaged binders

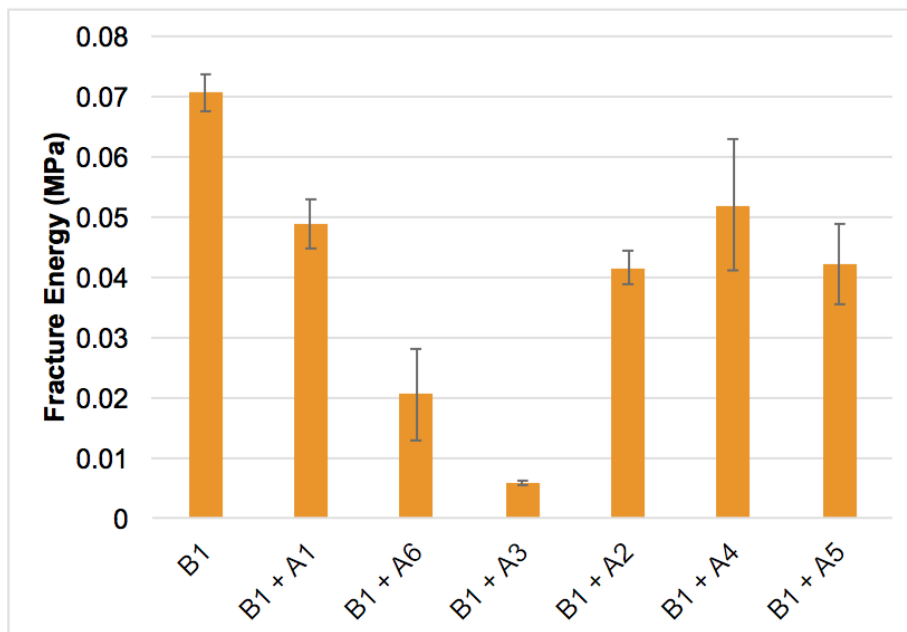
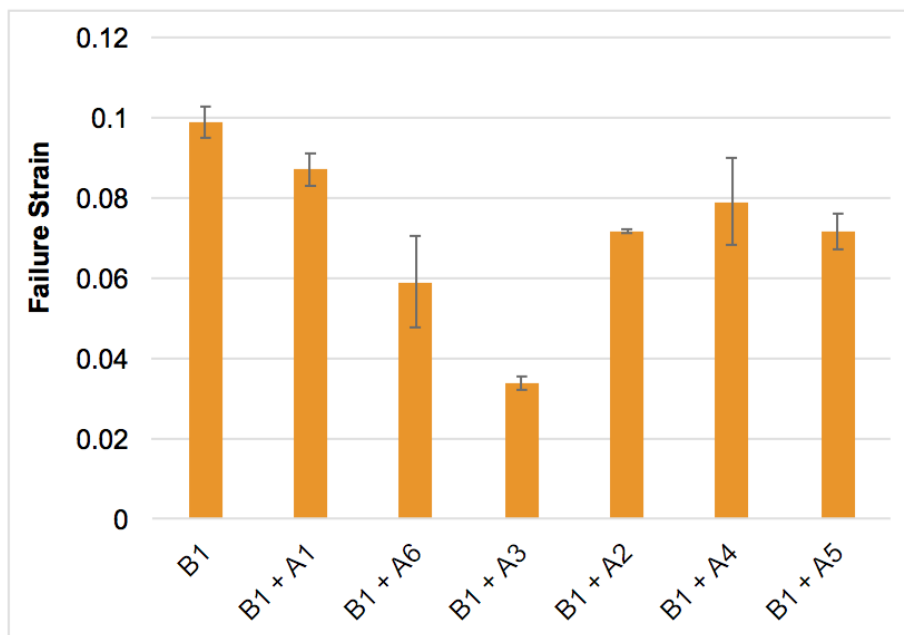


Figure 3.41. Poker chip fracture energy for unaged binders



**Figure 3.42. Poker chip failure strain for unaged binders**

### 3.6.1 Relationships between cracking indicators

In this study, it was important to explore whether any of the intermediate temperature cracking indicators were correlated to other cracking indicators. The plots that show these relationships are contained in Figures 3.43 - 3.52. It is notable that although all of these properties except for poker chip strength are related to linear viscoelastic behavior of the binder, few if any have a relationship with each other. Note also that the poker chip strength and fracture energy are related to each other very well, with the exception of one outlier (3.53).

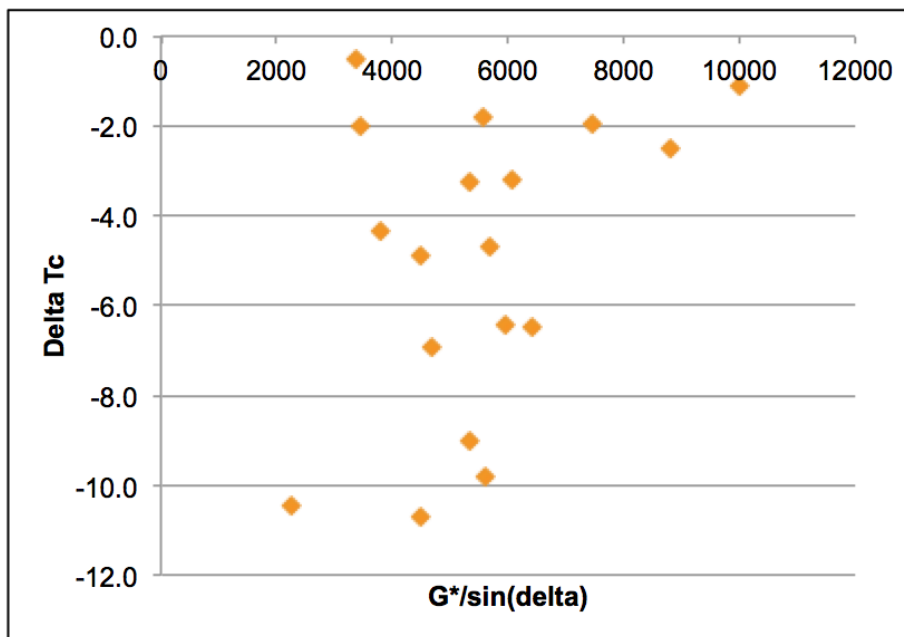


Figure 3.43. Current intermediate temperature parameter vs.  $\Delta T_c$

### 3.7 RECOVERED BINDERS FROM FIELD SECTIONS

As mentioned in a previous chapter, this project also incorporated binders that were recovered from field sections for which it was believed that binder was a potential reason for the performance of the mix. These binders were classified into two categories, binders that showed good performance and binders that showed bad performance in the field. For these binders, a frequency and temperature sweep was run in the DSR using the 4 mm plate technique discussed later in this chapter. In addition, a poker chip test was run on these binders to examine their strength. These techniques were chosen due to a small amount of binder

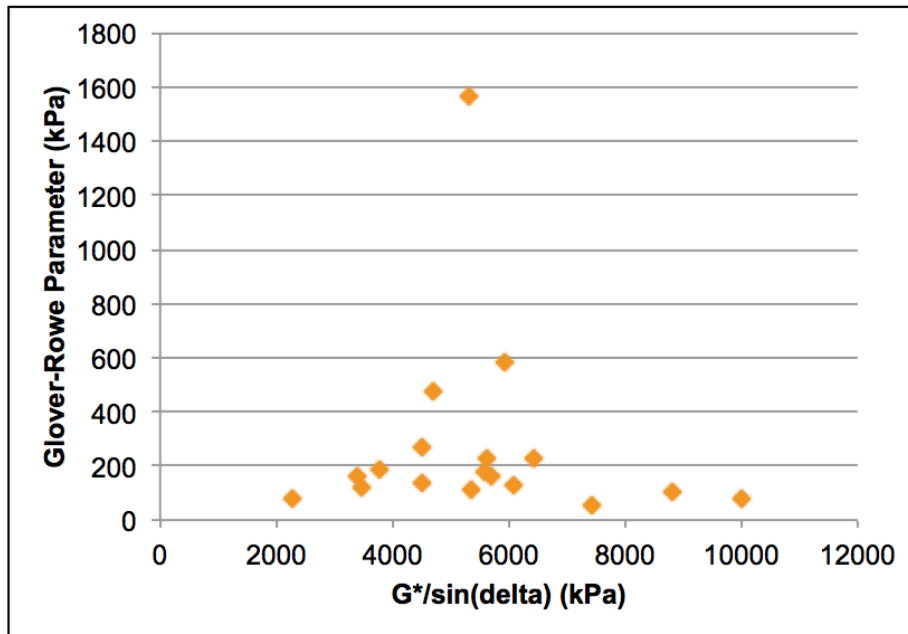


Figure 3.44. Current intermediate temperature parameter vs. Glover-Rowe parameter

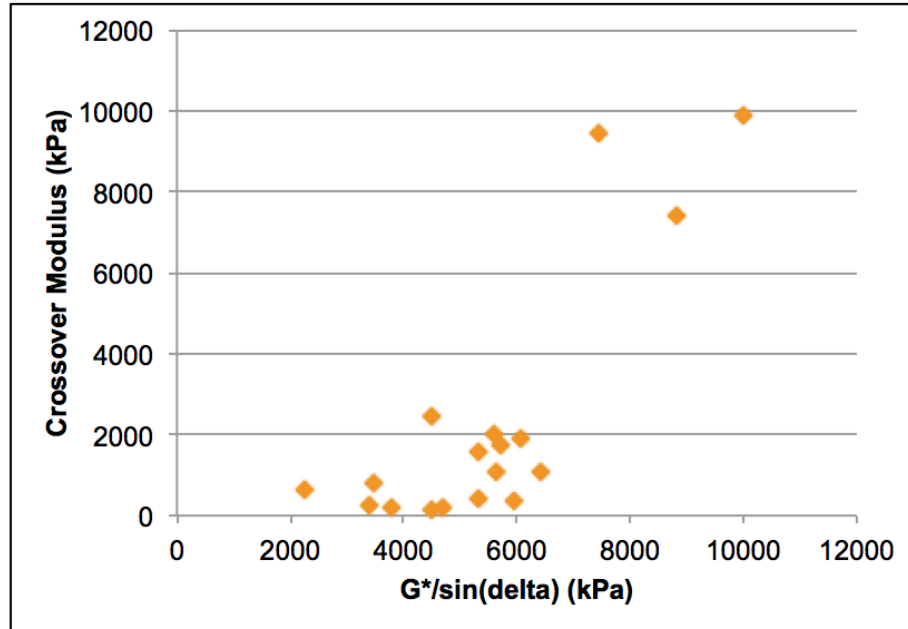


Figure 3.45. Current intermediate temperature parameter vs. crossover modulus

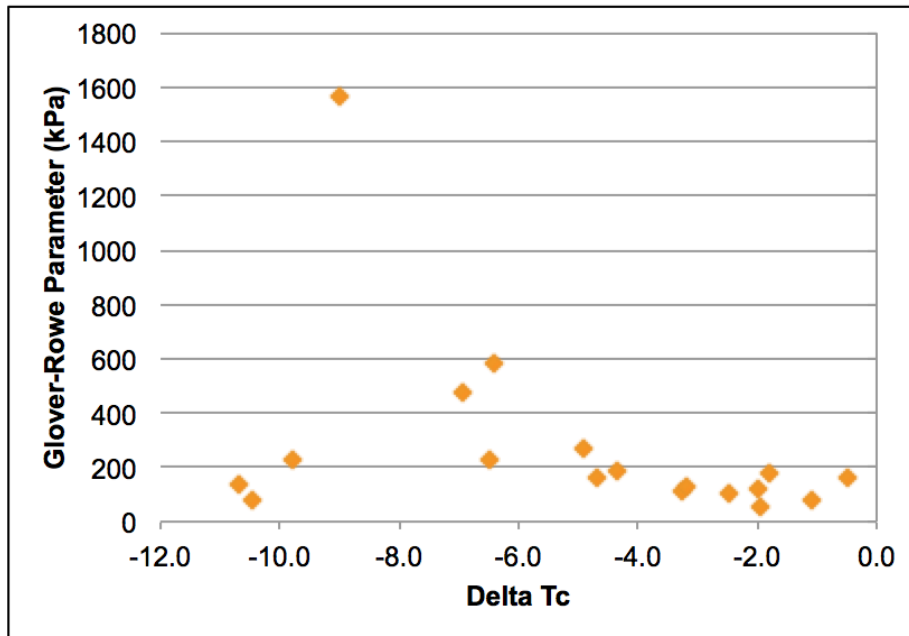


Figure 3.46.  $\Delta T_c$  vs. Glover-Rowe parameter

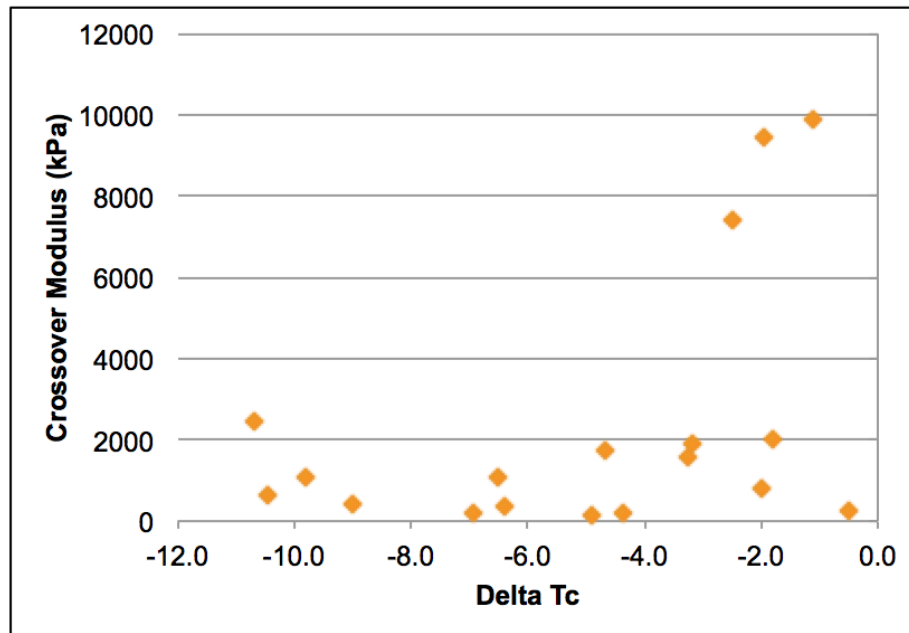


Figure 3.47.  $\Delta T_c$  vs. crossover modulus

that could be extracted from these mixes- leaving not enough material to run BBR tests or mixture tests. However, mixture performance was inferred qualitatively from the reports of

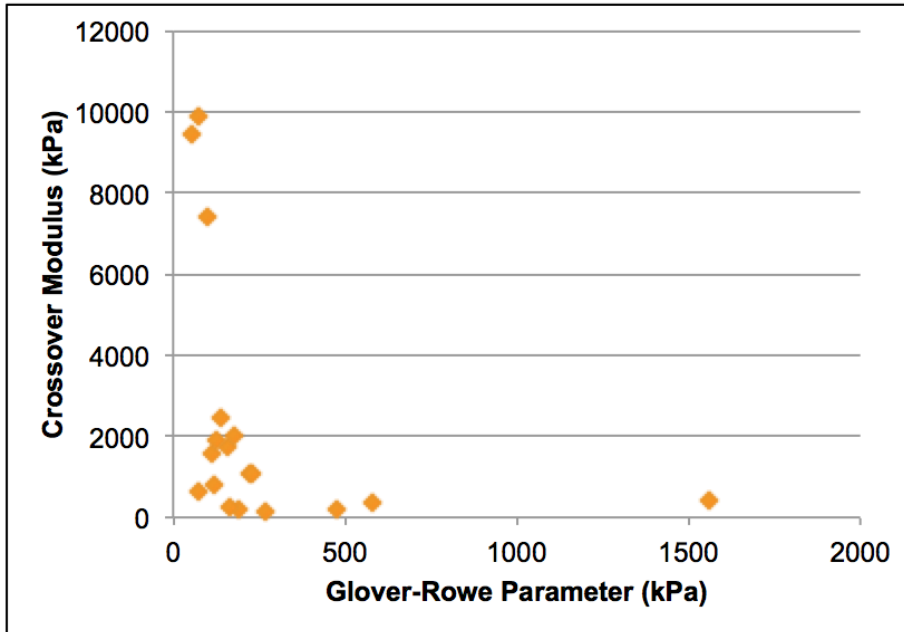


Figure 3.48. Glover-Rowe parameter vs. crossover modulus

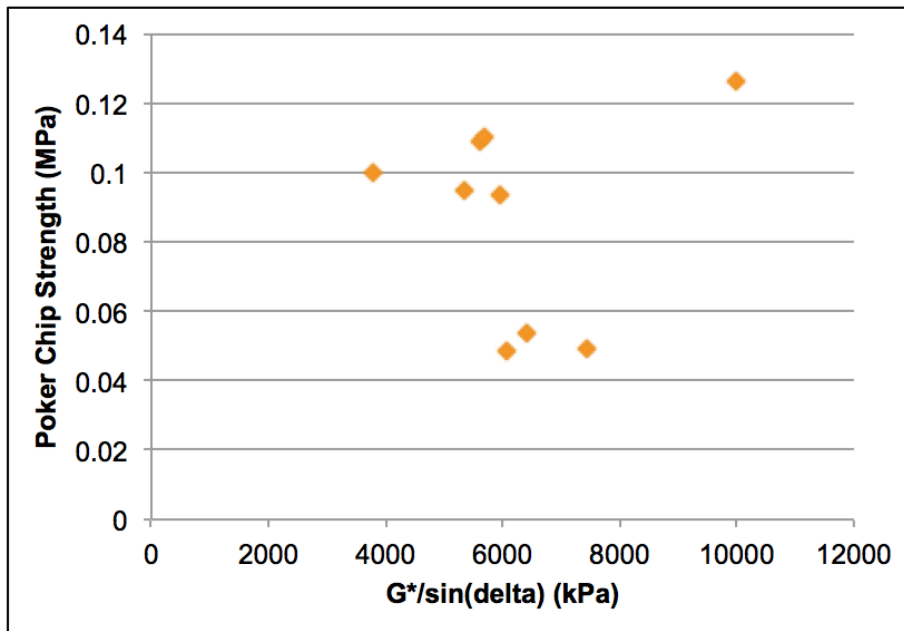


Figure 3.49. Current intermediate temperature parameter vs. poker chip test PAV strength

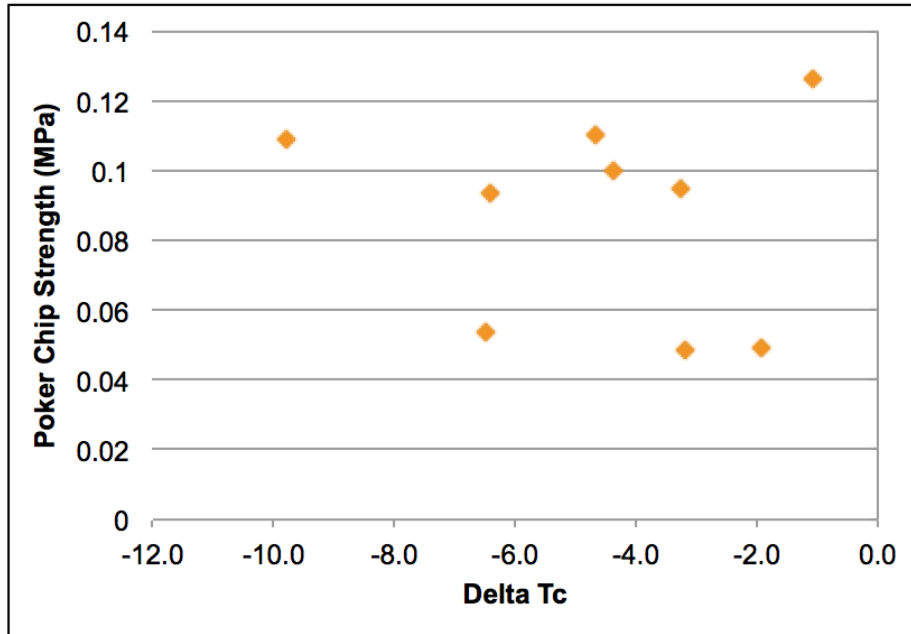


Figure 3.50.  $\Delta T_c$  vs. poker chip test PAV strength

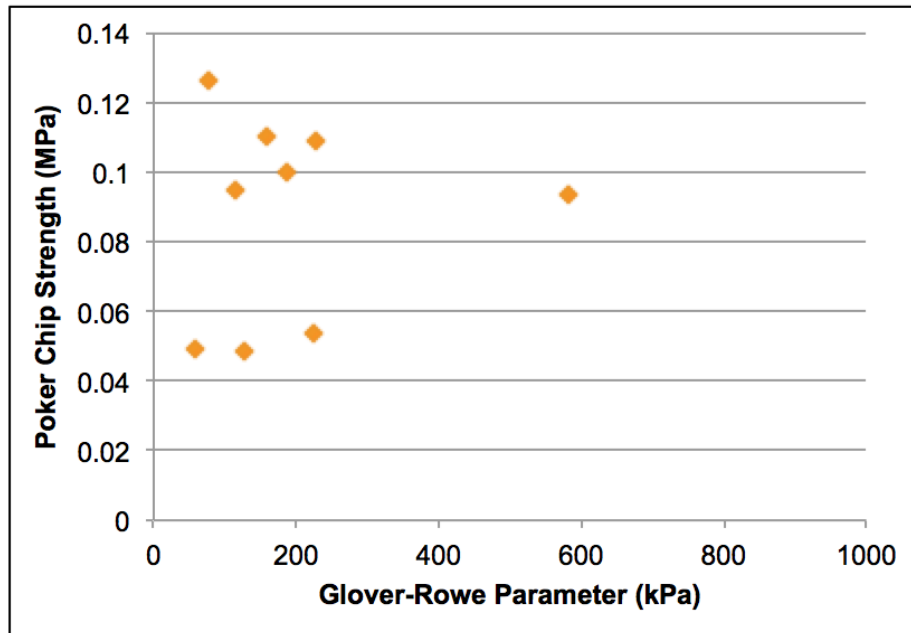


Figure 3.51. Glover-Rowe parameter vs. poker chip test PAV strength

the mix's performance in the field.

The results from the poker chip test are shown in Figure 3.54. From these results, it is

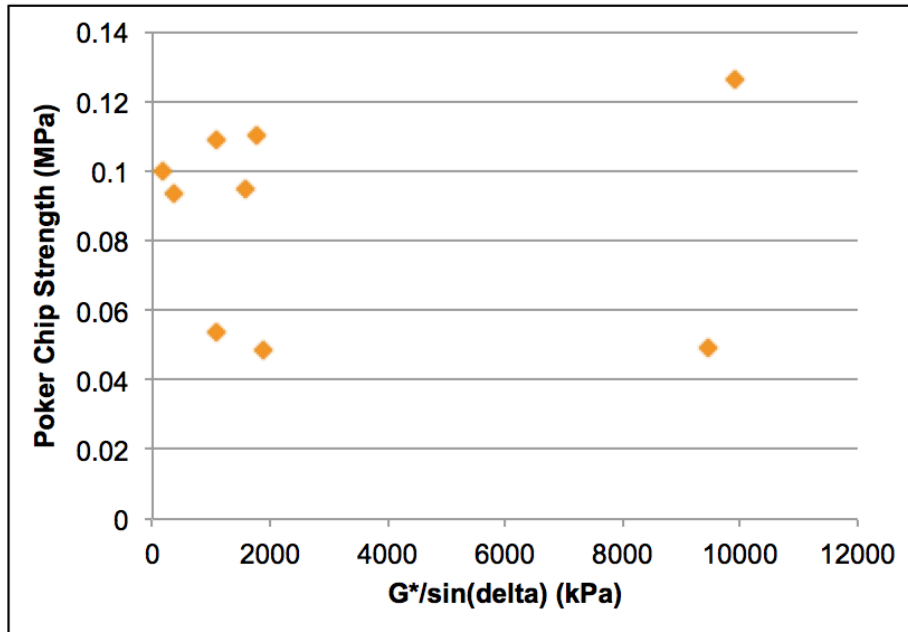


Figure 3.52. Crossover Modulus vs. poker chip test PAV strength

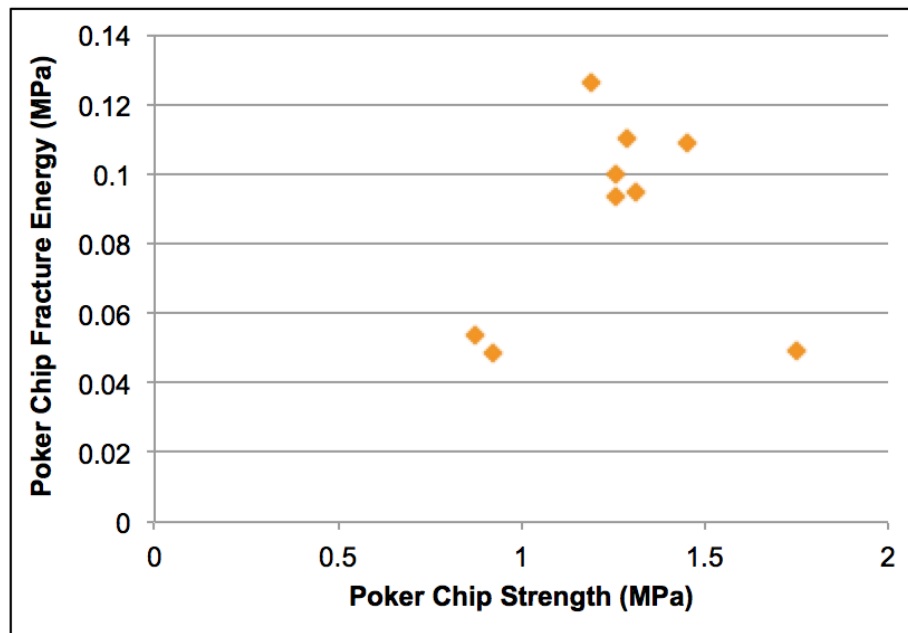
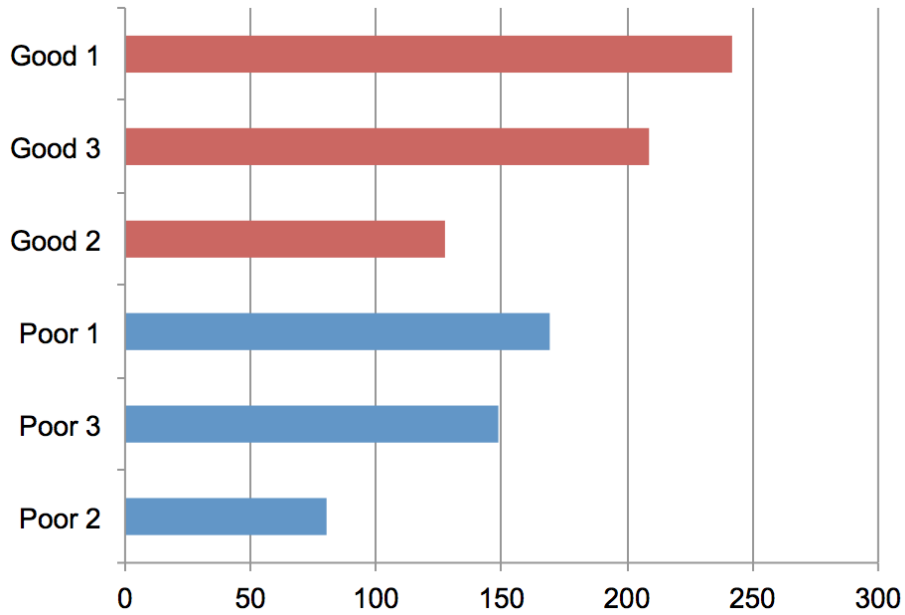


Figure 3.53. Poker chip test fracture energy vs. poker chip test PAV strength

believed that the poker chip test demonstrates some relationship with field performance for this set of binders. Figure 3.55 shows the low temperature true PG grades of the recovered

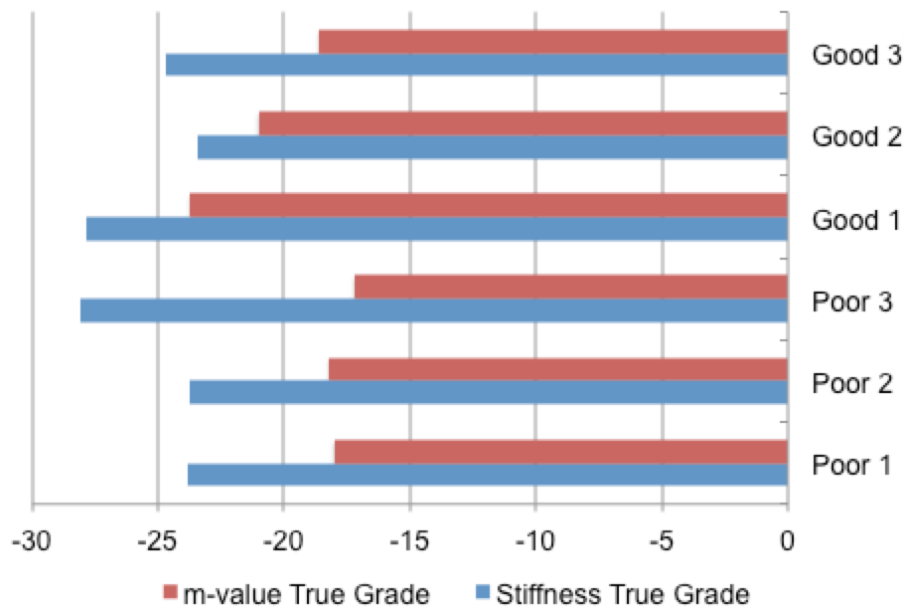


binders. There does appear to be some relationship between the good binders, and a lower true m-value grade.



Note: The performance designation is based on a broad analysis of contributions from material, mixture, and construction and materials come from different mix types and pavement structures

**Figure 3.54. Poker chip test strength for binders recovered from field mixes**



Note: The performance designation is based on a broad analysis of contributions from material, mixture, and construction and materials come from different mix types and pavement structures

**Figure 3.55. Low True Grade based on 4 mm plate DSR test for binders recovered from field mixes**

### 3.8 IMPROVING TESTING EFFICIENCY

*This section contains parts of an original version of a paper submitted for publication in Transportation Research Record: Journal of the Transportation Board (Hajj et al., 2019).*

The low temperature properties of the binder have attracted more attention during the recent years due to an increase in the use of reclaimed asphalt pavements (RAP). Traditional methods to evaluate low-temperature properties of the binder require a large amount of binder sample that needs to be recovered from RAP samples and used with a Bending Beam Rheometer (BBR). In order to economize on sample size for RAP materials and also for emulsion residues, previous researchers have explored the potential of using a 4 mm diameter specimen with a Dynamic Shear Rheometer (DSR) in lieu of the BBR (Sui2010, Sui2011, Farrar2015). Since the DSR measures the shear properties of the binder in time or frequency domain, the measurements from the DSR must be mathematically manipulated to be comparable to those from the BBR. Specifically, the DSR is most efficient at measuring complex shear modulus in frequency domain, whereas the parameters from the BBR

are obtained by conducting a flexural test (as opposed to shear) in time domain (as opposed to frequency). Previous research studies have also developed methods to accomplish these two conversions in order to compare data from the DSR with the BBR.

As discussed above, the BBR is the primary method that is used to evaluate asphalt binders at low temperatures in the United States. However, this method has some drawbacks, such as the requirement for a large sample size and a longer conditioning time to reach thermal equilibrium. In the past, testing PAV aged material at low temperatures in the DSR was not considered feasible, due to a requirement for large torque that was beyond the capability of traditional DSR units. However, in recent years, DSRs have evolved and have higher torque capacities. It is important to emphasize that the DSR is a very sensitive and high precision instrument. When the stiffness of the specimen (in this case aged binder at low temperatures) approaches the stiffness of the loading frame of the DSR, the measurements recorded by the unit include deformations within its loading apparatus. As such, it is critical to measure and discount for the compliance of the instrument itself while conducting such measurements (Sui et al. 2010). The scope of this study is to examine some of these methods from the literature and others based on the principles of linear viscoelastic interconversion using a set of eleven different binders.

Sui et al., in a study performed at Western Research Institute (WRI), proposed the use of a smaller plate diameter to achieve measurable deformation in the specimen while applying a torque that was within the capacity of the instrument (Sui et al. 2010). They also carefully examined the issue of correcting instrument compliance when making such measurements. Sui et al. (Sui et al., 2010) focused primarily on the correction for instrument compliance to match the data from the 4 mm plate with other size plates from the DSR. In another study, Sui et al. (2011) measured the linear viscoelastic properties of asphalt binder in frequency domain, and then interconverted these properties to time domain to generate a  $G(t)$  for asphalt binders. They then demonstrated a strong correlation between Stiffness and  $m$ -value measured in the BBR with  $G(t)$  and the slope of  $G(t)$  at 7200 seconds as measured and then inter-converted using the DSR 4 mm plate (Sui 2011).

In 2015, WRI released a white paper in which they provided further details and a proposed standard for the 4 mm plate (Farrar et al., 2015). Their revised criteria included computing  $G(t)$  60 seconds, instead of the previously recommended 7200 seconds, and new grading criteria, which assigned the binders a grade based on the low critical temperature + 10°C, the way that the BBR specification does. A subsequent study by Lu et al. (2017) used the aforementioned new criteria, but utilized a simpler model for Stiffness

(Equation 3.5) based on an approximation originally proposed by Anderson et al. (1994) The proposed model was further simplified by assuming a phase angle very close to zero, since the material was tested at low temperatures, where phase angles are small. An empirical relationship proposed by Anderson et al. (1994) was also used to approximate the m-value as  $\delta/90$  at the temperature and frequency of interest.

$$S(t) = \frac{3G^*(\omega)}{1 + 0.2\sin(\delta)} \quad (3.5)$$

where:

$$\omega = 1/t$$

$G^*$  = shear complex modulus

$\delta$  = phase angle

Lu et al. (2017) determined the Stiffness and m-value using the empirical functions proposed by Anderson et al. (1994) to estimate true grades of bitumens in their study based on the criteria proposed by Farrar et al. (2015) They generally found a good correlation between the Stiffness values as measured with the DSR with those measured with the BBR. However, they did not find much correlation between limiting temperatures based on m-values measured in the DSR and BBR. Part of their reasoning for some poor correlations was due to high wax contents in bitumens, but this could not fully explain the discrepancy in m-value.

Similarly, Oshone (Oshone, 2018) proposed an empirical function that could be used to determine Stiffness based on complex shear modulus (Equation 3.6) and m-value based on phase angle (Equation 3.7). These functions were based on a linear fit of DSR versus BBR data.

$$S(t) = 1.28G^*(\omega) + 19.2 \quad (3.6)$$

$$m = 0.008\delta + 0.1 \quad (3.7)$$

The functions provided by Oshone (2018) are similar to the ones used in the study by Lu et al. (2017), which are originally from Anderson et al. (1994) Both are designed to provide a simple criteria based on data that can be obtained from a DSR frequency sweep (complex modulus and phase angle). Both are also linear functions which are derived based on empirical correlations between DSR and BBR testing. In summary, the methods used

in the literature include both interconversion-based methods based on linear viscoelastic theory and approximation-based methods.

### 3.8.1 Methods and Materials

Eleven virgin asphalt binders were selected from various producers in the southern region of the United States. These binders were short-term aged for 85 minutes in the Rolling Thin Film Oven (RTFO), and then long-term aged for 20 hours in the Pressure Aging Vessel (PAV), as is typical for asphalt binders in the United States. Table 3.2 shows the binders selected for evaluation in this study. It is important to note that binders with a temperature interval of 92 or above (e.g. PG 70-22 or 76-22) are generally polymer-modified. Also, these binders were being used in the state of Texas that has an elastic recovery requirement for such binders, which is typically achieved using elastomers.

**Table 3.2. Asphalt Binders Evaluated in the Present Study**

<b>Binder</b>	<b>Label High Grade</b>	<b>Label Low Grade</b>
1	70	-22
2	64	-22
3	76	-22
4	64	-22
5	58	-28
6	76	-22
7	64	-22
8	76	-28
9	70	-28
10	70	-22
11	64	-22

Specimens of the PAV-aged binder were tested according to the standard ASTM procedure, D6648. The BBR test was conducted using at least two replicates for each binder at three different temperatures (16°C, 10°C, and 4°C above the lower grade temperatures). These data were then used to determine the continuous grade of the binder based on the Stiffness and m-value. Then, specimens of both RTFO and PAV-aged binder were tested using the 4 mm plate procedure. Before making these measurements the compliance of the instrument was measured by freezing the upper and lower DSR plates together using ice. An amplitude sweep was carried out using amplitudes ranging from 100 to 30000

$\mu N * m$  of torque at a frequency of 1 Hz. The torque versus displacement follows a linear relationship and its slope is used for compliance correction. This compliance correction is then subsequently used while measuring the properties of the asphalt binder similar to the procedure used in previous studies (Sui 2010, Sui 2011, Farrar 2015). Figure ?? shows typical raw data from the 4 mm plate test with an asphalt binder.

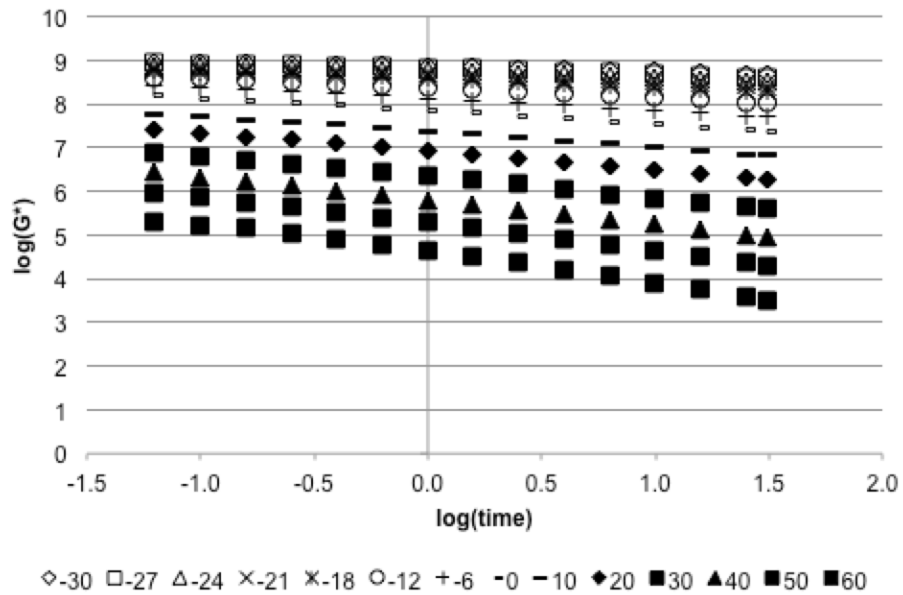


Figure 3.56. Raw data from 4 mm plate test

### 3.8.2 Analysis of Data

Irrespective of the specific (empirical or exact) method used to obtain Stiffness and m-value from the DSR test, as the first step, all methods involve conducting a frequency-temperature sweep test using the DSR followed by development of a master curve using these data. Two types of models were used by Sui et al. (2011) - the Generalized Maxwell model and the Christensen-Anderson-Marasteanu (CAM) model (Equations 3.8 & 3.9). In the present study, a sigmoidal function, shown in Equation 3.10 was also used. The sigmoidal function is often used to describe the behavior of bituminous mixtures, but can also be used to describe the behavior of binders, and has in some cases proven more effective in modeling the behavior of bitumen than other models (Yusoff et al., 2013).

$$G^*(\omega) = G_g \left[ 1 + \left( \frac{\omega_c}{\omega_r} \right)^v \right]^{-\frac{w}{v}} \quad (3.8)$$

$$\delta(\omega) = \frac{90w}{\left[1 + \left(\frac{\omega_c}{\omega_r}\right)^v\right]} \quad (3.9)$$

where:

$G_g$  = glassy modulus

$\omega_c$  = crossover frequency

$v$  = log(2/Rheological Index)

$w$  = constant related to phase angle

$\delta$  = phase angle

$\omega_r$  = reduced frequency

$$\log|G^*| = \delta + \frac{\alpha}{1 + e^{\beta + \gamma \log(\omega)}} \quad (3.10)$$

The time temperature superposition (in frequency domain) was applied to each binder to combine the measured data (Figure ??) into a single master curve (Figure 3.57). Note that the measurements are for complex shear modulus or  $G^*(\omega)$  in frequency domain. By definition, the complex compliance  $J^*(\omega)$  can be obtained from complex shear modulus  $G^*(\omega)$  as a reciprocal at any given frequency. As discussed earlier, there are two main transformations that are required to obtain BBR parameters from the DSR data: (i) converting properties from the frequency domain to the time domain, and (ii) converting shear response to uniaxial response. Therefore the first step is to convert the data from a frequency domain to a time domain.

In previous studies Sui et al. and Farrar et al. (2011, 2015) used the empirical equations proposed by Ninomiya and Ferry (?) (Equation 3.11) for this interconversion. This technique was applied in the present study to the data from the master curves to find  $J(t)$  using  $J^*(\omega)$ . Note that this approach can also be used to determine  $G(t)$  using  $G^*(\omega)$  and by replacing  $J'$  and  $J''$  with  $G'$  and  $G''$ , respectively.

$$J(t) = J'(\omega) - 0.4J''(0.4\omega) + 0.014J''(10\omega) \quad (3.11)$$

In their study, Sui et al. (2010) did not convert the shear compliance from the DSR to the axial compliance, which was relevant to the BBR. Instead, they examined the correlations between the BBR parameters at 60 seconds with shear relaxation modulus  $G(t)$  at 7200 seconds and m-value defined as the slope of  $G(t)$  at 7200 seconds Sui et al. (2010) reported that a good correlation was found and they suggested that a low temperature specification

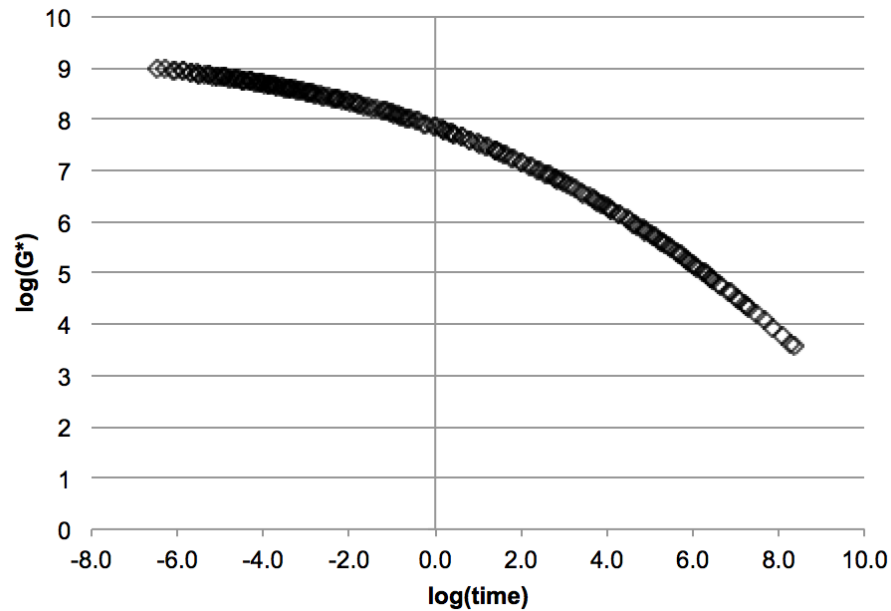


**Figure 3.57. Master curve generated from 4 mm plate test**

of  $G(t) < 160$  MPa and  $m > 0.26$  at the PG temperature was equivalent to the current Superpave specification of  $S(t) < 300$  MPa and  $m > 0.3$  at the PG temperature + 10°C. They later revised their proposed specification (Farrar 2015) to use an equivalent time of 60 seconds for  $G(t) > 143$  MPa and  $m > 0.28$  at the PG temperature + 10°C. Similar to Sui et al. (2010, 2011) and Farrar et al. (2015), Lu et al. (Lu et al., 2017) also proposed equivalent specifications directly based on data from the DSR as shown Table 1.1. Oshone (2018) also proposed criteria which stemmed from an empirical relationship between complex modulus and phase angle measured directly in the DSR and Stiffness and m-value, respectively, measured in the BBR. These relationships are shown in Table 1.1 as well as in Equations 3.6 and 3.7.

One of the objectives of the present study was to examine whether an exact viscoelastic interconversion from  $J^*(\omega)$  to  $J(t)$  followed by conversion from shear compliance to flexural compliance could be used to directly determine the low temperature grade of the binder while still using the criteria for BBR based parameters. The DSR time domain data can then be converted from shear compliance to compliance measured in flexural mode, which is relevant to the BBR test.

One critical assumption made in this study is that the Poisson's ratio is constant. Introducing this assumption not only simplifies the analysis but also avoids the need for



measuring the time-dependent Poisson's ratio, which would in turn require additional experimental modifications and setup. For the purpose of this study, a Poisson's ratio of 0.35 was assumed for all of the binders. Based on this assumption, it was possible to convert the shear compliance data to tensile compliance (Equation 3.12). It is important to highlight that the previous methods, whether drawing correlations between parameters based on  $G(t)$  with the BBR parameters or developing empirical models to correlate BBR stiffness with stiffness from DSR, implicitly assume that the Poisson's ratio is constant across time, temperature, and material.

$$D(t) = \frac{J(t)}{1 + 2\nu} \quad (3.12)$$

An observation from equation 3.12 is that the use of a constant Poisson's ratio has the same effect as vertically scaling the compliance values without necessarily affecting the shape of the curve (which would not be the case for a time-dependent Poisson's ratio). Therefore, the choice of the value of the Poisson's ratio will influence the value of the back calculated Stiffness but it would not influence the value of the back calculated m-value as long as it is reasonable to assume that Poisson's ratio is time independent. The effect of different choices of the constant Poisson's ratio is examined in a later section.

Finally, the BBR Stiffness is easily computed by inverting the individual data points on the creep compliance curve. The reason for doing this is that the BBR Stiffness is not the actual stiffness (relaxation modulus), but instead is obtained using a creep test, and computed as shown in Equation 3.13.

$$S(t) = \frac{PL^3}{48I\delta(t)} \quad (3.13)$$

where:

$P$  = applied load

$L$  = beam length

$I$  = moment of inertia of beam

$\delta(t)$  = time-dependent beam deflection

### 3.8.3 Results using different approaches

In previous studies, researchers have demonstrated an empirical correlation between results from the DSR using the 4 mm geometry and the BBR standard test (Sui 2011, Farrar 2015, Lu 2017) This section presents the results from using different approaches as outlined in

Table 1.1 and also described in the previous section. Results from this study are presented first, followed by results obtained using the approaches by Sui et al. (2010, 2011) and Farrar et al. (2015) and finally using approximate interconversion by Lu et al. (2017).

### **3.8.3.1 Use of sigmoidal function, interconversion to time domain, and conversion for axial loading**

As described earlier, the frequency-temperature data for the eleven binders in this study were obtained using the DSR and 4 mm diameter geometry following the method described earlier. The resulting data were combined to develop a master curve for  $J^*(\omega)$  using the sigmoidal function, which was then converted to  $J(t)$  using the Ninomiya and Ferry approach and finally to  $D(t)$  using Equation 3.12. The  $D(t)$  function was then converted to Stiffness versus time by inverting the compliance at different points in time. The Stiffness and m-value parameters were obtained from this curve at different temperatures and used to determine the continuous grade of the binder. This continuous grade was then compared to the continuous grade based on the Stiffness and m-value obtained at 60 seconds from the BBR test. As mentioned before, a constant Poisson's ratio of 0.35 was initially assumed for all binders and temperatures.

The comparison of DSR and BBR continuous grade based on the Stiffness parameter is shown in Figure 3.58 while the continuous grades based on m-value are compared in Figure 3.59. Overall, the Stiffness continuous grades using this approach were reasonably accurate, with an average error of 7%. However, the continuous grades based on m-value were not as accurate, and had an average error of 27%.

Therefore, other techniques were explored to determine the true low grade of the binder. It was observed that the sigmoidal function generally provided a very good fit for the shifted raw data while developing the master curve. However, the m-value is a highly sensitive parameter, so even though a good fit was obtained, small differences at the frequencies and temperatures of interest caused large variations in the m-value true grade due to compounding errors. Therefore, a second approach was attempted to determine the continuous grade based on the m-value. In this approach, a sigmoidal function was only fit to data from a single temperature without using time-temperature superposition or developing a master curve. This process (fitting the sigmoidal function) was repeated separately for each temperature corresponding to the BBR test, i.e. 16, 10, and 4° above the lower grade temperature of the binder.

As before, the sigmoidal function for  $J^*(\omega)$  was then used with Equation 3.11 to ob-

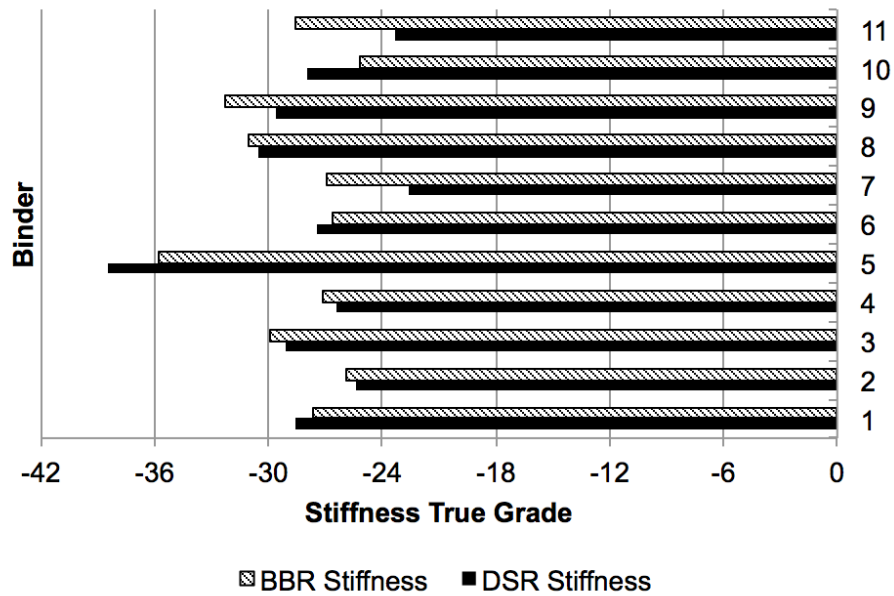


**Figure 3.58. Stiffness true grades of the binders in this study based on the master curve created using the sigmoidal function compared to BBR Stiffness true grades**

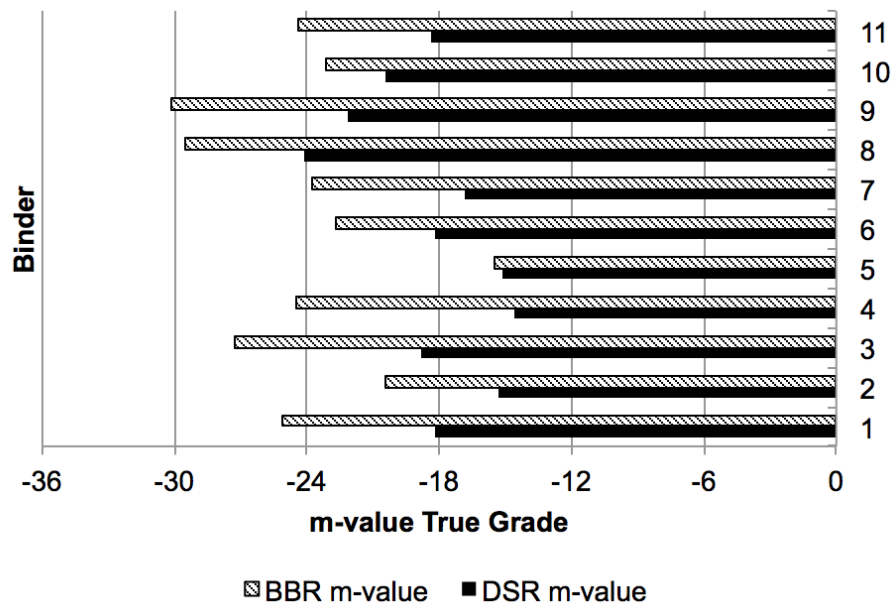


**Figure 3.59. m-value true grades of the binders in this study based on the master curve created using the sigmoidal function compared to BBR Stiffness true grades**

tain  $J(t)$  followed by computation of  $D(t)$  using Equation 3.12 and Stiffness and m-value by inverting  $D(t)$ . The main difference here was that the process was being carried out separately for each temperature instead of fitting a master curve.

A comparison of the m-value obtained from this process with the m-value from the BBR test revealed that there was a strong linear correlation between the two but with a slight bias (Figure 3.62). In order to address this, the m-value criterion proposed by Farrar et al. (Farrar et al., 2015) of 0.28 was applied instead of using 0.3 to determine the continuous grade. This provided a much more accurate estimate of continuous temperature grade based on m-value with an average error of 8% (Figure 3.60)

The overall linear relationship between Stiffness measured in the DSR and BBR using this method is shown in Figure 3.61. The linear relationship between m-value measured in the DSR and BBR using this approach is shown in Figure 3.62.

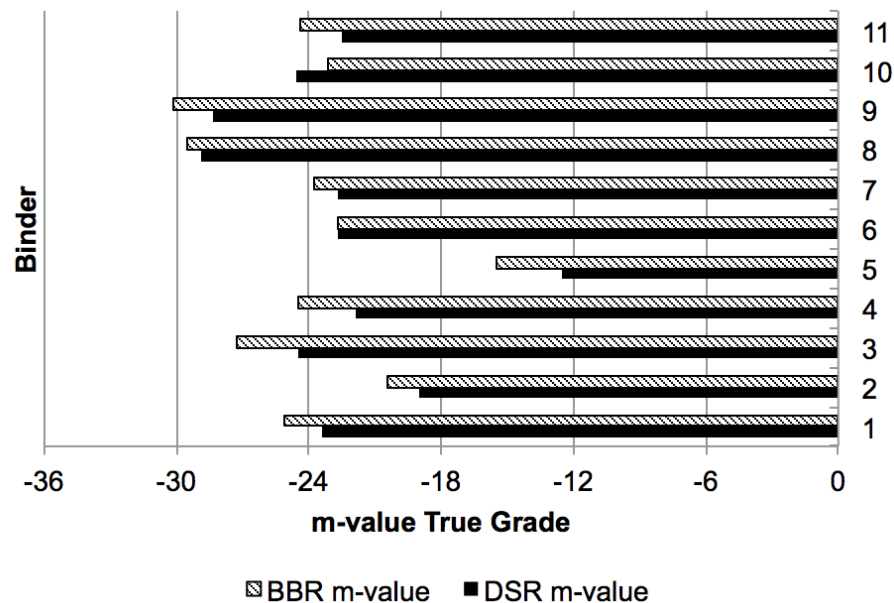


**Figure 3.60. m-value true grades of the binders in this study based on the raw data at BBR temperatures compared with BBR m-value true grades**

### 3.8.3.2 Use of CAM model, interconversion to time domain, and correlation with BBR S and m-value

The data from the 11 binders was also used with the methods developed by Sui et al. (2010, 2011) and Farrar et al. (2015). In this case, the data from the frequency-temperature

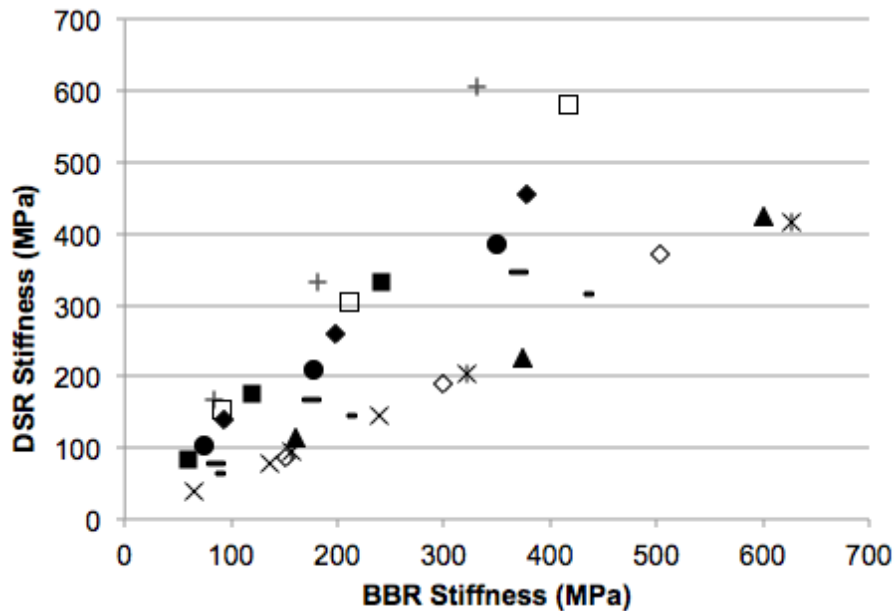


**Figure 3.61. Correlation between Stiffness measured in the DSR and BBR using the raw data at each temperature and Ninomiya-Ferry interconversion (each symbol represents one asphalt binder)**

sweep was used to develop a master curve using the CAM model and time-temperature superposition. The resulting master curve had a very good fit at lower temperatures, as has been shown with the use of the CAM model. For the data points taken below 0°C, the error was generally no more than 5% between the raw data and fitted function. Based on this fit followed by interconversion to time domain using the Ninomiya-Ferry (Equation 3.11), the equivalent  $G(t)$  and slope of the curve (m-value) were determined for each binder at the three BBR temperatures. This was then used to determine the limiting temperatures based on criterion for stiffness and m-value as described by Farrar et al. (2015). The limiting stiffness and m-value temperatures compared with their DSR counterparts for each binder are shown in Figures 3.63 and 3.64 respectively.

Overall, the method proposed by Farrar et al. resulted in a good estimate of the Stiffness true grade, with an average error of 10%. The m-value had an average error of 19%. However, it is notable that binder 5 was a significant outlier in this data set, and if this binder is removed, the error is only 11% on average overall. It is important to note that this binder's error was only observed when using the CAM model, but not with the sigmoidal model of the same data, and was consistently present among multiple replicates of data and

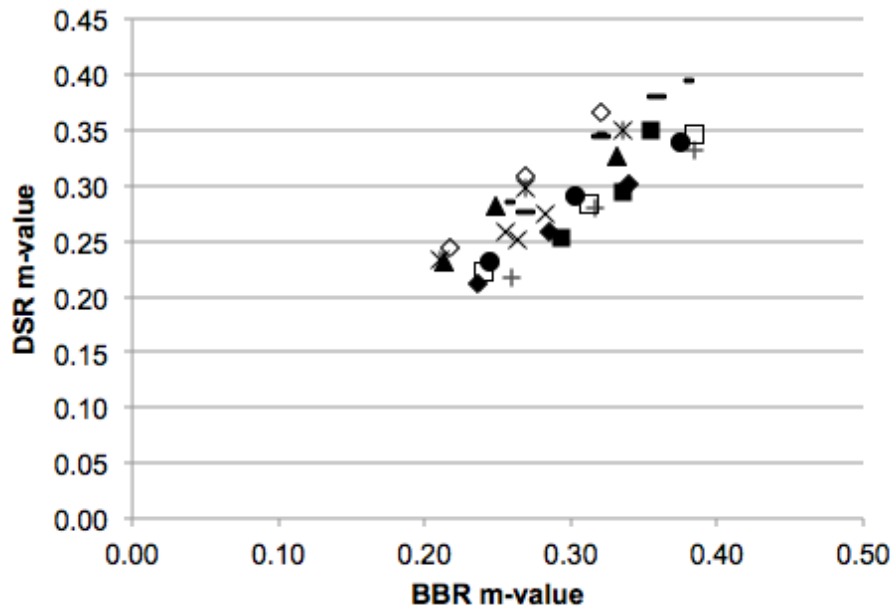


Figure 3.62. Correlation between m-value measured in the DSR and BBR using the raw data at each temperature and Ninomiya-Ferry interconversion (each symbol represents one asphalt binder)

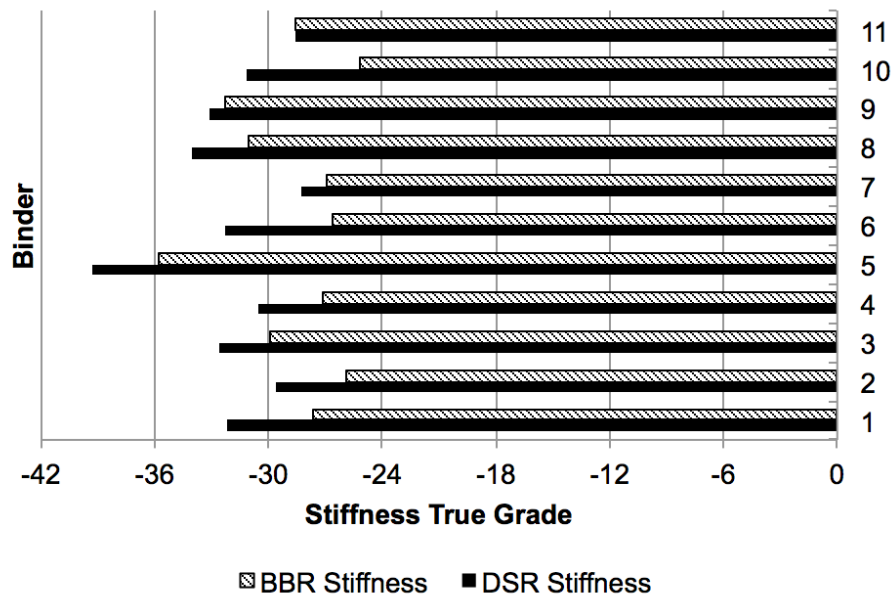
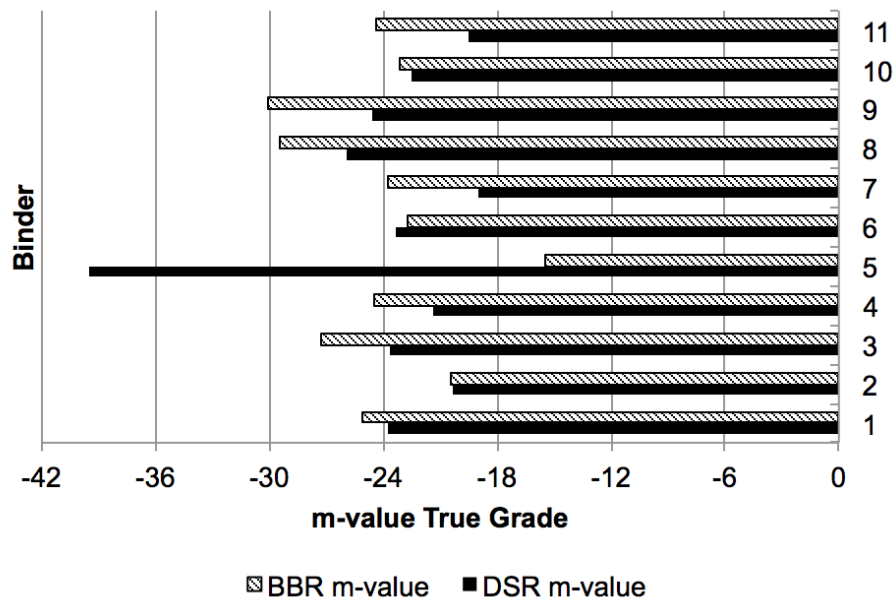


Figure 3.63. Stiffness true grades of the binders in this study based on the Farrar et al. method compared with BBR Stiffness true grades



**Figure 3.64. m-value true grades of the binders in this study based on the Farrar et al. method compared with BBR m-value true grades**

even after attempting to fit the CAM model with several different starting points.

### 3.8.3.3 Use of CAM model and approximate correlation with BBR S and m-value

In addition to the above methods, data from the 11 binders were also evaluated using the approximate method shown in Lu et al. (2017). This approximation as shown in Equation 3.5 was used to compute the shear relaxation modulus at a time that was defined as the inverse of the frequency. The approximation used to estimate the m-value was simply the phase angle at the time and temperature of interest divided by 90. The study by Lu et al. used the same criteria for grading the binders that Farrar et al. used, i.e. stiffness of 143 MPa and m-value of 0.28 at the equivalent time of 60 seconds. Note that Lu et al. used a module available in their rheometer software to construct the master curve. In the present study, since this module was not available, the CAM master curve used in the method developed by Sui et al. (Sui et al., 2011) and Farrar et al. (Farrar et al., 2015) was also used for this method.

The results from method are shown in Figures 3.65 and 3.66. The error between the DSR Stiffness using this method was 8%, while the error in computing the m-value true grade was 36%. In fact, this finding was consistent with the findings reported by Lu et al.

(2017) as well, i.e. the method had a good correlation with the Stiffness true grade, but not the m-value true grade.

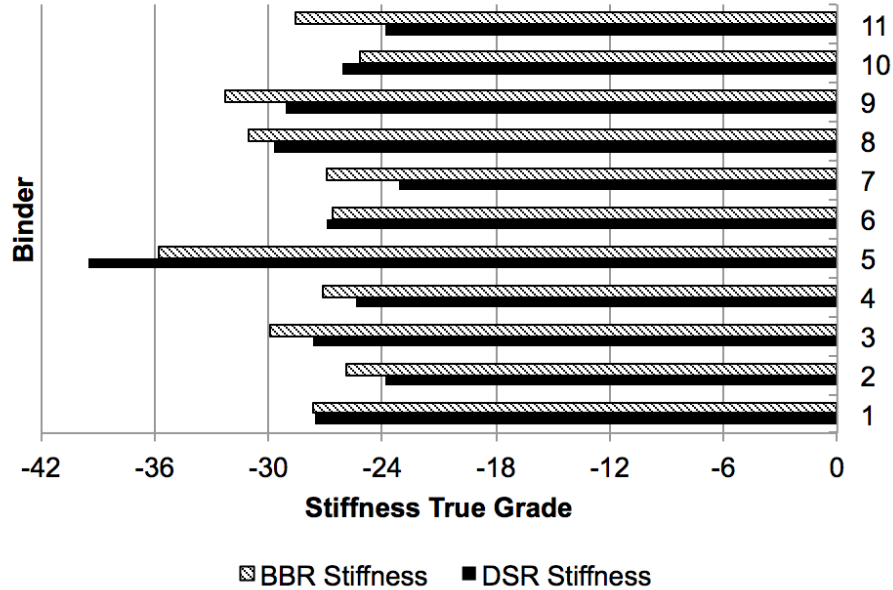


**Figure 3.65. Stiffness true grades of the binders in this study based on the method used by Lu et al. compared with BBR Stiffness true grades**

### 3.8.4 Sensitivity to Poisson’s Ratio

Some of the previous work in this area has avoided converting the data from shear stiffness measured in the DSR to flexural stiffness. Such a conversion requires the knowledge of the time-temperature-binder specific Poisson’s ratio. Measurement and use of time-temperature-material dependent Poisson’s ratio is possible but would require a substantial increase in experimental and analytical processing. Therefore, it is important to assess sensitivity and impact of assuming a constant Poisson’s ratio for all binders in the method described earlier. Note that this assumption is implicit even when the goal is not an exact conversion from shear to flexural properties but rather an empirical correlation between shear and flexural parameters.

In order to assess the sensitivity of the Poisson’s ratio on the Stiffness conversion, two different constant Poisson’s ratios were assumed, 0.35 and 0.45. As discussed earlier, when assumed to be time-independent, the Poisson’s ratio only effects the Stiffness parameter, but not the m-value parameter, as it results in a vertical scaling of the compliance curve, but



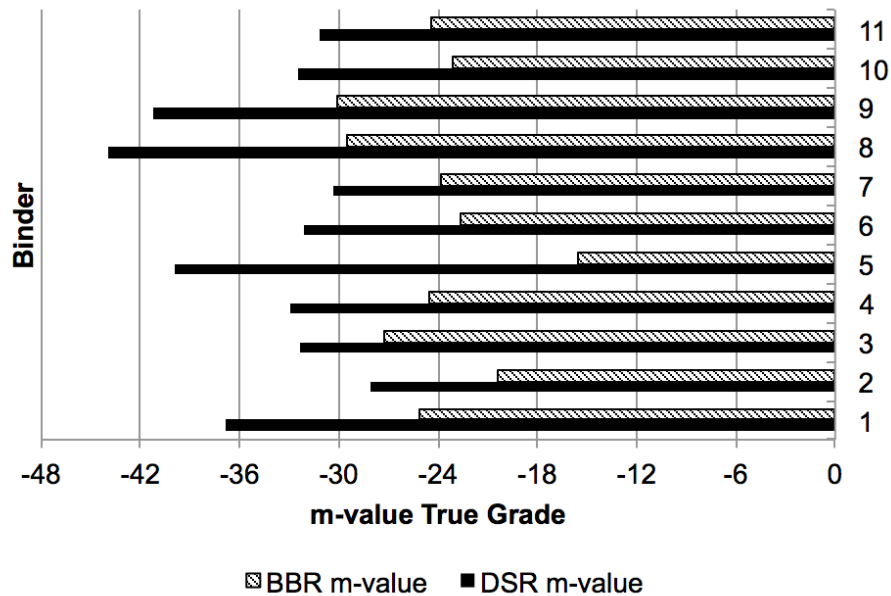


**Figure 3.66. m-value true grades of the binders in this study based on the method used by Lu et al. compared with BBR m-value true grades**

does not influence its slope. The encouraging results in predicting m-values suggests that it is reasonable to assume that the Poisson’s ratio is time dependent for different binders, particularly at the temperatures of interest. Results shown in Figure 3.67 indicate that a change of this magnitude only results in a small change in the overall continuous grade of the binder.

However, Figure 3.61 reveals that the Stiffness values obtained from inter converting shear to flexure appear to have a systematic bias when compared to the analogous parameter obtained using the BBR. Even more interesting is the fact that there appear to be two different linear trends for two different sets of binders. These linear trends (that converge to the origin) suggest that perhaps a temperature-dependent Poisson’s ratio would be more appropriate for use in such interconversion. To be more precise, perhaps two different temperature-dependent Poisson’s ratio may be more appropriate for each set of binder. However, estimating this a priori would defeat the purpose of using the 4 mm geometry. Notwithstanding this systematic bias, results from Figures 3.67 and 3.58 indicate that assuming a constant Poisson’s ratio across temperatures and binders does result in a reasonably accurate estimate for the stiffness of the binder, at least for the purposes of such interconversion and estimation.

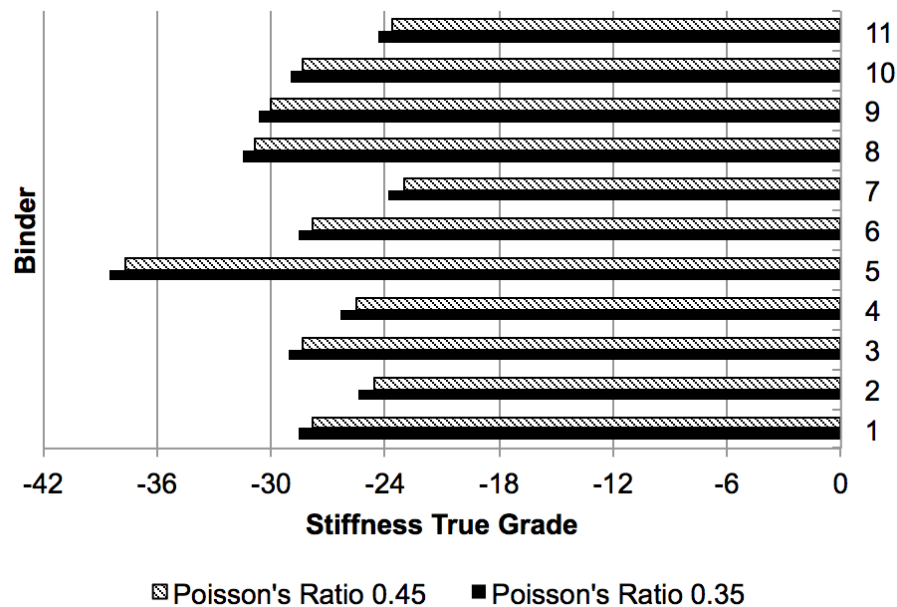


**Figure 3.67. Effect of assuming different Poisson ratios on the Stiffness true grade as computed in the present study**

### 3.8.5 Discussion of 4 mm plate

This study reviews many of the techniques available for analyzing data produced using the 4 mm diameter plate geometry with the Dynamic Shear Rheometer (DSR) and aged binders and evaluates the applicability of using the DSR for low temperature characterization of asphalt binders as an alternative to using the Bending Beam Rheometer (BBR).

The following conclusions are drawn from the results of this study:

1. Results from this study verify the feasibility of estimating the PG continuous low grade of a binder based on its Stiffness and m-value using data obtained from a frequency sweep test in the DSR.
2. The Stiffness based continuous low grade can be obtained by many methods with good accuracy, i.e. with an average of less than 10% error using BBR values as the benchmark. These methods include fitting the data to a master curve using time-temperature superposition with either sigmoidal or CAM model, and then interconverting the data to time domain. After this step it is either possible to assume a constant Poisson's ratio and predict the response from the BBR OR to use an empirical correlation between the DSR and BBR data to estimate the continuous grade

based on Stiffness.

3. The accuracy of the back calculated m-value continuous low grade using the DSR when compared to the BBR varied depending on the method of analysis. The method proposed by WRI (Sui 2010, Sui 2011, Farrar 2015) using the CAM model generally worked effectively for computing the true m-value low grade with the exception of one very soft binder. However, it is important to note that the m-value is a highly sensitive parameter, which can result in large errors when overall the data apparently fits very well to a master curve but may have small variances at the temperature and frequency of interest. The method from the present study, i.e. fitting data from frequency-temperature curve separately for each temperature and then converting to  $J(t)$  provides a better and more robust estimate for m-value.
4. The assumption of a constant Poisson's ratio amounts to a vertical scaling of the master curve and therefore does not have an impact on the m-value. The effect of Poisson's ratio on the continuous grade based on Stiffness is also minimal, as varying the Poisson's ratio from 0.35 to 0.45 changes the Stiffness true grade by less than 1 degree for all of the binders evaluated in this work. Further studies are required to determine the effect of the time-dependent Poisson's ratio on low temperature properties and the m-value.
5. The 4 mm plate test has good repeatability. The average single operator error for the m-value was lower than the allowable single operator error in the BBR specification. The average single operator error for the Stiffness parameter in the DSR was slightly higher than the allowable BBR error. Further work is necessary to determine if the operator error for the m-value is consistent and the error for the Stiffness parameter should be considered allowable or be improved.



## **CHAPTER 4. MIXTURE TESTING AND COMPARISON WITH BINDER TESTING**

### **4.1 MIXTURE TEST METHODS**

In the previous chapter, the binder tests performed were described in detail. However, the binder tests alone cannot provide insight into their effectiveness in predicting the binder's behavior in a mix. In this portion of the study, mixture tests were conducted to determine their relationship with the binder tests that were previously evaluated. The idea behind this study was to use a single mix design and keep aggregates, gradation, and binder content constant, while using different binders that were previously evaluated.

#### **4.1.1 Hamburg Wheel Tracking Device Test**

Two methods were selected for mixture evaluation. The Hamburg Wheel Tracking Device (HWTD) is commonly used by TxDOT to evaluate rutting resistance and moisture susceptibility of asphalt mixtures. The test is performed on two asphalt specimens with the ends cut off placed adjacent to each other in a polymer mold. These specimens are compacted using the Superpave Gyrotory Compactor (SGC). A steel wheel applies a total load of 156 lb to each pair of specimens at a rate of 50 passes per minute. During the test, the specimens are submerged underwater at a temperature of 50°C. Typically, the failure criteria is 0.5 inches of permanent deformation at the center of the specimen. However, the requirement to pass the current specification for this test is based on the high PG grade of the binder, which is thought to be very related to rutting resistance. A mix using PG 64 binder must pass at least 10,000 cycles of loading before the failure criteria is reached, while mixes of PG 70 and PG 76 must reach 15,000 and 20,000 cycles respectively to pass the current specification.

#### **4.1.2 Overlay Test**

To evaluate the fatigue cracking resistance of mixtures, the Texas Overlay Test was used in this study. The Overlay Test uses a specimen compacted using the SGC and then cut into a 3 inch wide, 1.5 inch thick test specimen. This specimen is glued using high strength epoxy to two metal plates with a 4.2 mm gap between them. The epoxy is allowed to cure overnight with a 5 lb weight on top of the specimen to ensure proper bonding. The specimen is then fixed into the testing apparatus and conditioned at 25°C. Once the specimen has

been fully conditioned, triangular loading cycles are applied at 10 seconds per cycle with a displacement-controlled amplitude of 0.6 mm. In the past, the primary parameter that has been used to define performance in this test is the number of cycles until some reduction in the maximum load was observed. However, new parameters have recently been proposed by TxDOT to better evaluate performance in this test and achieve better repeatability.

The first parameter is the critical fracture energy. This parameter is considered in order to evaluate the resistance of a mixture to forming an initial crack. This parameter is calculated based on the area under the load-displacement curve during the first cycle of loading until the peak load is achieved, which is defined as the fracture area. That parameter is then divided by the cross-sectional specimen area at the gap to determine the critical fracture energy (Equation 4.1).

$$G_c = \frac{W_c}{b * h} \quad (4.1)$$

where:

$W_c$  = fracture area

$b$  = specimen width

$h$  = specimen thickness

The second parameter considered is the crack resistance index. This parameter describes the mixture's resistance to crack growth, and in turn degradation of the peak load in each cycle. This parameter is determined by fitting the peak load vs. number of cycles curve to an exponential function (Equation 4.2). The crack resistance index is represented by the constant  $\beta$ .

$$y = x^{(0.0075\beta - 1)} \quad (4.2)$$

## 4.2 MIX DESIGN AND MATERIALS

The materials used were described in previous task summaries. To summarize, silicious and limestone aggregates were obtained from suppliers in central Texas. The binders used were those described from the binder testing chapter, with both the laboratory-produced binders and field binders tested. A Superpave mix design from an existing Job Mix Formula (JMF) used by a contractor for the TxDOT was adopted for this study. The gradation used is listed in Table 4.1. The optimum binder content from the JMF, 5.7% was used in this study.

**Table 4.1. Aggregate gradation**

Sieve size(inch)	Sieve size (mm)	Cumulative % passing
3/4"	19.50	100.0
1/2"	12.50	99.8
3/8"	9.50	93.2
No. 4	4.75	68.7
No. 8	2.36	42.1
No. 16	1.18	27.3
No. 30	0.60	18.6
No. 50	0.30	11.5
No. 200	0.08	5.1
Pan	0.00	0.0

### **4.3 MIXTURE TEST RESULTS**

Both the Hamburg Wheel Tracking Device and overlay tests were conducted on specimens compacted with many different binders from the study. The number of cycles versus rut depth for the HWTD test for mixtures with each binder that was evaluated is shown in Figure 4.1. Figure 4.2 shows the critical fracture energy for the mixtures using each different binder, and figure shows the crack resistance index for the same mixtures as obtained in the overlay test.

### **4.4 COMPARISON WITH BINDER TESTING**

It was critical in this study to determine the relationship between the new binder test methods and the mixture properties when those binders were used. The high temperature properties of the binder were evaluated compared to the HWTD, since this test deals with rutting resistance, while the intermediate and low temperature tests were evaluated against the results of the overlay test, since they are thought to be indicators for cracking.

The following parameters were compared for high temperature:

1. High PG Grade vs. HWTD Cycles to Failure (Figure 4.4)
2. MSCR  $J_n r$  (100 Pa) vs. HWTD Cycles to Failure (Figure 4.5)
3. MSCR %ER (100 Pa) vs. HWTD Cycles to Failure (Figure 4.6)
4. MSCR  $J_n r$  (3200 Pa) vs. HWTD Cycles to Failure (Figure 4.7)
5. MSCR %ER (3200 Pa) vs. HWTD Cycles to Failure (Figure 4.8)

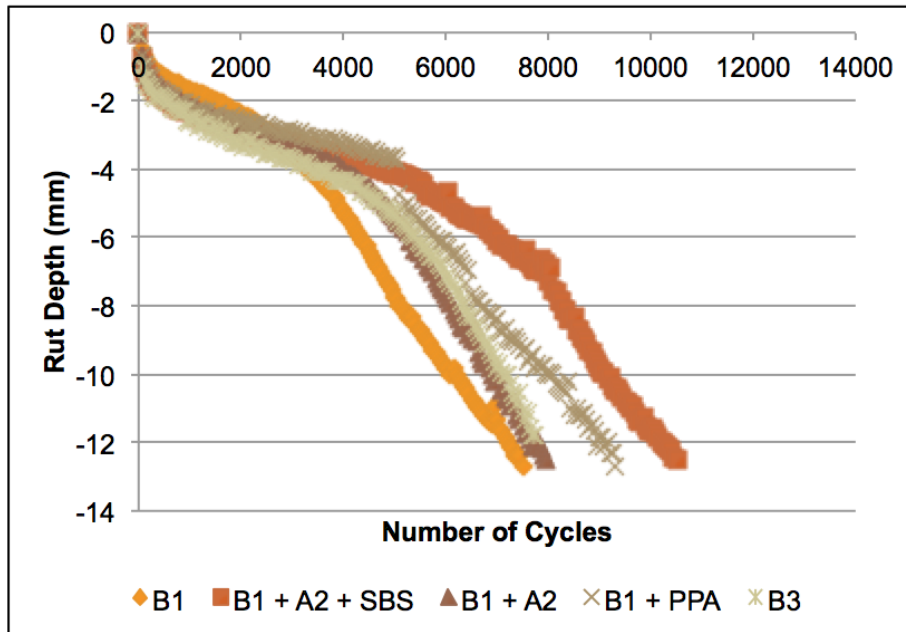


Figure 4.1. Results of Hamburg Wheel Tracking Device test for binders in this study

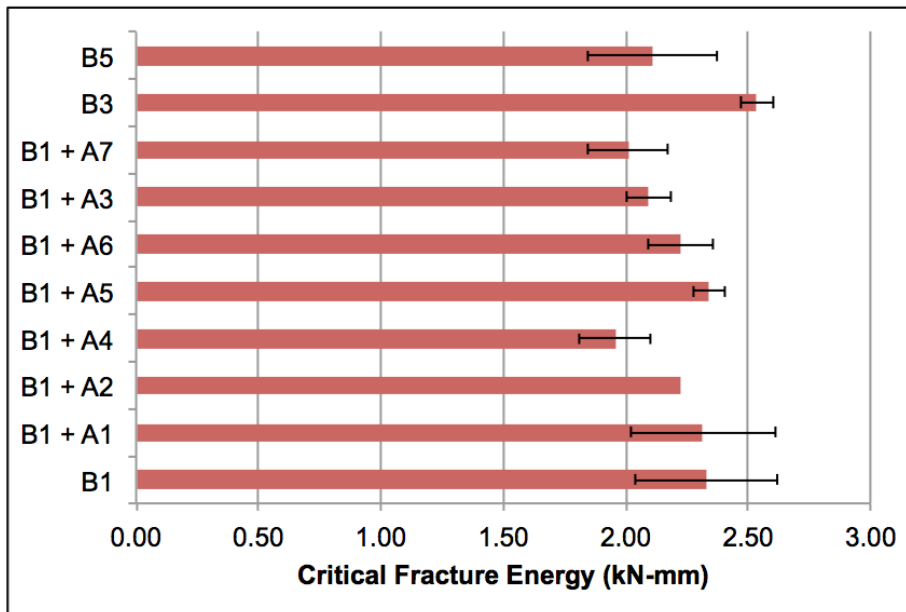


Figure 4.2. Critical Fracture Energy for mixes made with different binders from this study

For the purposes of this study, a temperature of 64°C was examined for the MSCR test, since this temperature has been shown to have good correlation in previous studies.



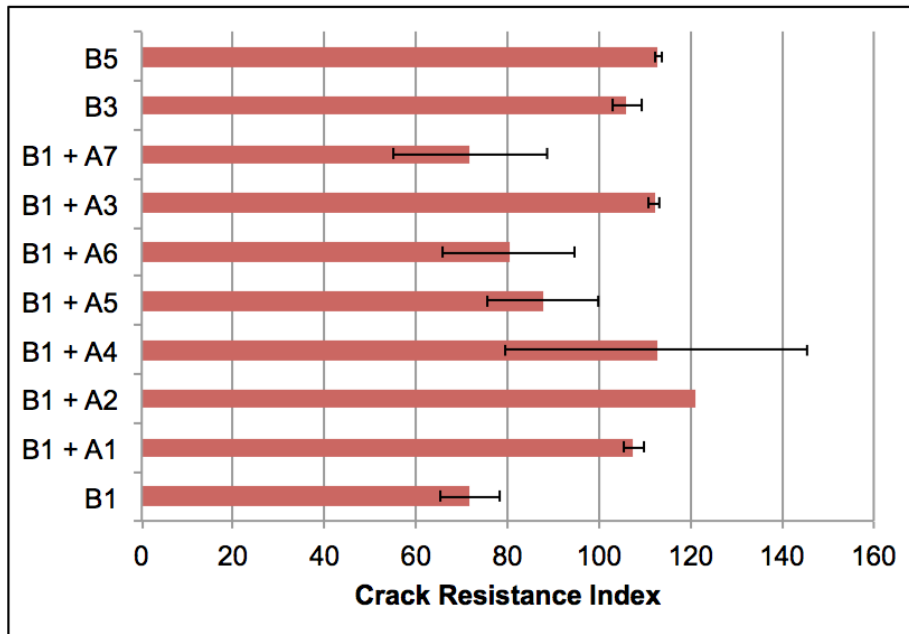


Figure 4.3. Crack Resistance Index for mixes made with different binders from this study

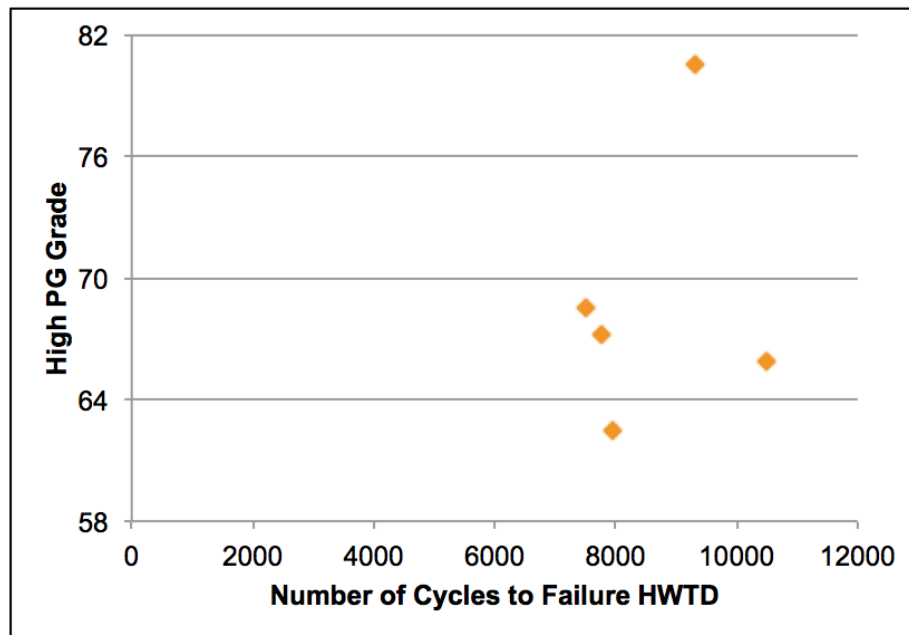
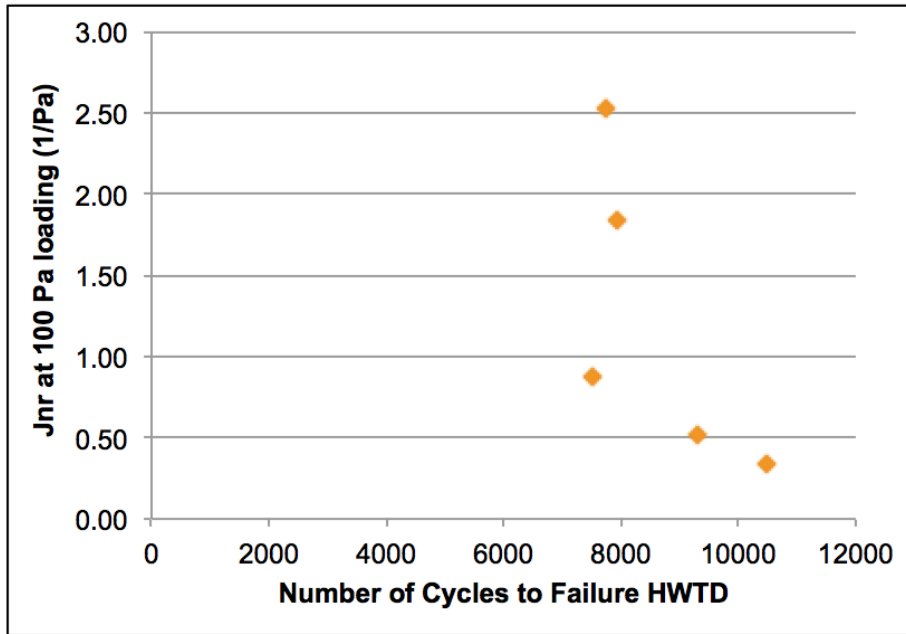
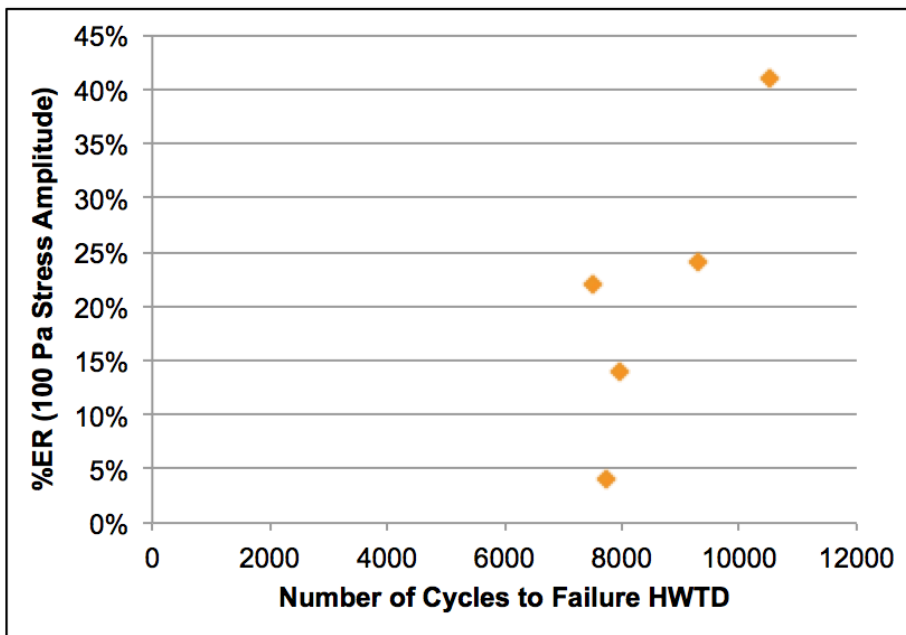


Figure 4.4. PG High Temperature vs. Number of Cycles to Failure



**Figure 4.5. Non-Recoverable Compliance at 100 Pa loading amplitude vs. Number of Cycles to Failure**



**Figure 4.6. Percent Elastic Recovery at 100 Pa loading amplitude vs. Number of Cycles to Failure**

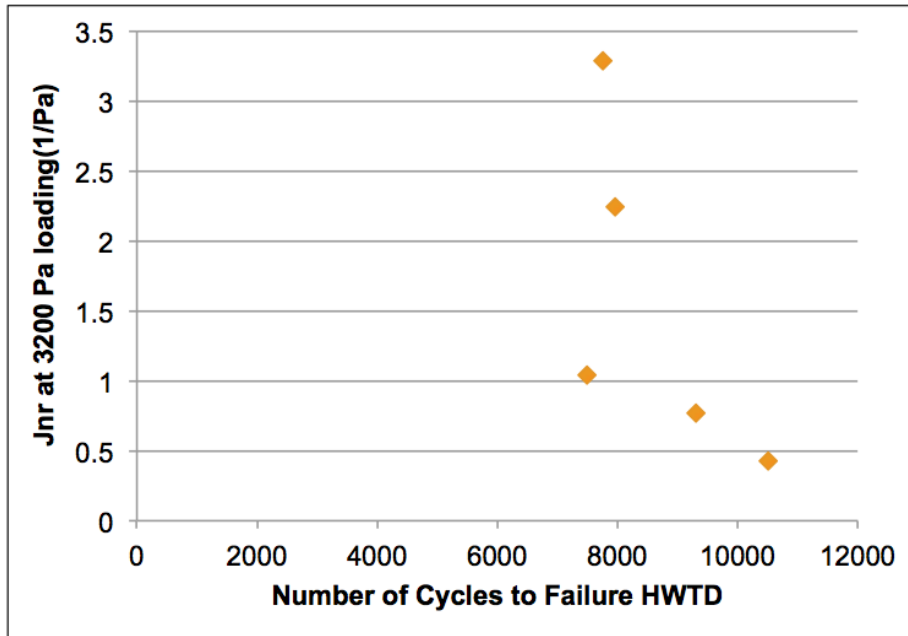


Figure 4.7. Non-Recoverable Compliance at 3200 Pa loading amplitude vs. Number of Cycles to Failure

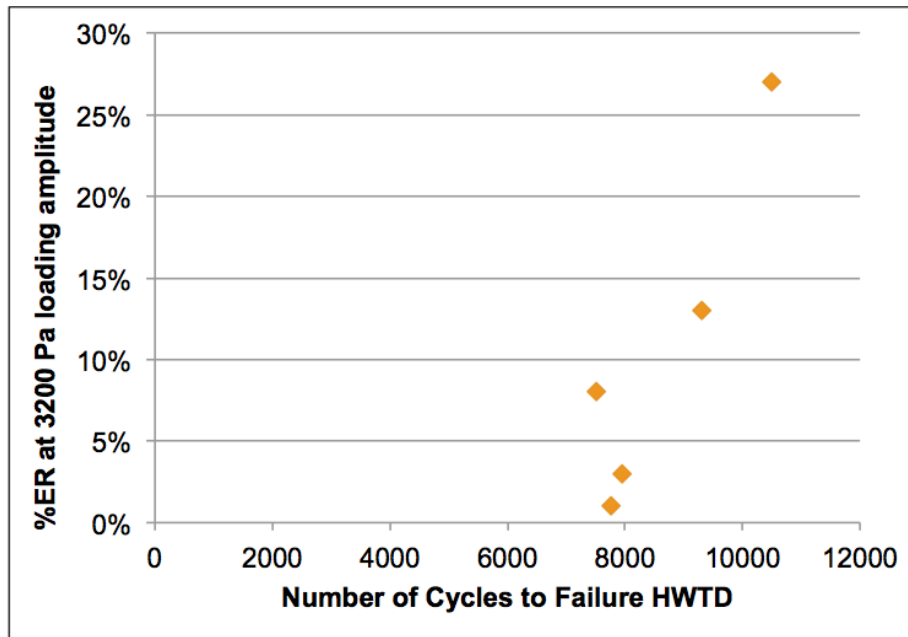


Figure 4.8. Percent Elastic Recovery at 3200 Pa loading amplitude vs. Number of Cycles to Failure

For the intermediate temperature properties, the following parameters were evaluated:

1. PG Intermediate Temperature Parameter vs. Critical Fracture Energy (Figure 4.9)
2. PG Intermediate Temperature Parameter vs. Crack Resistance Index (Figure 4.10)
3.  $\Delta T_c$  vs. Critical Fracture Energy (Figure 4.11)
4.  $\Delta T_c$  vs. Crack Resistance Index (Figure 4.12)
5. Glover-Rowe Parameter vs. Critical Fracture Energy (Figure 4.13)
6. Glover-Rowe Parameter vs. Crack Resistance Index (Figure 4.14)
7. Poker Chip Strength (PAV) vs. Critical Fracture Energy (Figure 4.15)
8. Poker Chip Strength (PAV) vs. Crack Resistance Index (Figure 4.16)
9. Poker Chip Strength (RTFO) vs. Critical Fracture Energy (Figure 4.17)
10. Poker Chip Strength (RTFO) vs. Crack Resistance Index (Figure 4.18)
11. Crossover Modulus vs. Critical Fracture Energy (Figure 4.19)
12. Crossover Modulus vs. Crack Resistance Index (Figure 4.20)

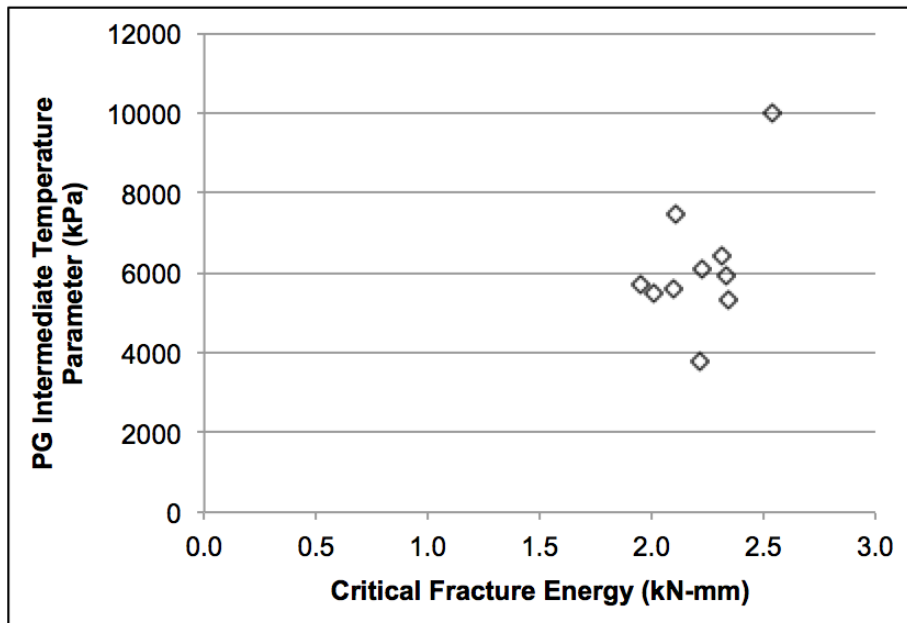


Figure 4.9. PG Intermediate Temperature Parameter vs. Critical Fracture Energy

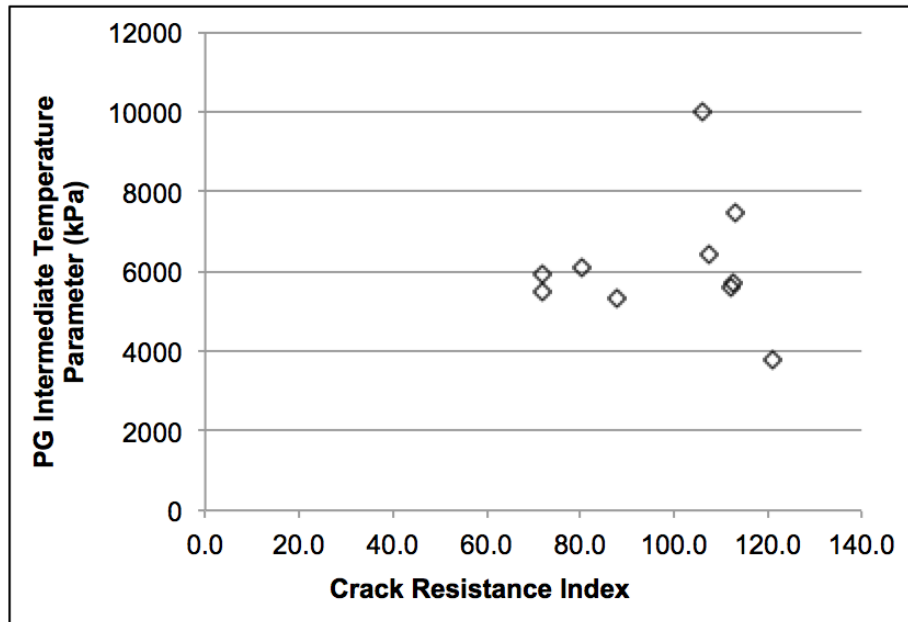


Figure 4.10. PG Intermediate Temperature Parameter vs. Crack Resistance Index

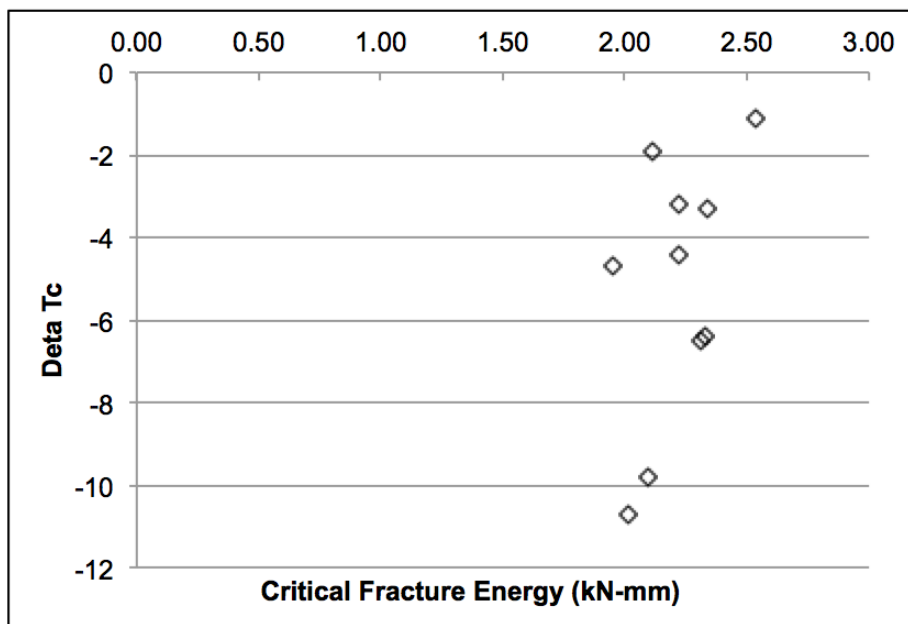


Figure 4.11.  $\Delta T_c$  vs. Critical Fracture Energy

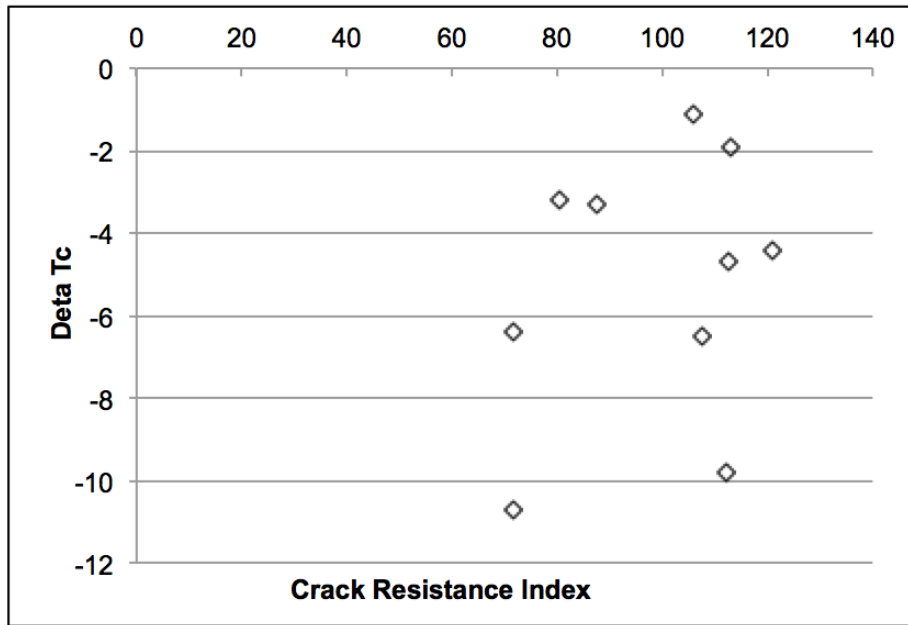


Figure 4.12.  $\Delta T_c$  vs. Crack Resistance Index

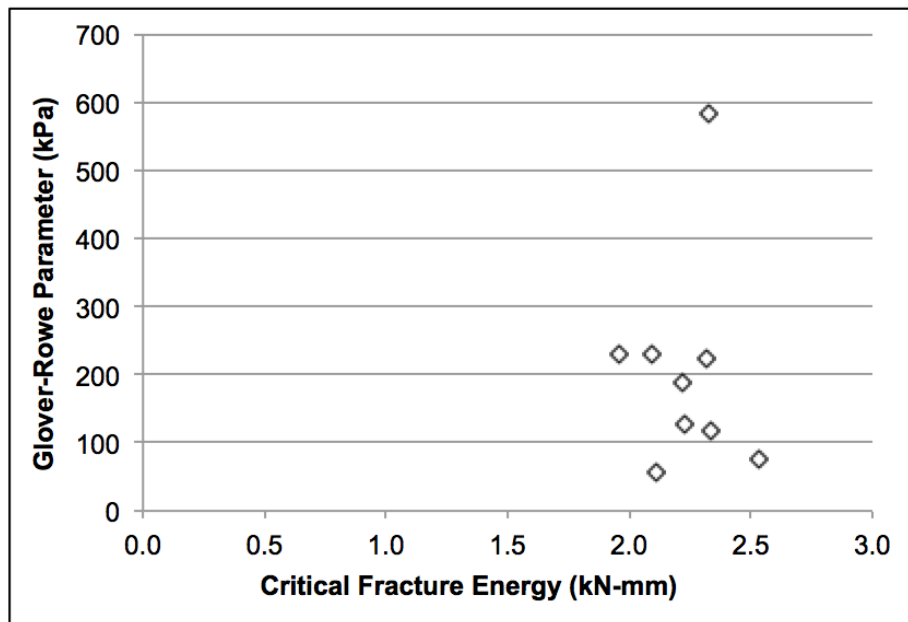


Figure 4.13. Glover-Rowe Parameter vs. Critical Fracture Energy

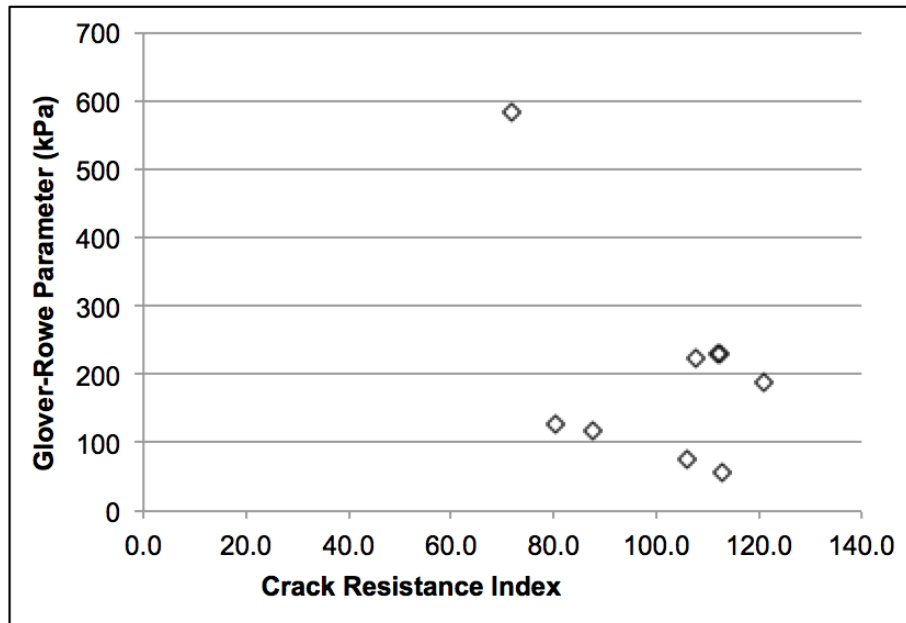


Figure 4.14. Glover-Rowe Parameter vs. Crack Resistance Index

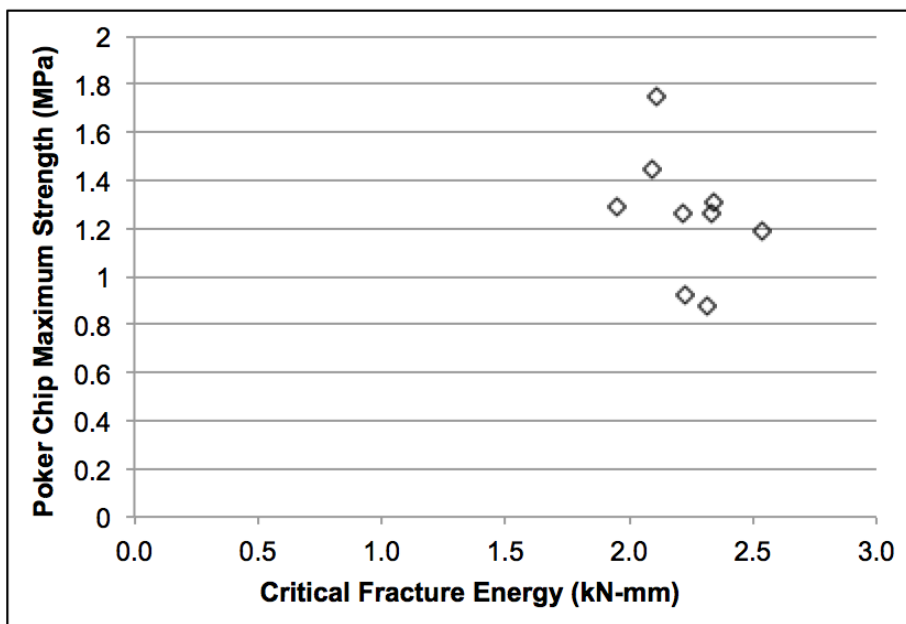


Figure 4.15. PAV-aged Poker Chip Strength vs. Critical Fracture Energy

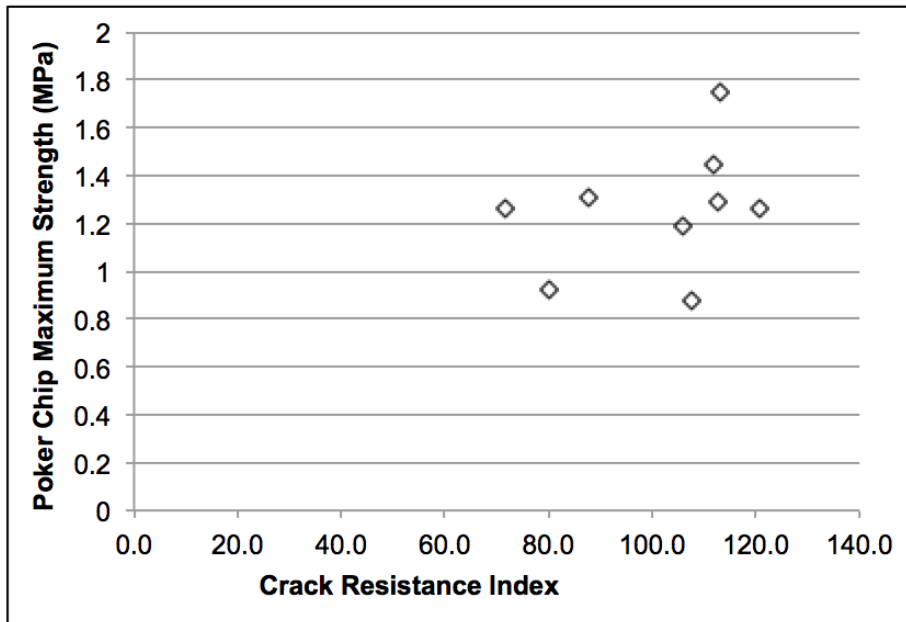


Figure 4.16. PAV-aged Poker Chip Strength vs. Crack Resistance Index

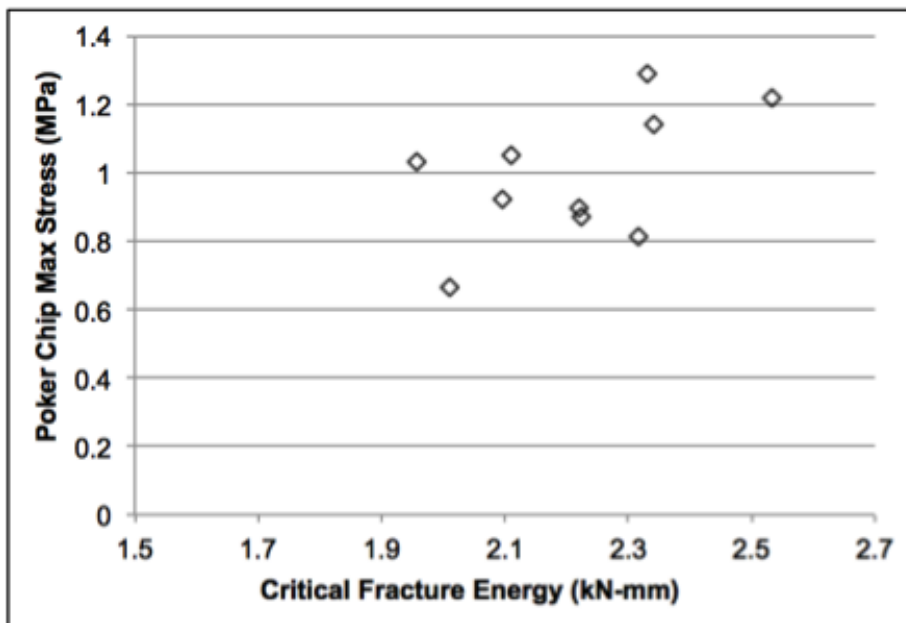


Figure 4.17. RTFO-aged Poker Chip Strength vs. Critical Fracture Energy



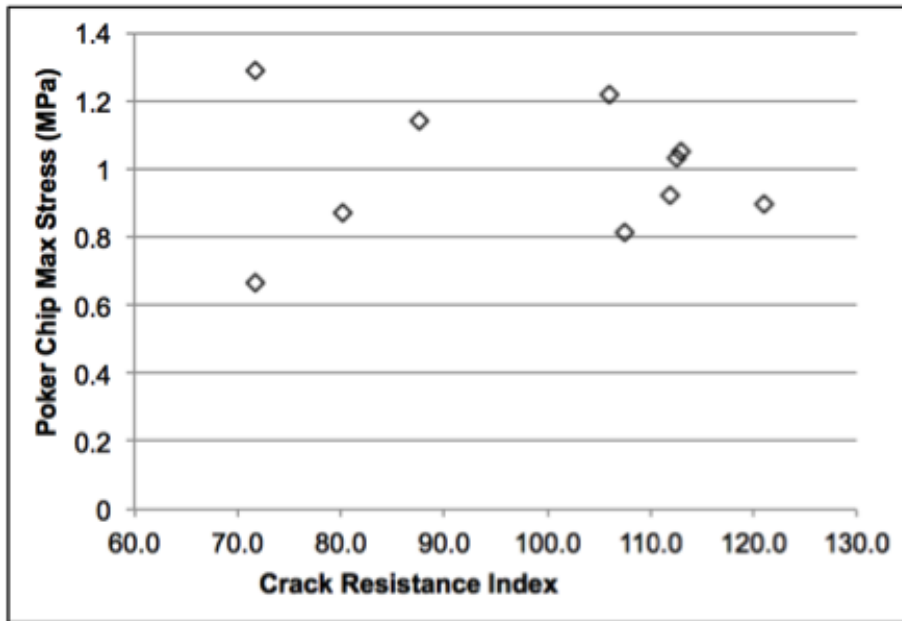


Figure 4.18. RTFO-aged Poker Chip Strength vs. Crack Resistance Index

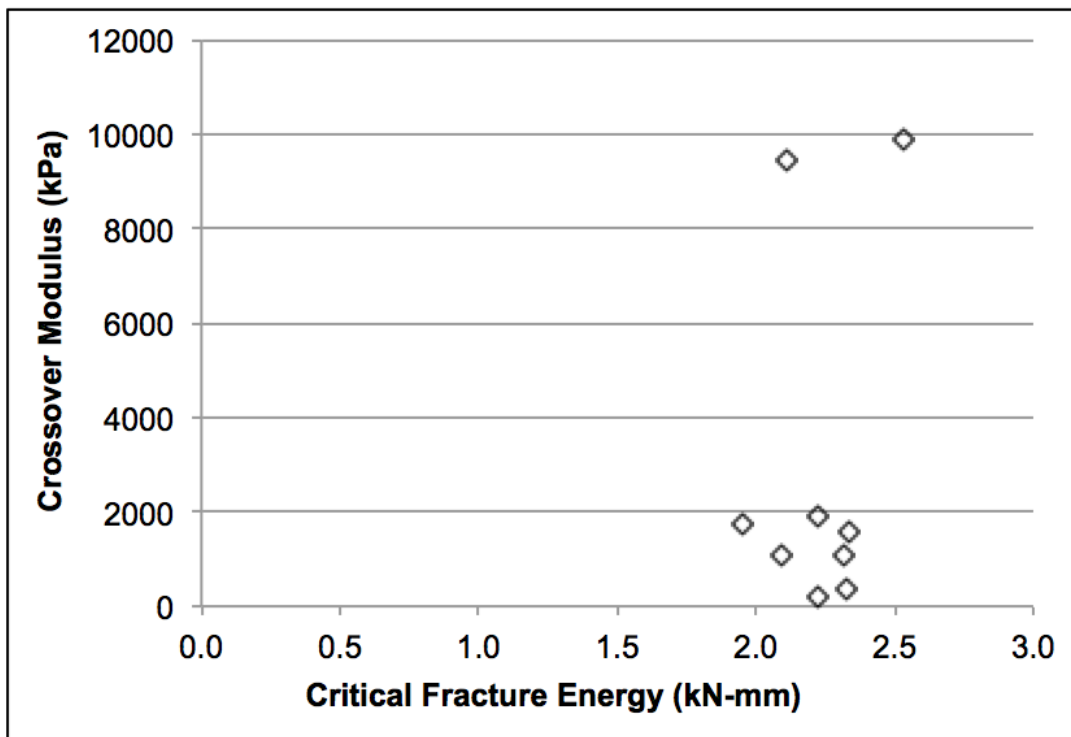


Figure 4.19. Crossover Modulus vs. Critical Fracture Energy

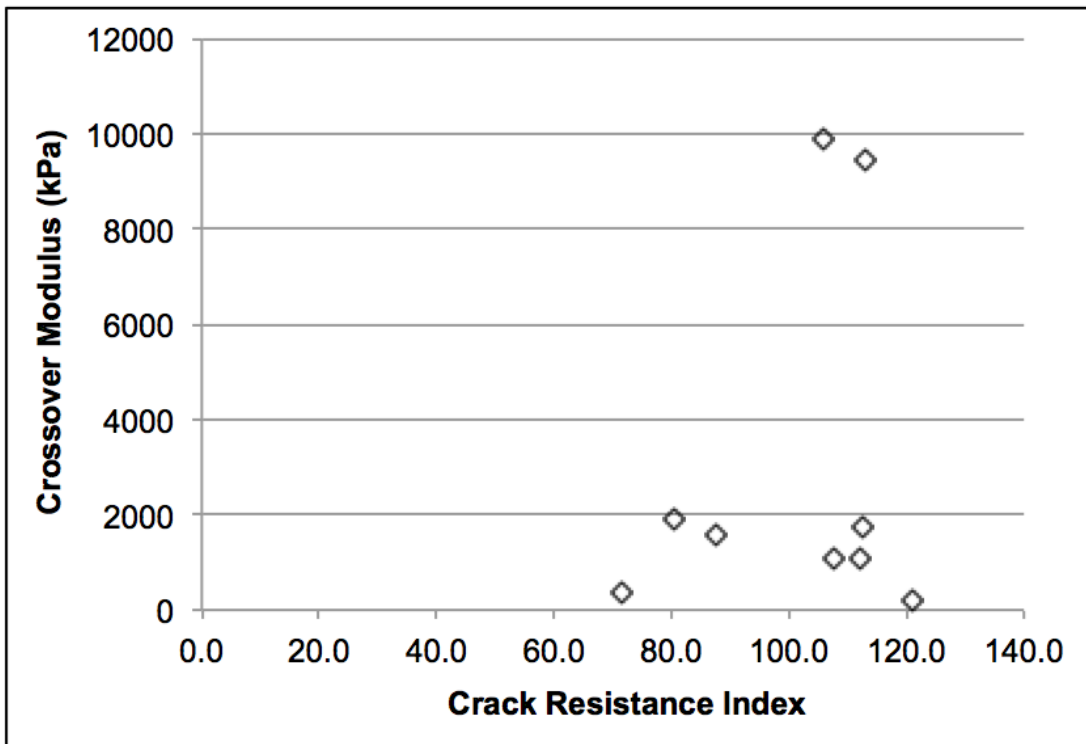


Figure 4.20. Crossover Modulus vs. Crack Resistance Index

# CHAPTER 5. EVALUATING REPEATABILITY OF SELECT TEST METHODS

## 5.1 OVERVIEW AND MATERIALS

The goal of this portion of the study was to assess whether some of the proposed test methods and concomitant parameters demonstrate a reasonable degree of repeatability when carried out using different instruments and operators. The primary goal of this information was to guide expectations in terms of future adoption of any specific test method and not necessarily serve as a substitute for a robustness test. The combinations of materials, operators, and instruments that were evaluated are listed below.

1.  $\Delta T_c$

- Binder B1:  
three samples with instrument #1 and operator #1  
two samples with instrument #1 and operator #2
  
- Binder B2:  
three samples with instrument #1 and operator #1  
two samples with instrument #1 and operator #2
  
- Binder B3:  
three samples with instrument #1 and operator #1  
two samples with instrument #1 and operator #2
  
- Binder B4:  
three samples with instrument #1 and operator #1  
two samples with instrument #2 and operator #2
  
- Binder B5:  
three samples with instrument #1 and operator #1  
two samples with instrument #2 and operator #2
  
- Binder B6:

three samples with instrument #1 and operator #1  
two samples with instrument #2 and operator #2

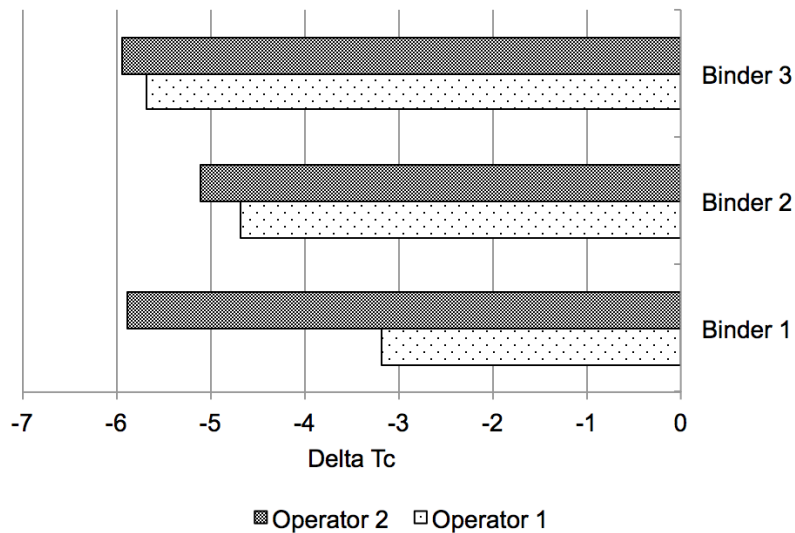
## 2. Glover-Rowe Parameter

- Binder B1:  
two samples with instrument #1 and operator #1  
two samples with instrument #1 and operator #2
  
- Binder B2:  
two samples with instrument #1 and operator #1  
two samples with instrument #1 and operator #2
  
- Binder B3:  
two samples with instrument #1 and operator #1  
one sample with instrument #1 and operator #2
  
- Binder B4:  
two samples with instrument #1 and operator #1  
two samples with instrument #2 and operator #2
  
- Binder B5:  
two samples with instrument #1 and operator #1  
two samples with instrument #2 and operator #2
  
- Binder B6:  
two samples with instrument #1 and operator #1  
two samples with instrument #2 and operator #2

Other parameters that have been evaluated in this study include the crossover modulus and crossover frequency, which were determined using the same test procedure as the Glover-Rowe parameter in the DSR, and are therefore not included in the repeatability section of this report, since they should experience similar effects from a change in operator. In addition, the Multiple Stress Creep and Recovery (MSCR) test was not evaluated for repeatability, because this has been done already in previous studies.

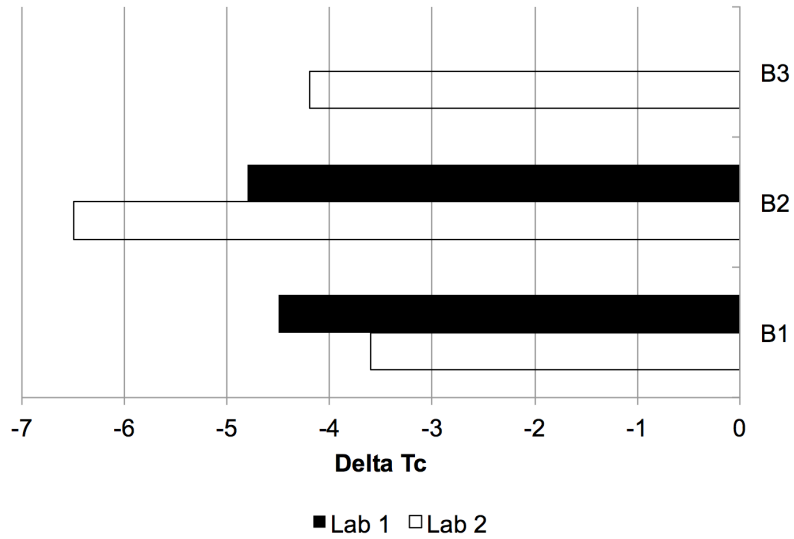
## 5.2 RESULTS

Figure 5.1 shows the results for  $\Delta T_c$  tested by two different operators using the same instrument. This figure shows that  $\Delta T_c$  generally has fair repeatability within the same instrument, and has very good repeatability for the same operator. Figure 5.2 shows the results for  $\Delta T_c$  tested by two different operators using different instruments. It is important to note that ASTM D6648 allows for some amount of error in determining the S and m-value true grades between operators, specifically 26.9% and 13%, respectively. However, since  $\Delta T_c$  requires multiple temperatures, these errors can be compounded. This can sometimes lead to substantial errors in repeatability, such as was seen for Binder 1, which has an error of 59.6% as a percent of the mean.



**Figure 5.1. Delta Tc tested by different operators using the same instrument**

Figure 5.1 shows the results for the Glover-Rowe Parameter tested by two different operators using the same instrument. This figure shows that the Glover-Rowe Parameter generally has good repeatability when performed by the same operator within the same instrument. However, substantial differences were observed when the operator changed, even using the same instrument.



**Figure 5.2. Delta Tc tested by different operators in different laboratories**

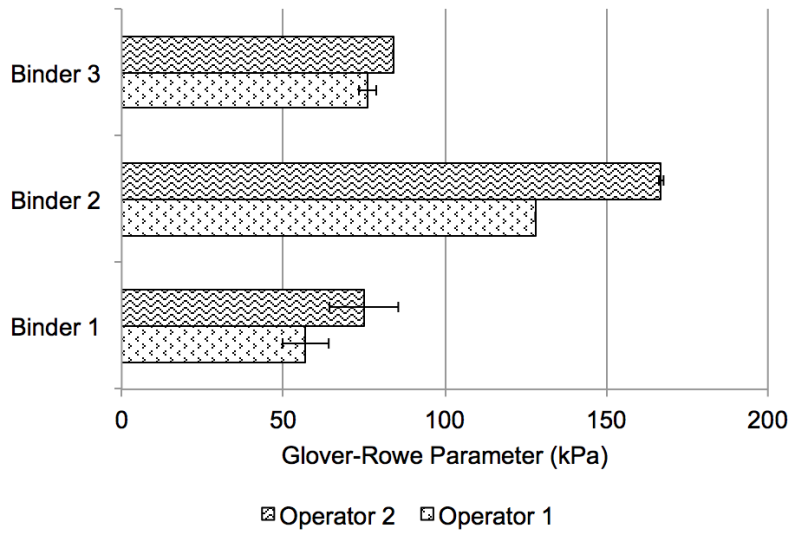


**Figure 5.3. Glover-Rowe Parameter tested by different operators using the same instrument**

## CHAPTER 6. SUMMARY AND CONCLUSIONS

This project conducted a comprehensive review of the Performance Grading (PG) specification and alternative tests that could potentially improve upon the PG framework. The early parts of the project examined the different methods that have been proposed to evaluate asphalt binder resistance to rutting, fatigue cracking, and low temperature cracking. A thorough literature review was conducted to determine what methods exist for binder testing for these distresses. Following this, the tests were narrowed down from the large variety of tests to tests that are simple to perform, do not require a large amount of time, and, to the extent possible, utilize existing equipment. After choosing a suite of tests, a selection of materials was performed, which involved three different types of binders- binders obtained from new construction sites, a wide variety of binders developed using a base binder with many different additives, and binders from recycled field sections. These binders were subjected to both the existing PG tests, and a suite of new tests. These binders were also used to produce full asphalt mixtures that were evaluated for their rutting and cracking resistance. The following are some of the key conclusions from this study.

1. The Multiple Stress Creep and Recovery (MSCR) test is a viable way to evaluate the rutting performance of binders. Results for both the non-recoverable compliance and the percent elastic recovery from this test were consistent with the binders performance based on mixture testing with the Hamburg Wheel Tracking Device.
2. The MSCR test can detect polymer modification (elastomers in particular) in a binder based on elastic recovery. However, the reverse is not true. In some cases polymer (elastomer) modification can result in low elastic recovery values, particularly when other additives are also included in the modification process. This means that polymer modification does not in itself provide a high elastic recovery. Therefore, it is not recommended to add a polymer requirement to the specification when high elastic recovery is desired.
3. Modification of the same base binder can result in drastically different properties depending on the type of modifier. In addition to having an effect on the chemical composition and microstructure of the binder, modifiers influence the overall performance-related properties of the binder, even when different modifiers result in a similar PG. The properties that were measured include  $\Delta T_c$ , the Glover-Rowe parameter, the crossover modulus and frequency, binder tensile strength, and fracture

- energy.
4. Overall, the critical fracture energy of asphalt mixtures from the Overlay test was shown to have a good correlation with the binder fracture energy from the poker chip test, when other elements of the mix (aggregate gradation and source, binder content, etc.) were held constant. This indicates that intermediate temperature cracking is heavily dependent on the properties of an asphalt binder, and that the fracture energy and tensile strength from the poker chip test are good indicators for a binder's resistance to formation of an initial crack.
  5. The  $\Delta T_c$  parameter showed a fair correlation with formation of cracks in the Overlay test as well. However, the viability of this test must be carefully considered in light of its repeatability due to the compounding errors from at least three different Bending Beam Rheometer (BBR) measurements, each of which has an allowable error between specimens.
  6. Other properties such as the Glover-Rowe parameter, the crossover modulus, the crossover frequency, and the current Superpave PG parameter were shown to be largely ineffective in predicting the mixture cracking performance when a specific binder is used in the mix with the Overlay test. It should be noted that all of these properties depend entirely on linear viscoelastic properties of the material, whereas the overlay test (and likely field cracking) occurs when the binder is subjected to large strains causing nonlinear damage. Further, the discrepancy between parameters such as the Glover-Rowe parameter and mixture performance is consistent with the findings reported in the literature by Glover and co-workers for polymer modified binders.
  7. The 4-mm plate geometry for the Dynamic Shear Rheometer (DSR) is a very important tool for the future of measuring low temperature properties of asphalt binder. A single low temperature frequency sweep test with shorter conditioning time in the DSR can provide Stiffness and m-value parameters that are consistent with those measured with the BBR for temperatures of interest. This test procedure is not only useful due to the improved efficiency of the method, but also because of the ability to measure low temperature properties using small amounts of material. For example, this can be a very useful tool to evaluate binder samples obtained from Recycled Asphalt Pavements (RAP), binder recovered from field cores, and emulsion residue.



## REFERENCES

- (2007). ASTM D113: Standard Test Method for Ductility of Bituminous Materials. In *ASTM D113-07*.
- (2016). ASTM D6373-16, Standard Specification for Performance Graded Asphalt Binder. Technical report, ASTM International, West Conshohocken, PA.
- (2017). AASHTO M320: Standard Specification for Performance Graded Asphalt Binder.
- Anderson, D. A., Hir, Y. M. L., Marasteanu, M. O., Planche, J.-p., Martin, D., and Gauthier, G. (2001). Evaluation of Fatigue Criteria for Asphalt Binders. *Transportation Research Record: Journal of the Transportation Research Board*, 1766:48–56.
- Anderson, M., Kriz, P., King, G., and Planche, J.-P. (2011a). Evaluation of the Relationship Between Asphalt Binder Properties and Non-load Related Cracking. *Journal of the Association of Asphalt Paving Technologists*, 80:615–664.
- Anderson, R., D'Angelo, J. A., and Bukowski, J. (2011b). Evaluation of the MSCR Test for Canadian Asphalt Binders. In *Proceedings of the Fifty-Sixth Annual Conference of the Canadian Technical Asphalt Association*.
- Andriescu, A., Hesp, S. A. M., and Youtcheff, J. S. (2004). Essential and Plastic Works of Ductile Fracture in Asphalt Binders. *Transportation Research Record: Journal of the Transportation Research Board*, 1875:1–8.
- Bahia, H., Hanson, D., Zeng, M., Zhai, H., Khatfi, M., and Anderson, R. (2001a). NCHRP 459: Characterization of Modified Asphalt Binders in Superpave Mix Design. Technical report.
- Bahia, H. U., Hanson, D. I., Zeng, M., Zhai, H., Khatri, M. A., and Anderson, R. M. (2001b). Characterization of modified asphalt binders in superpave mix design. Technical report, NCHRP Project 9-10.
- Bahia, H. U., Zhai, H., Bonnetti, K., and Kose, S. (1999). Non-Linear Viscoelastic and Fatigue Properties of Asphalt Binders. In *Association of Asphalt Paving Technologists*.

- Bonnetti, K. S., Nam, K., and Bahia, H. U. (2002). Measuring and Defining Fatigue Behavior of Asphalt Binders. *Transportation Research Record: Journal of the Transportation Research Board*, 1810:33–43.
- Clark, R. (1958). Practical results of asphalt hardening on pavement life. *Journal of the Association of Asphalt Paving Technologists*, 27:196–208.
- D'Angelo, J., Kluttz, R., Dongre, R. N., Stephens, K., and Zanzotto, L. (2007). Revision of the Superpave High Temperature Binder Specification: The Multiple Stress Creep Recovery Test. *Journal of the Association of Asphalt Paving Technologists*, 76:123–162.
- Doyle, P. (1958). Cracking characteristics of asphalt cement. *Proc of Assoc of Asphalt Paving Technologists*, 27:581–597.
- Dubois, E., Mehta, Y., and Nolan, A. (2014). Correlation between multiple stress creep recovery (MSCR) results and polymer modification of binder. *Construction and Building Materials*, 65:184–190.
- Elseifi, M. A., Asce, A. M., Mohammad, L. N., Glover, I., Negulescu, I., Daly, W. H., and Abadie, C. (2010). Relationship between Molecular Compositions and Rheological Properties of Neat Asphalt Binder at Low and Intermediate Temperatures. *Journal of Materials in Civil Engineering*, 22(December):1288–1294.
- Farrar, M. J., Sui, C., Salmans, S., and Qin, Q. (2015). Determining the Low-Temperature Rheological Properties of Asphalt Binder Using a Dynamic Shear Rheometer (DSR). Technical report, Western Research Institute, Laramie, WY.
- Glover, C. J., Davison, R. R., Domke, C. H., Ruan, Y., Juristyarini, P., Knorr, D. B., and Jung, S. H. (2005). Development of a New Method for Assessing Asphalt Binder Durability with Field Validation. Technical report, Texas Department of Transportation.
- Hajj, R. and Bhasin, A. (2018). The search for a measure of fatigue cracking in asphalt binders - A review of different approaches. *International Journal of Pavement Engineering*, 19(3):205–219.
- Hajj, R., Filonzi, A., Rahman, S., and Bhasin, A. (2019). Considerations for Using the 4 mm Plate Geometry in the Dynamic Shear Rheometer for Low Temperature Evaluation of Asphalt Binders. *Transportation Research Record: Journal of the Transportation Research Board*.

- Harvey, J. A. F. and Cebon, D. (2003). Failure mechanisms in viscoelastic films. *Journal of Materials Science*, 38(5):1021–1032.
- Hintz, C., Velasquez, R., Johnson, C., and Bahia, H. (2011). Modification and Validation of the Linear Amplitude Sweep Test for Binder Fatigue Specification. *Transportation Research Record: Journal of the Transportation Research Board*, 2207.
- Johnson, C. (2010). *Estimating Asphalt Binder Fatigue Resistance Using an Accelerated Test Method*. PhD thesis, University of Wisconsin- Madison.
- Johnson, C. M., Bahia, H., and Wen, H. (2007). Evaluation of Strain-Controlled Asphalt Binder Fatigue Testing in the Dynamic Shear Rheometer. In *4th International SIIV Congress*.
- Kennedy, T. W., Huber, G., Cominsky, R., Hughes, C., Von Quintus, H., and Moulthrop, J. (1994). Superior performing asphalt pavements (Superpave): The product of the SHRP asphalt research program. Technical report.
- Lu, X., Uhlback, P., and Soenen, H. (2017). Investigation of bitumen low temperature properties using a dynamic shear rheometer with 4 mm parallel plates. *International Journal of Pavement Research and Technology*, 10:15–22.
- Marasteanu, M. O., Li, X., Clyne, T. R., Voller, V., Timm, D. H., and Newcomb, D. (2004). Low Temperature Cracking of Asphalt Concrete Pavement. Technical report, Retrieved from the University of Minnesota Digital Conservancy.
- Marek, C. and Herrin, M. (1968). Tensile Behavior and Failure Characteristics of Asphalt Cements in Thin Films. In *Association of Asphalt Paving Technologists Proceedings*, pages 1–54.
- Masad, E., Somadevan, N., Bahia, H., and Kose, S. (2001). Modeling and Experimental Measurements of Strain Distribution in Asphalt Mixes. *Journal of Transportation Engineering*, 127(December):477–485.
- McGennis, R. B., Shuler, S., and Bahia, H. U. (1994). Background of Superpave Asphalt Binder Test Methods. Technical Report July, Federal Highway Administration, Office of Technology Applications.

- Motamed, A., Bhasin, A., and Liechti, K. M. (2014). Using the poker-chip test for determining the bulk modulus of asphalt binders. *Mechanics of Time-Dependent Materials*, pages 197–215.
- Oshone, M. T. (2018). *Performance Based Evaluation of Cracking in Asphalt Concrete Using Viscoelastic and Fracture Properties*. PhD thesis, University of New Hampshire.
- Poulikakos, L. D. and Partl, M. N. (2011). Micro Scale Tensile Behaviour of thin bitumen films. *Proceedings of the Society for Experimental Mechanics, Inc.*, 51(7):1171–1183.
- Rowe, G. M., King, G., and Anderson, M. (2014). The Influence of Binder Rheology on the Cracking of Asphalt Mixes in Airport and Highway Projects. *Journal of Testing and Evaluation*, 42(5).
- Ruan, Y., Davison, R. R., and Glover, C. J. (2003). An investigation of asphalt durability: Relationships between ductility and rheological properties for unmodified asphalts. *Petroleum Science and Technology*, 21(1 & 2):231–254.
- Stuart, K. and Mogawer, D. (2002). Validation of the Superpave Asphalt Binder Fatigue Cracking Parameter Using the FHWA's Accelerated Loading Facility. In *Asphalt Paving Technology*.
- Sui, C., Farrar, M., Harnsberger, P., Tuminello, W., and Turner, T. (2011). New Low-Temperature Performance-Grading Method. *Transportation Research Record: Journal of the Transportation Research Board*, 2207:43–48.
- Sui, C., Farrar, M. J., Tuminello, W. H., and Turner, T. F. (2010). New Technique for Measuring Low-Temperature Properties of Asphalt Binders with Small Amounts of Material. *Transportation Research Record: Journal of the Transportation Research Board*, (2179):23–28.
- Sultana, S. and Bhasin, A. (2014). Effect of chemical composition on rheology and mechanical properties of asphalt binder. *Construction and Building Materials*, 72:293–300.
- Sultana, S., Bhasin, A., and Liechti, K. M. (2014). Rate and confinement effects on the tensile strength of asphalt binder. *Construction and Building Materials*, 53:604–611.
- Tabatabaee, H. A., Clopotel, C., Arshadi, A., and Bahia, H. (2013). Critical Problems with Using the Asphalt Ductility Test as a Performance Index for Modified Binders. *Transportation Research Record: Journal of the Transportation Research Board*, 2370:84–91.

- Tsai, B.-W. and Monismith, C. (2005). Influence of Asphalt Binder Properties on the Fatigue Performance of Asphalt Concrete Pavements. *Journal of the Association of Asphalt Paving Technologists*, 74(January).
- Wen, H. and Bahia, H. (2009). Characterizing Fatigue of Asphalt Binders with Viscoelastic Continuum Damage Mechanics. *Transportation Research Record: Journal of the Transportation Research Board*, 2126:55–62.
- Yusoff, N. I. M., Jakarni, F. M., Nguyen, V. H., Hainin, M. R., and Airey, G. D. (2013). Modelling the rheological properties of bituminous binders using mathematical equations. *Construction and Building Materials*, 40:174–188.
- Zhou, F., Li, H., Chen, P., and Scullion, T. (2014). Laboratory evaluation of asphalt binder rutting, fracture, and adhesion tests. Technical report, No. FHWA/TX-14/0-6674-1. Texas. Dept. of Transportation. Research and Technology Implementation Office.



**APPENDIX A.**  
**PROPOSED TEST METHOD FOR 4 MM DSR GEOMETRY**





---

## Test Procedure for Measuring Low Temperature Properties of Asphalt Binder Using a Dynamic Shear Rheometer



**TxDOT Designation: XXXXX**

**Effective Date: XXXXXX**

---

### 1. SCOPE

- 1.1 This procedure provides a test method for measuring the low temperature properties of asphalt binder that are typically used for assigning the binder a Performance Grade (PG). In the past, these values have been measured only using the Bending Beam Rheometer (BBR).
- 1.2 The values given in parentheses (if provided) are not standard and may not be exact mathematical conversions. Use each system of units separately. Combining values from the two systems may result in nonconformance with the standard.
- 

### 2. APPARATUS

- 2.1 *Dynamic Shear Rheometer (DSR)* – a device designed to measure rheological properties of viscoelastic materials in shear using the parallel plate geometry.
- 2.1.1 4 mm plate geometry attachment for DSR.
- 2.1.2 Environmental Test Chamber (ETC) or other apparatus for DSR capable of reaching temperatures as low as -30 °C (-22 °F). Temperature control should be  $\pm 0.1$  °C ( $\pm 0.2$  °F).
- 2.1.3 Follow manufacturer's instructions for calibration of DSR to ensure accurate measurements. DSR should be properly calibrated as recommended by the manufacturer.
- 2.1.4 Software with DSR measurement tools should output linear viscoelastic properties.
- 

### 3. MATERIALS

- 3.1 *Asphalt Binder* – Use binder as specified per the pertinent TxDOT Specification Items in the applicable project plans. Asphalt binders should be aged in the Rolling Thin Film Oven (RTFO) as specified in Tex-541-C and subsequently in the Pressure Aging Vessel (PAV) as specified in AASHTO R-28.
- 

### 4. PROCEDURE

- 4.1 *Laboratory-Aged Specimens:* PAV-aged specimens of asphalt binder should be prepared and molded into small cylinders weighing 1 g each.
-

- 4.2 A machine compliance correction must be performed to correct for very stiff material being used in the DSR as follows:
- 4.2.1 Perform the zero gap in the DSR at a temperature of 0 °C (32 °F).
  - 4.2.2 Raise the top DSR plate to the loading gap.
  - 4.2.3 Apply a drop of distilled water to the bottom plate.
  - 4.2.4 Lower the top plate to create a gap of 50 µm with water between it.
  - 4.2.5 Lower the temperature of the plate to -5 °C (23 °F). Hold at this temperature for 5 minutes until ice is completely frozen.
  - 4.2.6 Apply a 1 N ± 0.5 N tensile load.
  - 4.2.7 Set the gap to dynamically adjust to maintain this tensile load of 1 N ± 0.5 N throughout the compliance correction process.
  - 4.2.8 Lower the temperature to -30 °C (-22 °F) and allow the gap to manually adjust to maintain the tensile load during cooling to avoid shrinkage fracture of the ice.
  - 4.2.9 Condition the specimen at -30 °C for 200 seconds.
  - 4.2.10 At this temperature, run an amplitude sweep at 1 Hz with amplitudes between 100 and 30000 µN of torque. Measure 5 points per decade.
  - 4.2.11 Plot the linear data with torque on the x-axis and displacement on the y-axis. The slope of this line is the compliance correction value.

#### 4.3 *Mounting Specimens in the DSR:*

- 4.3.1 After the DSR has been cleaned of all water and returned to room temperature, heat the plates slightly so that the specimen can be adhered to them.
- 4.3.2 Set the temperature to 10 °C (50 °F). Place the specimen on the lower plate and gradually reduce the gap to 2800 μm as the specimen cools. Perform the first trim of the specimen after the gap is reduced and the normal force is less than 5 N.
- 4.3.3 Set the temperature to 0 °C (32 °F) and reduce the gap to 2400 μm. Again, perform a second trim and wait for the normal force to be less than 5 N.
- 4.3.4 Reduce the gap to 2000 μm as the specimen is cooled to -30 °C (-22 °F).

#### 4.4 *Testing Specimens in the DSR:*

- 4.4.1 Perform a frequency sweep test as described below:
- 4.4.2 Test the asphalt binder at temperatures including -30 °C (-22 °F), -27 °C (-16.6 °F), -24 °C (-11.2 °F), -21 °C (-5.8 °F), -18 °C (-0.4 °F), -12 °C (10.4 °F), -6 °C (21.2 °F), 0 °C (32 °F), 10 °C (50 °F), 20 °C (68 °F), 30 °C (86 °F), 40 °C (104 °F), 50 °C (122 °F), 60 °C (140 °F).
- 4.4.3 Each temperature should be preceded by a conditioning time of 300 seconds.
- 4.4.4 Test frequencies should range from 0.1 to 100 rad/s with at least 5 points per decade.
- 4.4.5 Temperatures should be run from low to high, while frequencies should be run from high

---

## 5. REPORT

- 5.1 Report the following for each specimen:
- G' and G'' at each temperature-frequency combination

---

## 6. ANALYSIS

- 6.1 Fit each temperature of interest's G' and G'' vs. frequency data to individual curves using the sigmoidal function below:

$$\log|G'| = \delta + \frac{\alpha}{1 + e^{\beta + \gamma \log(\omega)}}$$

- 6.2 Use Ninomiya-Ferry interconversion to convert the frequency domain data to time domain as shown below:

$$J(t) = J'(\omega) - 0.4J''(0.4\omega) + 0.014J''(10\omega)$$

- 6.3 Convert the data from shear to axial loading as shown below assuming a Poisson's ratio of 0.35 for the binder at low temperatures:

- 6.4 Convert the data from compliance to BBR creep Stiffness by inverting it directly.
- 6.5 Report the Stiffness in MPa at 60 seconds at each temperature of interest.
- 6.6 The m-value can be computed by taking a local slope of the Stiffness vs. time curve at 60 seconds. Report this m-value as well.
- 6.7 The grading criteria are a maximum of 300 MPa for Stiffness and a minimum m-value of 0.28.





**APPENDIX B.**  
**PROPOSED TEST METHOD FOR POKER CHIP TEST**





---

## Test Procedure for Measuring Intermediate Temperature Fracture Properties of Asphalt Binder Using the Poker Chip Test

**TxDOT Designation: XXXXX**

**Effective Date: XXXXXX**



---

### 1. SCOPE

- 1.1 This procedure provides a test method for measuring the intermediate temperature fracture properties of asphalt binder for determination of the load-related cracking resistance of a binder.
- 1.2 The values given in parentheses (if provided) are not standard and may not be exact mathematical conversions. Use each system of units separately. Combining values from the two systems may result in nonconformance with the standard.

---

### 2. APPARATUS

- 2.1 Commercial device available for testing of thin films of adhesives in tension, including those used for Dynamic Mechanical Analysis (DMA)
  - 2.1.1 15 mm rigid metal plates (2).
  - 2.1.2 A test chamber capable of maintaining a uniform temperature of  $18\text{ }^{\circ}\text{C} \pm 1\text{ }^{\circ}\text{C}$ .
  - 2.1.3 A load cell with at least 2 kN capability.
  - 2.1.4 An actuator capable of controlling displacement with good precision.
  - 2.1.5 Follow manufacturer's instructions for calibration of the test equipment and temperature control device. Calibration of the device is extremely important to perform to ensure accurate measurements of load and displacement.

---

### 3. MATERIALS

- 3.1 *Asphalt Binder* – Use binder as specified per the pertinent TxDOT Specification Items in the applicable project plans. Asphalt binders should be aged in the Rolling Thin Film Oven (RTFO) as specified in Tex-541-C and subsequently in the Pressure Aging Vessel (PAV) as specified in AASHTO R-28.

---

### 4. PROCEDURE

- 4.1 *Laboratory-Aged Specimens:* PAV-aged specimens of asphalt binder should be prepared in

films at least 1 mm (0.04 in) thick with a diameter of at least 20 mm (0.8 in).

- 4.2 Rigid plates should be mounted in the device so that they are perpendicular to each other.
- 4.2.1 Set the temperature in the chamber to the test temperature, 18 °C and condition the plates at this temperature for at least 10 minutes.
- 4.2.2 Perform a zero gap action at this temperature by bringing the plates close together until they are touching, at which point the load cell will detect a force.
- 4.2.3 Set this as the zero point, and bring the plates far from each other.
- 4.2.4 Heat the bottom plate, and place the asphalt binder specimen on it.
- 4.2.5 Heat, and then lower the top plate immediately to 0.7 mm (0.028 in).
- 4.2.6 Over the next 10 minutes, manually decrease the specimen thickness to 0.35 mm (0.014 in) as the specimen cools, while taking care to avoid applying loads larger than 20 N to the specimen.
- 4.2.7 Condition the specimen at this gap and temperature for 15 minutes. During this time, allow the gap to adjust dynamically to account for any changes in the load larger than 20 N in either direction.
- 4.2.8 Begin the test. The test should apply uniaxial tension to the top plate while holding the bottom plate in place. Tests should be displacement-controlled at a rate of 0.1 mm/min.

---

## 5. REPORT

- 5.1 Plot the stress (load divided by initial cross-sectional area of the specimen) vs. strain (change in thickness divided by original thickness of the specimen) curve for each specimen.
- 5.2 Report the following for each specimen:
- Maximum load (N)
  - Area under stress-strain curve until maximum load
  - Strain at failure
  - Photos of the failed specimen

---

## 6. ANALYSIS

- 6.1 Engineering stress can be calculated as shown below:

$$\sigma = \frac{F}{A_0}$$

where:

F = load (N)

A<sub>0</sub> = original cross sectional area of the specimen (mm<sup>2</sup>)

6.2 Engineering strain can be calculated as shown below:

$$\varepsilon = \frac{\Delta L}{L_0}$$

where:

ΔL = change in thickness of specimen (mm)

L<sub>0</sub> = original thickness of specimen (mm)